

AR-A/35 853

COMPARISON OF THE LONGITUDINAL FLYING QUALITIES OF AN
OPTIMAL PILOT MODEL (U) AIR FORCE INST OF TECH
WRIGHT PATTERSON AFB OH SCHOOL OF ENGI... J M PAYNE
SEP 83 AFIT/GAE/AA/835-5

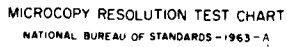
1/2

UNCLASSIFIED

1/6 14/2

HL

20



MICROCOPY RESOLUTION TEST CHART
NATIONAL BUREAU OF STANDARDS-1963-A

AD-A135853



①

COMPARISON OF THE LONGITUDINAL
FLYING QUALITIES OF AN OPTIMAL
PILOT MODEL, A GROUND-BASED
SIMULATOR, AND AN AIRBORNE SIMULATOR

THESIS

DISTRIBUTION STATEMENT A

Approved for public release
Distribution Unlimited

**DTIC
ELECTE**

DEC 14 1983

B

DEPARTMENT OF THE AIR FORCE
AIR UNIVERSITY (ATC)

AIR FORCE INSTITUTE OF TECHNOLOGY

DTIC FILE COPY

Wright-Patterson Air Force Base, Ohio

83 12 13 250

AFIT/GAE/AA/83S-5

COMPARISON OF THE LONGITUDINAL
FLYING QUALITIES OF AN OPTIMAL
PILOT MODEL, A GROUND-BASED
SIMULATOR, AND AN AIRBORNE SIMULATOR

THESIS

AFIT/GAE/AA/83S-5 James M. Payne
 Captain USAF

Approved for public release; distribution unlimited.

DTIC
ELECTE
S DEC 14 1983 D
B

AFIT/GAE/AA/83S-5

COMPARISON OF THE LONGITUDINAL
FLYING QUALITIES OF AN OPTIMAL PILOT MODEL,
A GROUND-BASED SIMULATOR, AND AN AIRBORNE SIMULATOR

THESIS

Presented to the Faculty of the School of Engineering
of the Air Force Institute of Technology
Air University
in Partial Fulfillment of the
Requirements for the Degree of
Master of Science

by
James M. Payne, B.S.
Captain USAF
Graduate Aeronautical Engineering
September 1983

Approved for public release; distribution unlimited.

Preface

This thesis is one of the first accomplished for the Air Force Institute of Technology/Test Pilot School Education Program. It represents the culmination of study at Wright-Patterson AFB, Ohio, and Edwards AFB, California.

Many people made contributions. Dr. Robert Calico, my advisor, provided aid during the analysis. Captain (Dr.) James Silverthorn, who transferred from AFIT to TPS at the same time as I moved, provided invaluable advice and continuity of support. The TPS staff and CALSPAN Corporation provided the NT-33A support. Major Thomas Melody, the staff NT-33A project monitor, provided the SAFTD simulator expertise that made the ground-based simulation work. My TPS classmates, Captains Charles Stewart, Terry Tomeny, Kevin McNellis, Thomas Day, and First Lieutenant Thomas Akers were all valuable partners in the NT-33A Test Team.

A special thanks goes to my wife, Jackie, who preserved and survived as a great Mom for "two under two."



Accession For	
NTIS	<input checked="" type="checkbox"/>
DTIC TAB	<input type="checkbox"/>
Unannounced	<input type="checkbox"/>
Justification	
By	
Distribution/	
Availability Codes	
Dist	Avail and/or Special
A-1	

Contents

	Page
Preface	ii
List of Figures	iv
List of Tables	v
List of symbols	vi
Abstract	viii
I. Introduction	1
II. Test Objective	3
III. Test Item Description	3
Optimal Pilot Model	3
SAFTD	8
NT-33A	9
IV. Test Methods and Conditions	12
Overall	12
Analytical Model	13
Simulation	13
V. Test Results	18
VI. Analysis	29
VII. Conclusions and Recommendations	34
Bibliography	36
Appendix A: Analysis of the Effects of Load Factor on Frequency Response of the NT-33A	38
Appendix B: Computer Listings and Bode Plots	46
Appendix C: Data Plots	68
Appendix D: Digital Tape Parameters	99
Appendix E: Pilot Background	102
Vita	104

List of Figures

<u>Figure</u>		<u>Page</u>
1	Diagram of Optimal Pilot Model	4
2	SAFTD Layout	9
3	NT-33A Control System Layout	10
4	NT-33A HUD Layout	11
5	Sample Analog Match	12
6	The Cooper-Harper Scale	14
7	Preprogrammed Pitch Tracking Tasks	15
8	OPSACT "Pilot" Performance	18
9A	Confidence Intervals for SAFTD at 1g	20
9B	Cooper-Harper Ranges for SAFTD at 1g	20
10A	Confidence Intervals for SAFTD at 2g	21
10B	Cooper-Harper Ranges for SAFTD at 2g	22
11	SAFTD Tracking Error Versus Frequency	23
12A	Confidence Intervals for NT-33A at 1g	25
12B	Cooper-Harper Ranges for NT-33A at 1g	25
13A	Confidence Intervals for NT-33A at 2g	26
13B	Cooper-Harper Ranges for NT-33A at 2g	26
14	NT-33A Error Count Versus Frequency	27
15	Cooper-Harper Trends at 1g	28
16	SAFTD Tracking Error Versus Cooper-Harper	30
17	NT-33A Error Count Versus Cooper-Harper	31
18	Pilot #2 Error Count Versus Frequency	32

List of Tables

<u>Table</u>		<u>Page</u>
1	Selected Dynamic Parameters	17
2	SAFTD Ground Simulator Pilot Comments	19
3	NT-33A Pilot Comments	24

List of Symbols

Note: Underlined variables in this thesis indicate column vectors. Capital letters in vector equations are matrices.

A	System Plant Matrix
<u>b</u>	System control vector
F _s	Force applied to control stick
H	System observation matrix
g	Acceleration of gravity (32.2 feet per second ²)
K _f	Stick force sensitivity
K _L	Control linkage gain
k	Strength of noise
M _α , M _{α̇}	Aircraft stability derivatives relating pitching moment to angle of attack and angle of attack rate
M _δ	Aircraft stability derivative relating pitching moment to elevator deflection
M _q	Aircraft stability derivative relating pitching moment to pitch rate
n	Normal load factor
Q _x	State weighting matrix
Q _y	Weighting matrix for observed variables
q	Pitch rate
t	Time
U _o	Trim velocity
u	Pilot control input to system
u _c	Commanded control input
v _u	Motor noise
v _y	Observation noise
w	Noise input to system dynamics
<u>x</u>	State vector

Y_p	Noise corrupted observation vector
Y_r	Minimum Cooper-Harper rating
Y_s	Maximum Cooper-Harper rating
$Z_{\alpha}, Z_{\dot{\alpha}}$	Aircraft stability derivatives relating normal force to angle of attack angle of attack rate
Z_{δ}	Aircraft stability derivative relating normal force to elevator deflection
α	Angle of attack
δ	Elevator deflection angle
δ_c	Commanded elevator deflection angle
ϵ	Tracking error angle
$\dot{\epsilon}$	Rate of change of tracking error angle
ω_{sp}	Short period natural frequency
Σ	Dummy noise variable
\bar{y}	Median Cooper-Harper rating
θ	Pitch angle
θ_c	Commanded pitch angle
τ	Pilot time delay
τ_a	Time constant of actuator
τ_n	Pilot neuro-muscular time constant
τ_h	Time constant of noise
τ_{θ_c}	Time constant of pitch command
ζ	Damping ratio

Abstract

This thesis presents a comparison of the longitudinal flying qualities as predicted by an analytical computer model, a ground-based simulator, and an airborne simulator. The comparison was designed to correlate the results and judge whether ground tests could forecast airborne results. The objective was to determine and compare the pilot performance in the three cases, and to determine and compare the pilot ratings in the simulators. Secondary objectives included an investigation of the effects of different load factors in both simulators and the effects of visual and motion cues in the NT-33A. Identical aircraft dynamics, flight control characteristics, and tracking tasks were used in each case. The handling characteristics for short period natural frequencies of 2, 4, 6, 8, and 10 radians per second were rated using the Cooper-Harper rating scale. In the analytical model, pilot performance improved as the frequency was increased. In the ground simulator, the pilot ratings were primarily a function of how well he could track the preprogrammed task. Performance improved as frequency was increased. In the airborne NT-33A tests, pilots preferred 4 to 6 radians per second. Lower frequencies were too slow and higher frequencies were too abrupt and uncomfortable despite better tracking performance. The inconsistent pilot preference above 6 radians per second in the two simulators is due to the absence of motion cues. The lack of correlation at the higher frequencies indicates that ground based simulation cannot entirely replace airborne testing.

I. INTRODUCTION

↓
This thesis presents a comparison of the longitudinal flying qualities as predicted by an analytical computer model, a ground-based simulator, and an airborne simulator. The comparison was designed to correlate the results and judge whether ground tests could forecast airborne results. Project tests were conducted using the Optimal Pilot Single Axis Control Task (OPSACT) computer program, the ground based Simulator for Aircraft Flight Test and Development (SAFTD), and the variable stability, USAF NT-33A aircraft. The objective of this evaluation was to determine and compare the pilot performance in the three cases, and to determine and compare the pilot ratings in the simulators. Secondary objectives included an investigation of the effects of different load factors in the two simulators and the effects of visual and motion cues in the NT-33A.

Tight experimental control was maintained by programming identical aircraft dynamics into the models and setting optimum values for both the short period damping and the control system dynamics such as forces, gradients, and stick displacements. These values were obtained from previous research at the same flight condition which corresponds to an n/α of 29 g's per radian. A stochastic pitch tracking task was used in the computer model while identical pitch tracking tasks were programmed into the SAFTD TV display and the NT-33A HUD. In the OPSACT, the root mean square of the tracking error was

determined. In the two simulators, pilot comments were recorded and tracking ability at short period natural frequencies of 2, 4, 6, 8, and 10 radians per second was rated using the Cooper-Harper rating scale. Actual tracking error was also recorded on strip charts in the SAFTD and a magnetic tape data recorder in the NT-33A. These sources provided a quantitative measure of actual pilot performance. In addition, HUD camera film was also used to record airborne tracking tasks.

Computer testing of the analytical model took place on the Cyber computers at Wright-Patterson Air Force Base, Ohio, and Edwards Air Force Base, California. Ground simulation was conducted in the SAFTD at Edwards Air Force Base, California, between 28 April and 20 May 1983. During 26 hours of SAFTD testing, 125 1g test points and 37 2g test points were accomplished. Airborne testing was conducted at Edwards AFB, California from 20 April to 6 May 1983, consisting of 20 NT-33A sorties for a total of 24.4 flying hours. During NT-33A tests, 153 1g and 71 2g test points were accomplished with 33 being flown with outside visual reference denied using canopy and visor filters.

The Optimal Pilot Model has been used by Harvey (Ref.1) to predict the long term (100 seconds) performance of an aircraft with a lead computing sight. Mullen (Ref. 5) compared the short term (10 seconds) performance prediction of the OPM to a simulation with less success than Harvey.

II. TEST OBJECTIVE

The objective of this evaluation was to determine and compare the pilot pitch tracking performance in the three cases, and to determine and compare the pilot ratings in the simulators. From this comparison, a correlation between the computer model or the ground-based simulator and the inflight simulator would indicate the value of each.

Secondary objectives included determining the effects of a higher load factor (2g) on pilot opinion in the two simulators and the effects of visual and motion cues in the NT-33A. The testing at different load factors was designed to test the assumption that preferred flying qualities at 1g are also preferred at higher load factors. The investigation of the visual and motion cues was designed to determine which cues are most important to the pilot's ratings.

III. TEST ITEM DESCRIPTION

THE OPTIMAL PILOT MODEL

The optimal pilot model used in the analytical portion of this study was the Optimal Pilot Single Axis Control Task (OPSACT). This computer program has been previously used to predict pilot opinion of longitudinal tracking tasks (Ref. 3 and 5).

Based upon optimal stochastic control theory, the original concept for the model was developed by Kleinman, Baron, and Levison (Ref. 2). It relies on the assumption that a human operator with good training behaves in an optimal manner for a

given control task. OPSACT was assembled by Enright using this concept of Kleinman et al. (Ref. 3).

The model incorporates a closed loop system that includes the system dynamics of the aircraft and the tracking task, the display of these dynamics, and the pilot's perception and control actions (Figure 1). The uncertainties of the real process are modeled by stochastic noises which enter the system as a random target load factor, errors in pilot perception, and errors in the pilot control inputs.

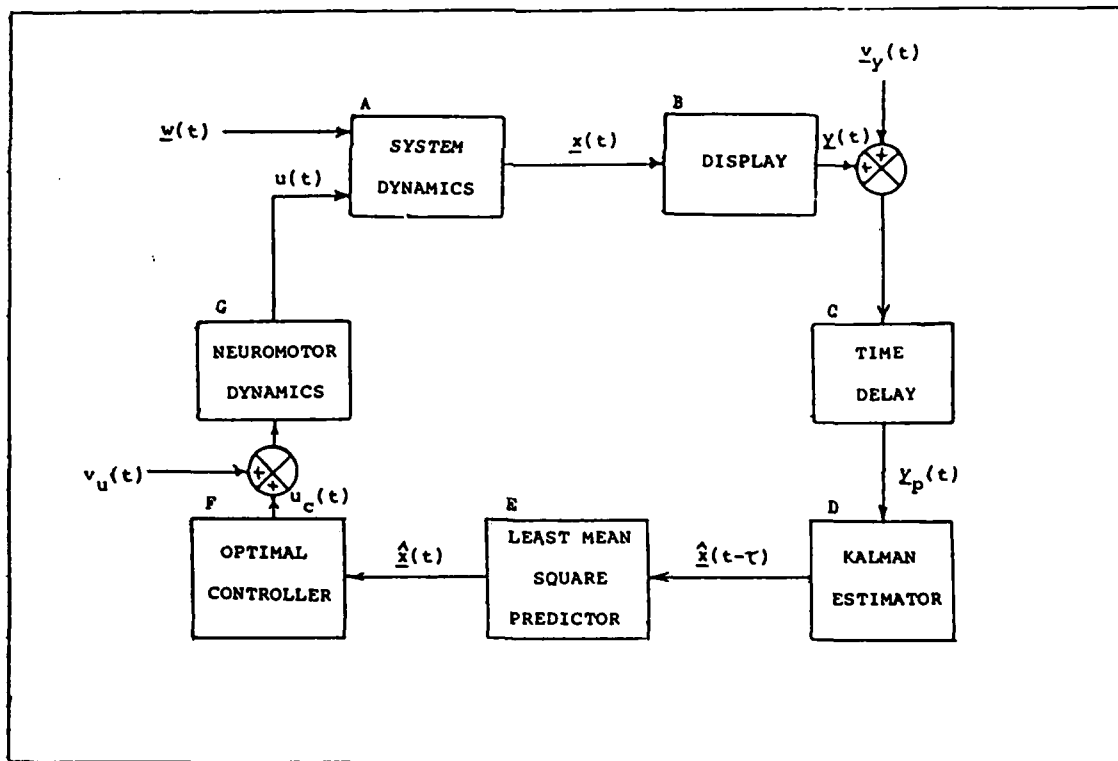


Figure 1. Diagram of the Optimal Pilot Model

The systems dynamics (Block A) are a combination of the aircraft dynamics and the pitch tracking dynamics. One of the assumptions in the development of this model was that the lg flying qualities of an aircraft are not significantly altered when the load factor is increased. Appendix A lists the results of an investigation that showed this to be true as the frequency response of the NT-33A aircraft was not change significantly as the load factor was increased.

The tracking task used in this model was a stochastic pitch tracking task designed to simulate the pitch tracking task that the pilots flew in the simulators. It is a zero mean pitch command with a deviation and time constant similar to the task programmed into the SAFTD display and the NT-33A HUD.

The state equations of motion were formed using the following state variables:

$$x_1 = \delta$$

$$x_4 = \Theta$$

$$x_2 = q$$

$$x_5 = \Theta_c$$

$$x_3 = \alpha$$

$$x_6 = \text{dummy noise state, } \Sigma$$

$$\text{and } u \equiv \delta_c = -K_f F_s$$

The equations of motion and target dynamics are combined into matrix notation

$$\dot{x} = Ax(t) + Bu(t) + W(t)$$

in which the "A" matrix is

$$\begin{bmatrix} -1/\tau_a & 0 & 0 & 0 & 0 & 0 & -K_f F_s \\ M \frac{M_z Z_\delta}{U_0} & M_q + M_{\dot{\alpha}} & M_{\alpha} + M_z \frac{Z_\alpha}{U_0} & 0 & 0 & 0 & 0 \\ \frac{Z_\delta}{U_0} & 1 & \frac{Z_\alpha}{U_0} & 0 & 0 & 0 & 0 \\ 0 & 1 & 0 & 0 & 0 & 0 & 0 \\ 0 & 0 & 0 & 0 & -1/\tau_{\theta_e} & k & 0 \\ 0 & 0 & 0 & 0 & 0 & -1/\tau_n & 0 \\ 0 & 0 & 0 & 0 & 0 & 0 & 0 \end{bmatrix}$$

For 300 KIAS and $\omega_{sp} = 2$ radians per second, the A matrix is

$$\begin{bmatrix} -20 & 0 & 0 & 0 & 0 & 0 & -1.339 \\ -22.28 & -0.994 & -2.204 & 0 & 0 & 0 & 0 \\ -0.105 & 1 & -1.81 & 0 & 0 & 0 & 0 \\ 0 & 1 & 0 & 0 & 0 & 0 & 0 \\ 0 & 0 & 0 & 0 & -0.40 & 0.114 & 0 \\ 0 & 0 & 0 & 0 & 0 & -20 & 0 \\ 0 & 0 & 0 & 0 & 0 & 0 & 0 \end{bmatrix}$$

Also, $B = \text{col } [0 \ 0 \ 0 \ 0 \ 0 \ 0 \ 1]$

and $W(t) = \text{col } [0 \ 0 \ 0 \ 0 \ 0 \ w \ 0]$

where w = white Gaussian driving noise.

The pilot sees the pitch tracking error (Block B), ϵ , which is $\theta - \theta_c$, and the rate of change of the error, $\dot{\epsilon}$. The model of this is

$$y(t) = H x(t)$$

with $y(t) = \text{col} [\epsilon \quad \dot{\epsilon}]$

and the output or observation matrix H is

$$\begin{bmatrix} 0 & 0 & 0 & 1 & -1 & 0 & 0 \\ 0 & 1 & 0 & 0 & 1/\tau_{re} & -k & 0 \end{bmatrix}$$

The time delays that are associated with the relaying and processing of visual images in the brain are modeled by lumping them into a single equivalent time delay (Block C). This delay, τ , is nominally 0.2 ± 0.05 seconds.

A Kalman estimator (Block D) works in series with a least mean square predictor (Block E) to yield a "best estimate" of the system state vector from a time delayed, noisy observation vector. The estimate is then weighted by a set of optimal feedback gains which are determined from the solution of an optimal control problem. This weighted estimate is used to produce a scalar command control input (Block F), $u_c(t)$, which is a longitudinal stick force.

The neuromotor dynamics are modeled by including a first order lag (Block G). This lag accounts for the pilot's inability or reticence to make rapid or excessive control inputs.

Controller remnant accounts for the inherent random errors associated with the preception of displayed variables and in the pilot control inputs.

Since the model is linear, these errors are consolidated as observation noises, v_y , and motor noise, v_u . These v_y and v_u are assumed independent, zero mean Gaussian noises with enough bandwidth to be considered white noise processes.

A detailed description of OPSACT is contained in References 3 and 5.

THE GROUND SIMULATOR (SAFTD)

The Simulator for Aircraft Flight Test and Development (SAFTD) is a real-time simulator laboratory used to support flight test programs at the Air Force Flight Test Center. The Test Pilot School's simulator model was developed from an existing F-16 model. Two digital computers arranged in a distributive processing network were used with a generic fixed base fighter cockpit with a moveable center stick as shown in Figure 2. The stick was connected to a McFadden artificial feel system which generated the stick dynamics. Simulator operation was controlled using an interactive alphanumeric cathode ray tube (CRT) display and data entry keyboard. Two synchronous processors used aerodynamic coefficient lookup tables while integrating the appropriate equations of motion. Thus the simulator modeled the aircraft for all values of airspeed and angle of attack (AOA). A series of test pulses identical to those used in the NT-33A were fed to a pitch steering bar displayed on a 25 inch raster scan TV. The 25 inch TV was partially covered to match the dimensions of the NT-33A HUD. The maximum time delay between the stick input and update of the TV display was three frames or 48 milliseconds. This is well below the pilot perceptual threshold of approximately 100 milliseconds (Ref. 18). A time history of eight key flight parameters were displayed on strip charts (Appendix D).

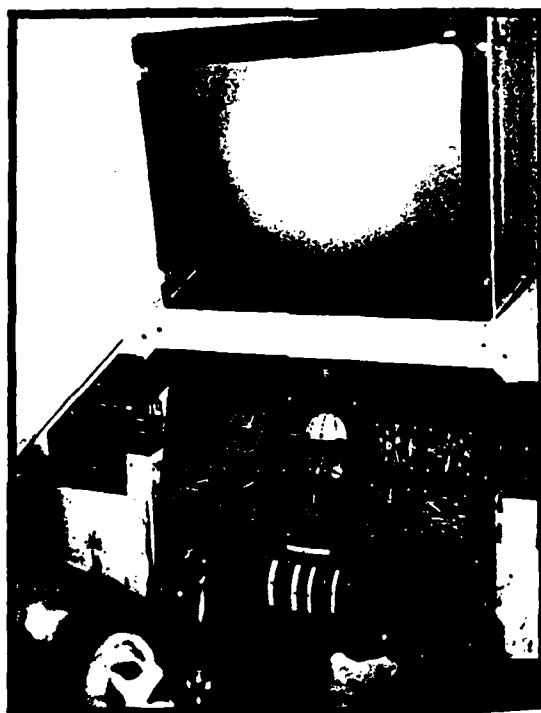


Figure 2. SAFTD Layout

THE NT-33A

The test aircraft, NT-33A Serial Number 51-4120, is a T-33A modified with a variable stability system by CALSPAN Corporation, Buffalo, New York. This variable stability system uses response feedback to modify the static and dynamic responses of the basic NT-33A by commanding control surface positions through full authority electrohydraulic servos. System components include a programmable analog computer, associated aircraft response sensors, control surface servos, and an electrohydraulic force-feel system. The rear seat pilot can vary the computer gains through controls located in the rear cockpit allowing

changes in airplane dynamics and control system characteristics in flight. Stick friction and breakout forces, stick deflection gradients, and stick force gradients were achieved through an electrohydraulic system. A schematic of the aircraft flight control system is presented in Figure 3.

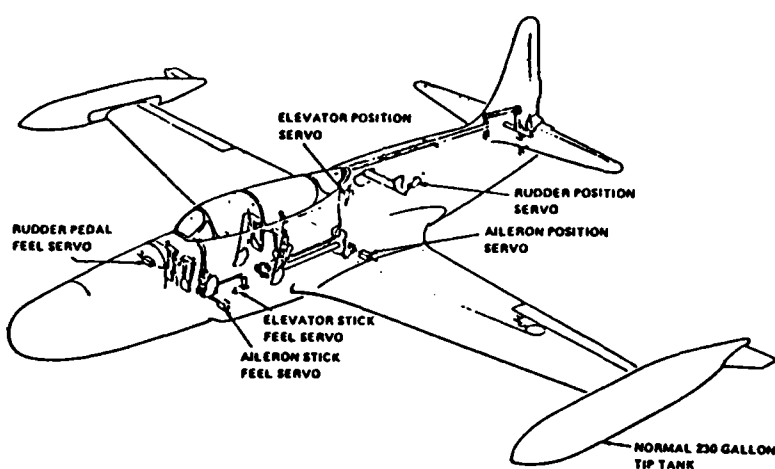


Figure 3. NT-33A Control System Layout

An on-board Leach MTR 3200 magnetic tape recording system was utilized to record aircraft flight conditions, flight control positions, and the tracking task parameters. A front cockpit AVQ-7 HUD displayed the tracking task. The system incorporated a general purpose digital computer and programmable display generator. This system has a processing time delay of 32 milliseconds. The pitch tracking task that appeared on the HUD was preprogrammed on magnetic tape. A 16mm HUD camera was used

to record a tracking time history. The layout of the HUD display is presented in Figure 4. The primary symbols used by the pilots were the pitch command bar, waterline marker, and horizon line.

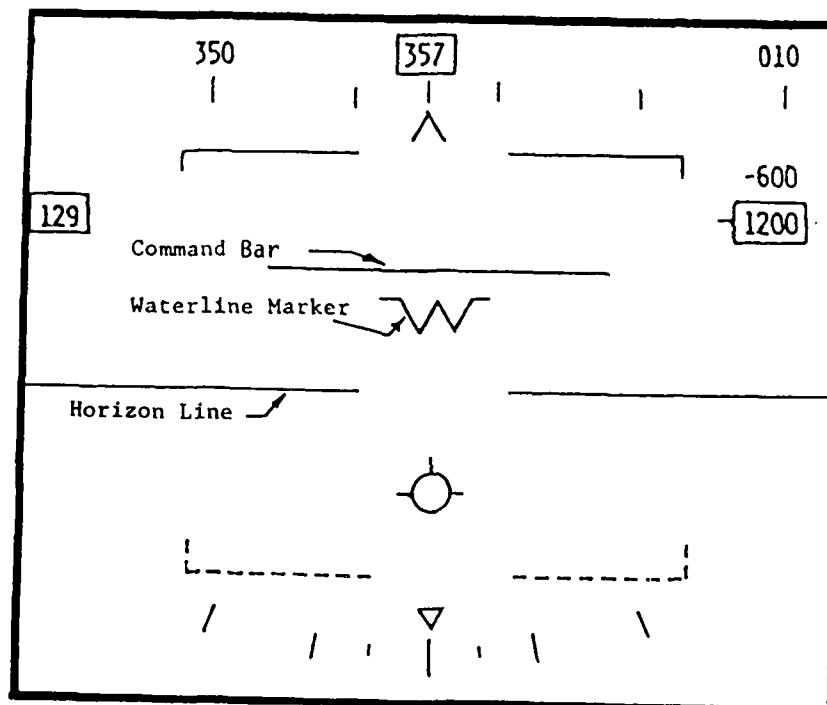


Figure 4. NT-33A HUD Format

IV. TEST METHODS AND CONDITIONS

OVERALL

An important element in the achievement of valid results was the matching of the dynamics of the various tests. The analytical model used the short period approximation to model the aircraft. Baseline testing was accomplished in the SAFTD and NT-33A to verify that the configuration of each matched the dynamics of the short period approximation. This was accomplished by analog matching open loop strip chart data with computer generated response plots. Figure 5 shows an example of the analog matching.

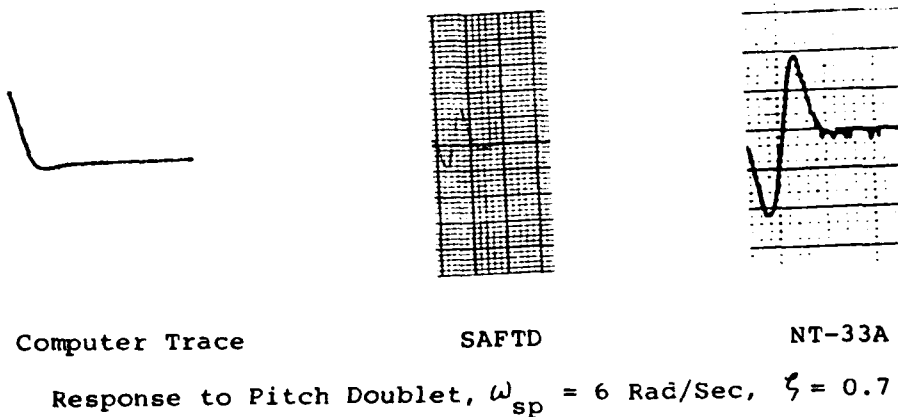


Figure 5. Sample Analog Match

Also, the breakout force, friction force, stick deflection gradient, stick force gradient, and the stick damping in the

simulators were compared and verified using force gauges and strip charts.

ANALYTICAL MODEL

Tests with the analytical model were conducted using aerodynamic derivatives from the NT-33A at the flight conditions as the inflight tests. These conditions corresponded to 300 KIAS at 13,000 feet MSL. This gives a normal load factor per angle of attack (n/α) of 29 g's per radian.

The short period natural frequency was varied by changing M_α with M_q being changed to maintain a constant 0.7 damping ratio. The elevator linkage gain was varied to maintain a constant stick force per g. This corresponded to the technique used in the SAFTD and the NT-33A.

SIMULATION

Data collection was accomplished by performing identical HUD pitch tracking tasks at the same flight condition in both the SAFTD and NT-33A simulators at specific short period natural frequencies. During each 90-second task, only one frequency was tested and tracking ability was then rated using the Cooper-Harper rating scale (Figure 6) and pilot comments.

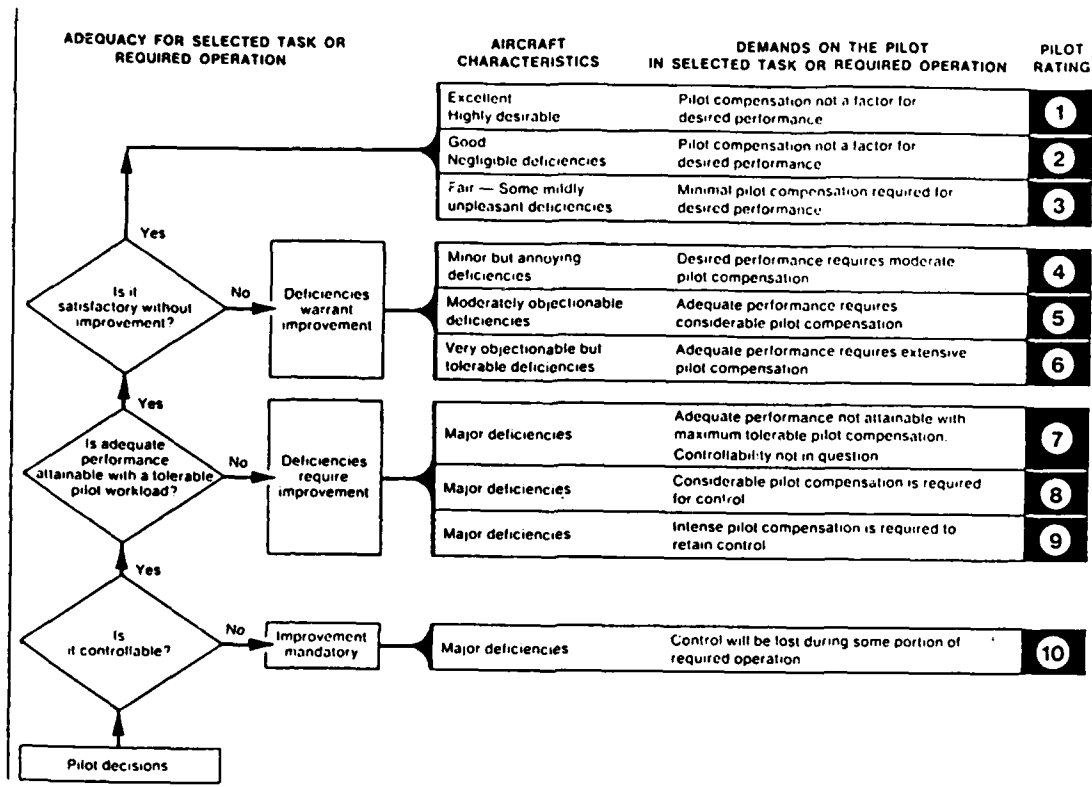


Figure 6. The Cooper-Harper Rating Scale

The pitch tracking tasks consisted of a 90-second series of steps and ramps which commanded up to ± 4 degrees from the initial level flight reference. The two different pulse trains, presented in Figure 7, were used to prevent pilots from memorizing the task. Both tasks were designed by CALSPAN to excite longitudinal dynamic modes that were important for successful air-to-air pitch tracking.

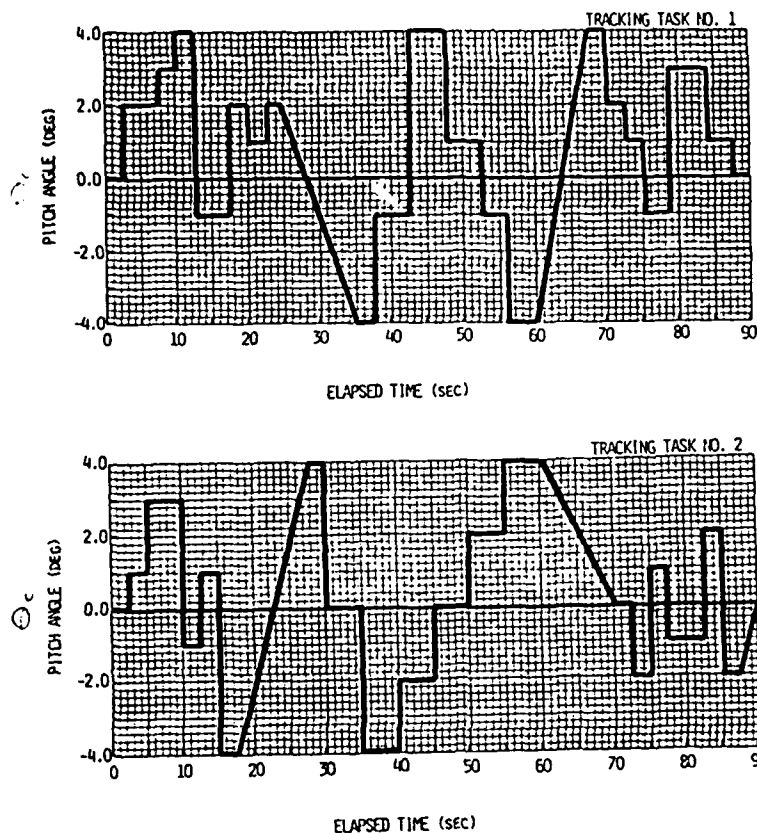


Figure 7. Preprogrammed Pitch Tracking Tasks

The pitch command bar was programmed to move in pitch according to the tracking sequence. The SAFTD task was displayed on a television screen while the NT-33A display was on a HUD combining glass. The project pilot attempted to track the moving command bar with the top of the "W" (waterline marker) in both simulators. The "W" was the same size in each simulator (5.3 milliradians). A moveable centerstick controller was used for

all tests in both simulators. Desired performance in both simulators was defined as acquisition of the moving pitch command bar with the top of the "W" within one second and then maintain pitch attitude within a "W" width for the duration of the test pulse. Adequate performance was acquisition within two seconds and then maintain pitch attitude within two "W" widths of the pitch command bar for the duration of the pulse.

The tracking task was repeated in each simulator varying only the short period natural frequency (ω_{sp}), which was varied in even increments from 2 to 12 radians per second in the SAFTD and from 2 to 10 radians per second in the NT-33A. Twelve radians per second could not be tested in the NT-33A because of structural mode excitation. At this frequency, an unstable AOA feedback to the elevator caused the variable stability system to exceed its design limits and automatically disengage. All other aircraft and control system variables were selected to provide good flying qualities. These optimized values were obtained from previous testing at an n/α of 29 g's per radian and are listed in Table 1 (Ref 12). The lateral directional characteristics were chosen to provide good control harmony.

The ratio of n/α was maintained at 29 g's per radian in both simulators by controlling altitude and airspeed at $13,000 \pm 1,000$ feet pressure altitude and 300 ± 15 KIAS respectively. The SAFTD was programmed to simulate the NT-33A at this flight condition.

Table 1 SELECTED DYNAMIC PARAMETERS (13,000 ft PA, 300 KIAS)	
<u>PARAMETER</u>	<u>VALUE</u>
Short period natural frequency	2 - 12 (rad/sec)
Short period damping	0.70
Normal g per alpha	29.00 (g/rad)
Dutch roll natural frequency	3.20 (rad/sec)
Dutch roll damping	0.35
Phi to beta ratio	2.00
Roll mode time constant	0.35 (sec)
Phugoid natural frequency	0.09 (rad/sec)
Phugoid damping	0.05
Longitudinal stick force per g	6.50 (lb/g)
Longitudinal stick force per inch	8.00 (lb/in)

Test points were selected to allow equal pilot exposure to each configuration. The value of ω_{sp} was unknown to the project pilot and the sequencing order of ω_{sp} 's tested was determined with a random number generator.

Limited testing was done in both simulators at a nominal 2g's by trimming for 1g level flight and then maintaining a nominal 60 degree banked turn throughout the tracking sequence.

The effects of outside visual cues on pilot ratings in the NT-33A were investigated by denying outside references. Temporary restricted vision was accomplished with a blue helmet visor and an amber NT-33A cockpit screen. This combination made the HUD clearly visible while making the scene beyond the HUD appear as darkness.

V. TEST RESULTS

Test results are presented in three parts: the OPSACT results, the SAFTD results, the NT-33A results, and a comparison of the three.

In the OPSACT model, the performance of the "pilot" got progressively better as the frequency was increased (Figure 8). The Q_y matrix is the relative weight of the tracking error and the rate of change of the tracking error.

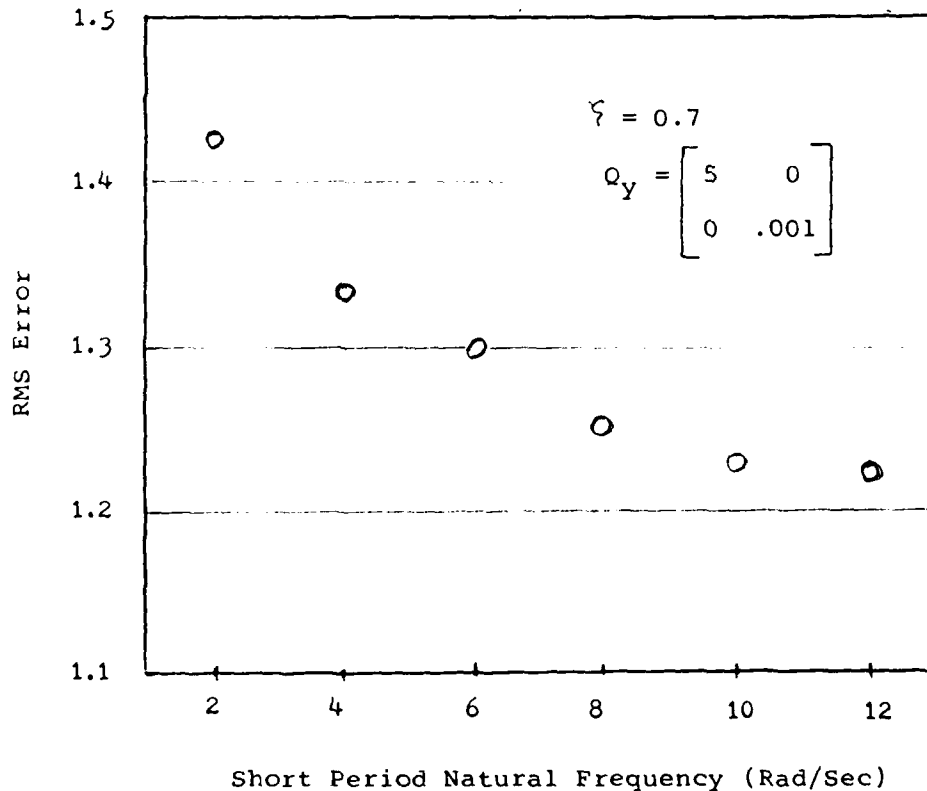


Figure 8. OPSACT "Pilot" Performance

In the SAFTD, pilots rated the low frequency dynamics as

1
poor and gave successively better ratings as short period frequency was increased. Representative pilot comments for tested short period frequencies are summarized in Table 2.

Table 2	
SAFTD GROUND SIMULATOR PILOT COMMENTS	
ω_{sp}	COMMENTS
2	Very slow, poor predictability, large overshoots, sluggish
4	Slightly slow, fairly predictable, moderate overshoots, large inputs
6	Quick, moderate predictability, small overshoots, lots of compensation
8	Quick, good predictability, small oscillations
10	Really quick, good predictability, small overshoot, hardly any PIO
12	Very quick, good predictability, small overshoot, pretty comfortable, no PIO problem

In addition to the pilots' word picture, graphs of Cooper-Harper ratings versus short period frequency are plotted in Figures 9A and 9B.

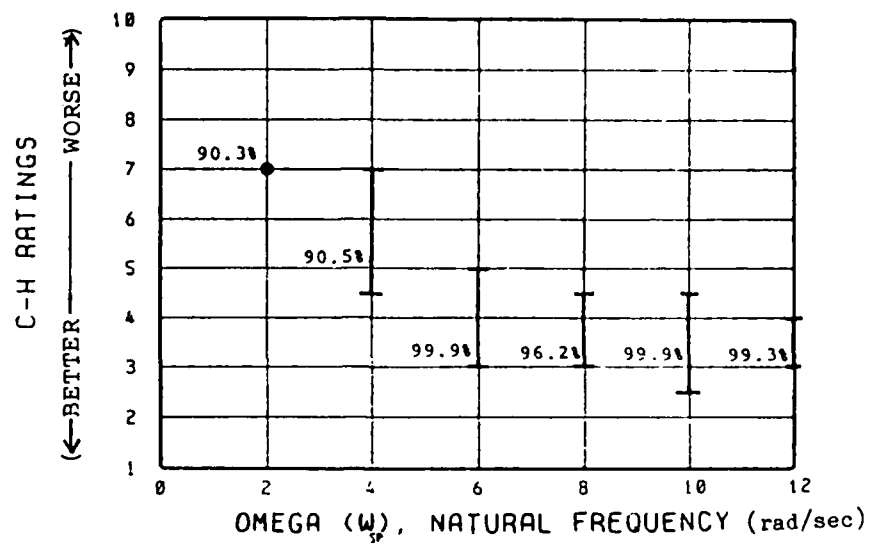


Figure 9A. Confidence Intervals for SAFTD at 1g

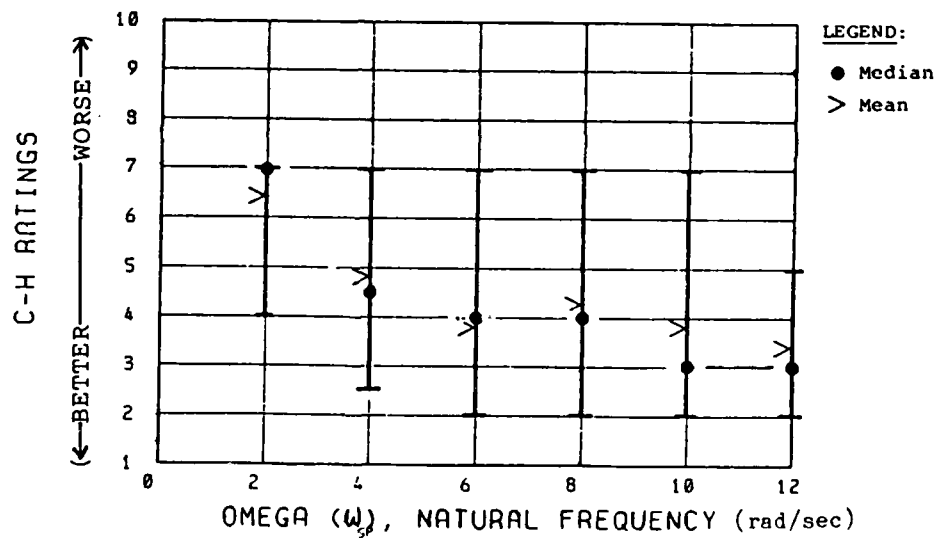


Figure 9B. Cooper-Harper Ranges for SAFTD at 1g

Figure 9A depicts statistical confidence intervals showing the predominant Cooper-Harper ratings for each tested frequency. It is not possible to plot exact statistical intervals such as 90

or 95 percent for each frequency as the Cooper-Harper ratings are discrete values. The confidence interval was determined by the formula:

$$\Pr(Y_r < \bar{Y} < Y_s) = \sum_{k=r}^{s-1} \binom{n}{k} (1/2)^n$$

This states that there is a fixed probability that \bar{Y} , the median Cooper Harper rating, will be between a minimum and maximum rating, Y_r and Y_s . If the ratings are rank ordered, r is the position of the first occurrence of the lower rating and s is the last occurrence of the higher rating. The relationship applies regardless of the distribution of the sample or the value of the median. Figure 9B shows the absolute range of Cooper-Harper ratings for each tested frequency as well as the median and mean value. Figures 10A and 10B present the 2g test results for the SAFTD in the same format.

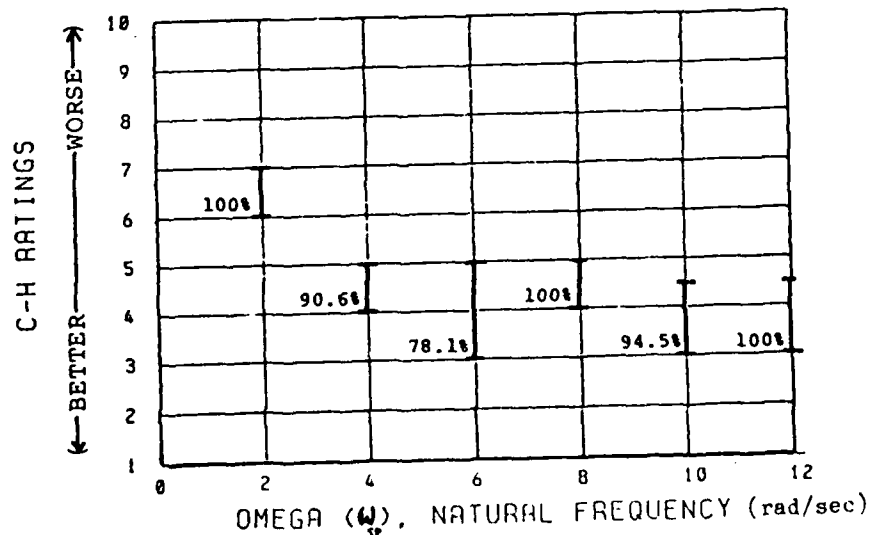


Figure 10A. Confidence Intervals for SAFTD at 2g

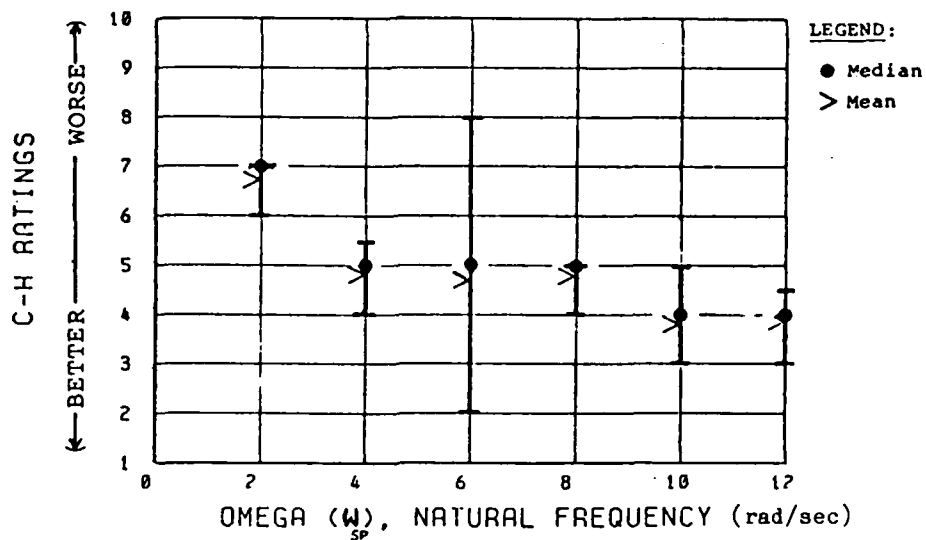


Figure 10B. Cooper-Harper Ranges for SAFTD at 2g

The SAFTD results show an increasing pilot preference for higher frequencies. SAFTD rating confidence intervals show a negligible difference between 1g and 2g testing while the mean ratings are worse at 2g. The preferred frequencies are the same at 1g and 2g, supporting the assumption that flying qualities that get the better ratings at low load factors will get the better ratings at higher load factors.

Figure 11 shows how the SAFTD pilot performance improved as the short period natural frequency was increased.

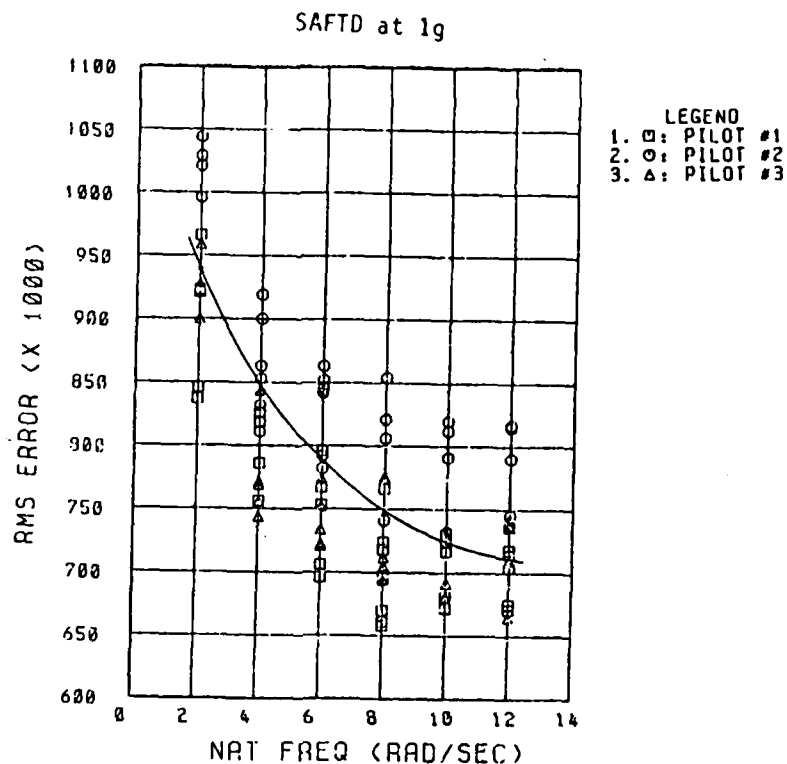


Figure 11. SAFTD Tracking Error Versus Frequency

The NT-33A in-flight results follow other flight test results. The pilots disliked the very low frequencies, liked the predictable medium response area, and disliked the uncomfortably abrupt high frequencies. As in the SAFTD, there was no significant difference in pilot opinion and Cooper-Harper ratings between 1g and 2g tests, with the numerical differences primarily attributed to sample size. Here, there was not the difference in mean ratings that occurred in the SAFTD. Testing with no outside visual references had a negligible effect on ratings. The pilots focused on the HUD during the tracking task in either situation,

eliminating background visual cues as a major factor in pilot ratings.

The NT-33A 1g results are presented in Table 3 and Figures 12A and 12B. Table 3 summarizes the pilot opinions concerning response, predictability, PIO tendency, and work load. Figure 12A presents the statistical confidence interval on the median Cooper-Harper rating and Figure 12B shows the absolute range of ratings given to each tested frequency as well as the sample median and mathematical mean.

Table 3	
NT-33A PILOT COMMENTS	
ω_{sp}	COMMENTS
2	Sluggish, poor predictability, large overshoots, a lot of compensation
4	Good response, good predictability, comfortable, minimal compensation
6	Good response, not abrupt, good predictability, feels good
8	Quick response, abrupt, less predictable, a little uncomfortable, some PIO tendency
10	Jerky, too jumpy, increased work load, large compensation, uncomfortable, bobbles, PIO prone

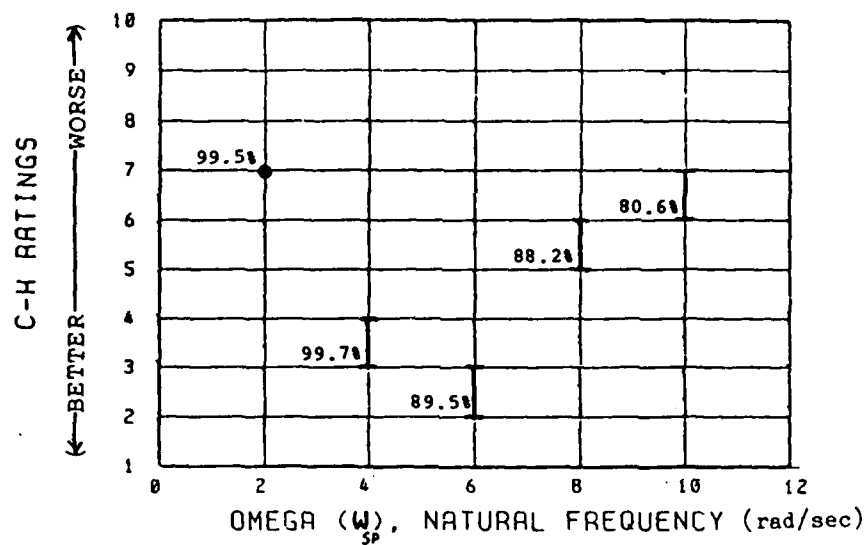


Figure 12A. Confidence Intervals for NT-33A at 1g

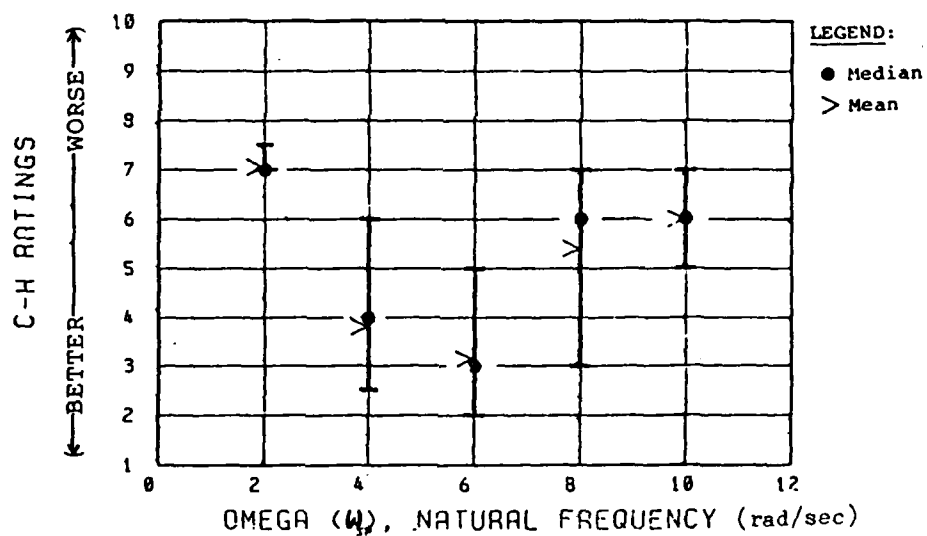


Figure 12B. Cooper-Harper Ranges for NT-33A at 1g

The 2g test results for the NT-33A are presented in Figures 13A and 13B. Like the SAFTD results, there was a negligible difference between 1g and 2g ratings.

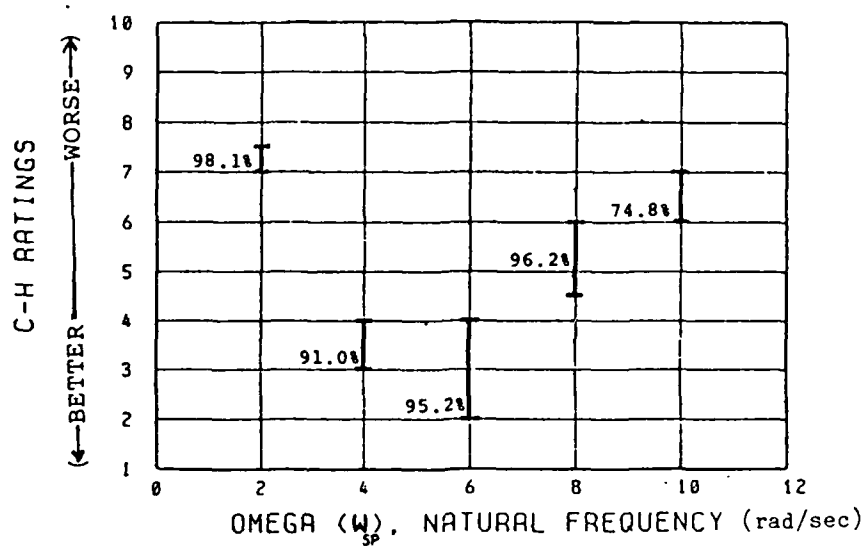


Figure 13A. Confidence Intervals for NT-33A at 2g

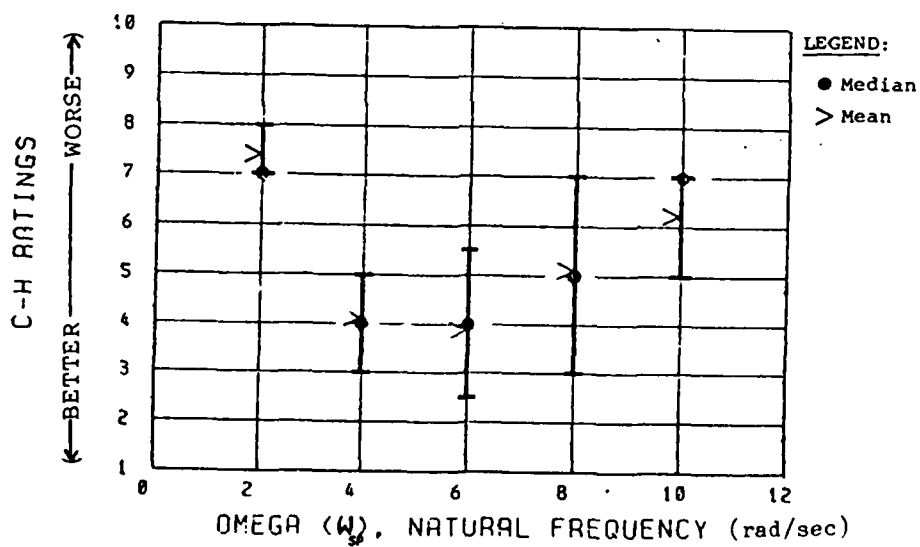


Figure 13B. Cooper-Harper Ranges for NT-33A at 2g

Figure 14 is a plot of pilot performance versus short period natural frequency in the NT-33A. RMS error was not available because of format incompatibilities between the NT-33A data

acquisition system and the Test Pilot School computer. Error counts were manually produced from strip charts by determining the area under the curve which was the error between the pitch command and the actual pitch angle. This provides the same relative indication of performance versus frequency as RMS error.

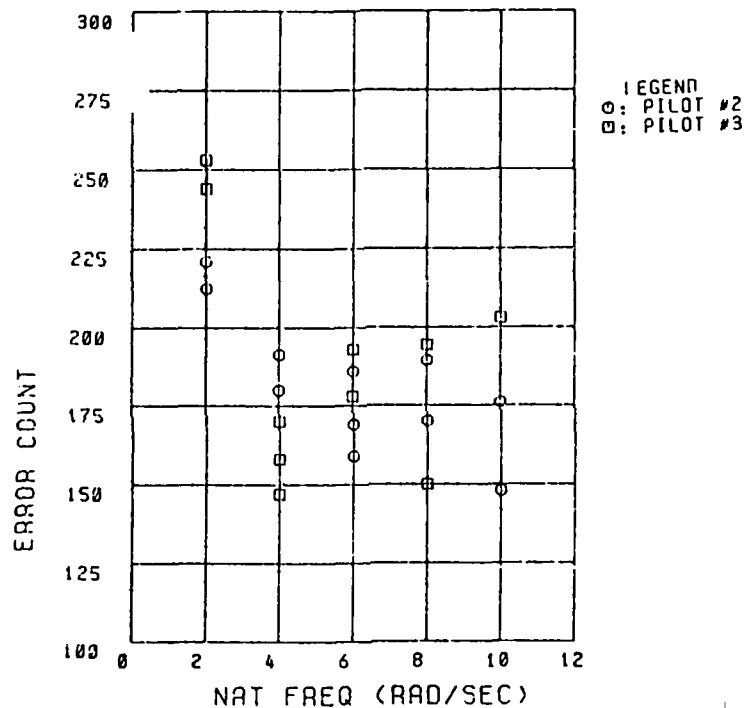


Figure 14. NT-33A Error Count Versus Frequency

The project objective was to compare the OPSACT results, the SAFTD results, and the NT-33 in-flight results and see if ground tests could forecast airborne opinions. Tight experimental control was maintained so that any correlation between the ground and in-flight simulators was not biased or circumstantial.

The OPSACT and SAFTD RMS performance improved as the short period natural frequency was increased. The NT-33A performance was not well defined at high frequency where it tended to be worse.

The Cooper-Harper ratings summary in Figure 15 shows that the ground simulator results correlate positively with NT-33 results at 1g for low and medium short period frequencies (2, 4, and 6 radians per second). At higher frequencies (8 and 10 radians per second), the ground simulator ratings and performance continued to improve while in-flight ratings worsened.

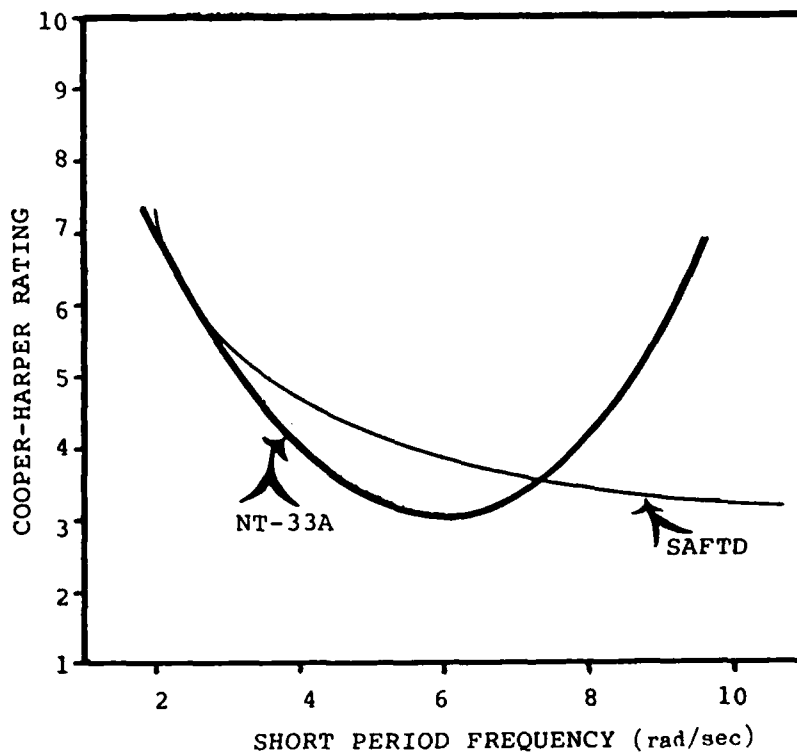


Figure 15. Cooper-Harper Trends at 1g

VI. ANALYSIS

This section offers an explanation for the considerable difference at the higher frequencies between the ground-based studies and the airborne simulation despite each case having identical equations of motion and control dynamics.

Performance error or root mean square (RMS) error was measured as the difference between the preprogrammed pitch angle commanded and the actual pitch angle which the pilot controlled. A small RMS error figure signifies that the command bar was quickly and accurately acquired while a large number implies slow response and/or tracking difficulty. Charting performance was not a measure of the "best pilot", but rather provided insight as to why a pilot preferred certain frequencies and could indicate whether a pilot performed consistently in different runs testing the same frequency.

The OPSACT allows weighting of the pilot's control inputs due to tracking error and rate of change of tracking error. This study found that any weight greater than one percent on the rate cause the pilot to prefer the lower frequency of two radians per second. If the weighting was such that that the OPSACT performance at two radians per second paralleled the SAFTD and NT-33A, the OPSACT results followed the SAFTD.

Since the SAFTD could not provide "feel" cues, the performance criterion dominated pilot opinion at all frequencies during the ground test phase. In the SAFTD, Cooper-Harper ratings were directly proportional to RMS performance which improved with successively higher frequency. Figure 16 depicts

the pilots' performance versus the Cooper-Harper ratings assigned. This evidences linear behavior with an 80 percent correlation. Figure 11 depicts the RMS error versus short period frequency as a second order behavior. The graph indicates that performance improves as frequency increases. A second order fit had a 74 percent statistical correlation. This suggests the hypothesis that performance is the primary variable affecting pilot ratings in the ground simulator. Unlike the NT-33A, there are no uncomfortable motion cues at the higher frequencies. Therefore, Cooper-Harper ratings in the SAFTD tend to improve as frequency increases.

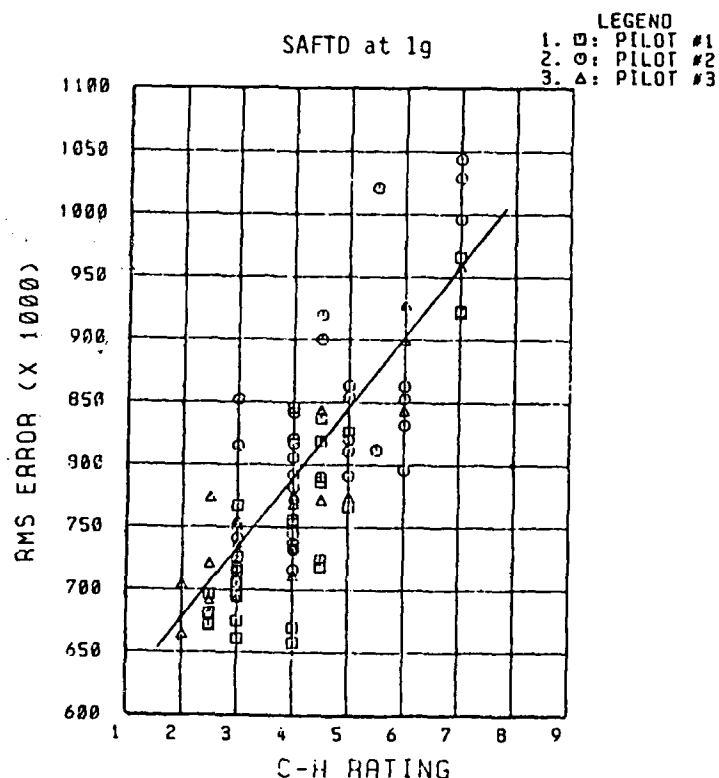


Figure 16. SAFTD Tracking Error Versus Cooper-Harper

In the NT-33A tests, the pilot opinions were driven by three factors: tracking accuracy (performance), comfort, and pilot compensation. These factors changed in relative importance as the frequency changed. The pilots' comments indicated that performance or ability to accurately track the pitch command bar was a primary variable in determining the flying quality ratings for low and medium frequencies. At higher frequencies, however, "jerkiness" or uncomfortably abrupt motions forced the pilot to make large compensations and drove the ratings to worse levels. Plots of performance versus Cooper-Harper ratings and short period frequency in the NT-33A appear in Figures 17 and 14.

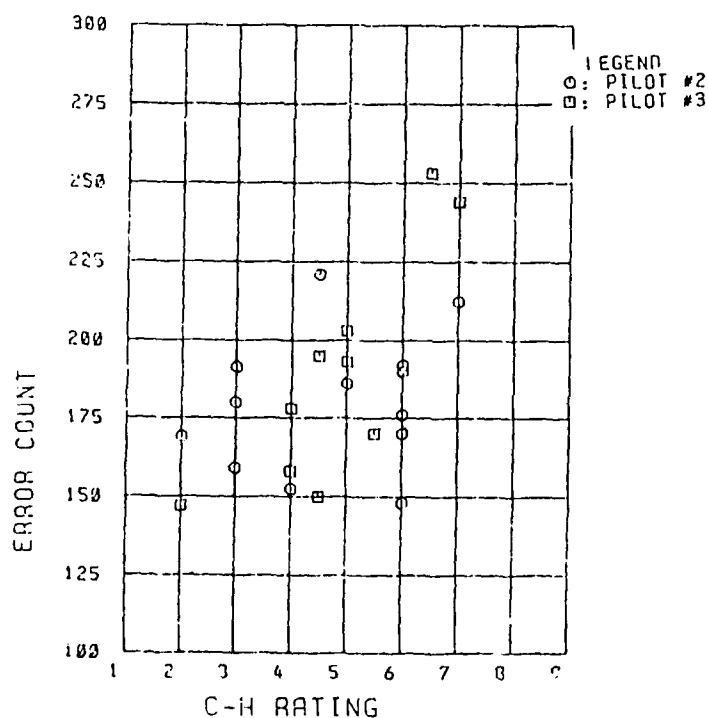


Figure 17. NT-33A Error Count Versus Cooper-Harper

Unlike the SAFTD results, where a direct linear relationship between Cooper-Harper ratings and performance was established, NT-33A results did not correlate well as other factors affected the ratings. One of these factors was g onset rate, which was rapid enough at high frequencies to cause problems in maintaining steady stick inputs, and in some cases, made focusing on the HUD difficult. Despite the abrupt motion cues, one pilot showed the same increase in performance with higher frequency that the ground simulator results suggested. Figure 18 presents this

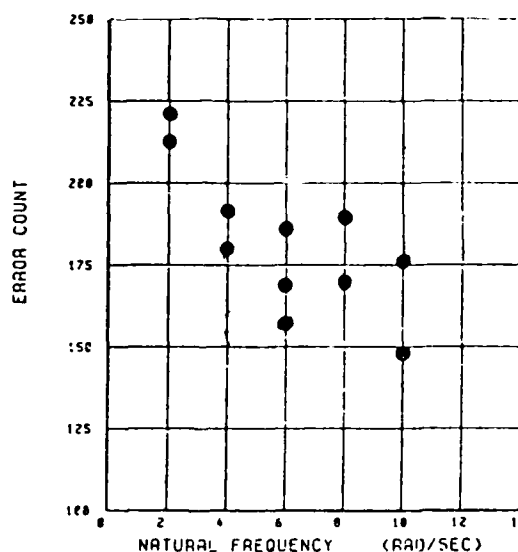


Figure 18. Pilot #2 Error Count Versus Frequency

Hand reduced tracking error data indicated two different behavior patterns at 10 radians per second, the highest tested frequency in the NT-33A. Either the pilot aggressively tracked the commanded task and ignored the very abrupt motions or the aggressive tracking was tempered to maintain a comfort level.

The resulting error counts reflect this different level of aggressiveness. Therefore, it is possible that pilot performance could be improved with frequency if the effects of the other factors could be mitigated. This "other factor" hypothesis is amply evidenced by the low correlation between RMS versus Cooper-Harper plot in Figure 17.

The Cooper-Harper rating system defines major thresholds based on a combination of performance, work load, and pilot compensation. Thus, performance is not an overriding factor in pilot opinion. Further research on analytical modeling and ground simulation needs to incorporate items such as pilot workload and pilot compensation to keep the g onset rate comfortable into the prediction.

There was no significant difference between 1g and 2g results during project tests. These results are consistent with the analysis shown in Appendix A. Therefore, the Military Specification contention that 1g predictions characterize higher load factors cannot be refuted. Since the project was primarily aimed at a 1g comparison of simulators, 2g was only tested for a statistically significant sample size. The loaded testing should be continued at higher load factors and in different aircraft. Testing in the NT-33A at the 300 KIAS, 13,000 feet MSL flight condition at no more than 2g allowed the aircraft to remain in the linear portion of the lift curve. Testing at higher g in the non-linear portion of the curve or testing aircraft with different lift slopes may produce a different conclusion than this limited evaluation.

VII. CONCLUSIONS AND RECOMMENDATIONS

The computer pilot model and ground based simulator modeled the airborne pilot performance trends well. However, performance is not the only criteria that a pilot uses to rate the flying qualities of an aircraft. The pilot considers other factors such as g onset rate when he forms his opinion. Therefore, any model which uses performance as a dominate criteria will not generally be successful. The model can, however, be used in parallel with the airborne simulator or test article to reduce airborne test.

Further work with the weighting matrix in the analytical model might produce a combination that would more closely parallel the airborne tests. One method of finding this weighting would be to generate a time history of the pilot model. By comparing the time history to a time history of the simulators, the behavior of the model could be adjusted to be similar to actual pilots.

The assumption that the preferred 1g flying qualities will also be preferred at 2g and higher cannot be refuted by this study, and, at least for longitudinal dynamics, is supported by the analysis in Appendix A. More testing at higher load factors is recommended.

For this type of task, which has the high fidelity of a HUD, denying outside visual references did not have a significant effect on pilot performance or ratings. This means that the difference between the SAFTD and NT-33A were dominated by the

effects of motion. Therefore, using a HUD type task with high fidelity reduces the number of variables between the studies.

Bibliography

1. Harvey, Thomas R. Application of an Optimal Control Pilot Model to Air-to-Air Combat. AFIT Thesis GA/MA/74M-1. Wright-Patterson Air Force Base, Ohio: Air Force Institute of Technology, March, 1974.
2. Kleiman, D. L., S. Baron and W. H. Levison. "An Optimal Control Model of Human Response, Part 1," Automatica, 6: 357-363 (May 1970).
3. Enright, Randall. Predicting Pilot Opinion Rating of Flying Qualities of Highly Control-Augmented Aircraft Using Optimal Pilot Model. AFIT Thesis GAE/AA/80D-3. Wright-Patterson Air Force Base, Ohio: Air Force Institute of Technology, December 1980.
4. Maybeck, Peter S. Stochastic Models, Estimation and Control, Vol. 1, Academic Press, 111 Fifth Ave., New York, New York; 1979.
5. Mullen, Patrick A. Prediction of Short Term Tracking Tasks Using an Optimal Pilot Model. AFIT Thesis GAE/AA/81D-21. Wright-Patterson Air Force Base, Ohio: Air Force Institute of Technology, March 1982.
6. Heffley, R.K. and W.F. Jewell. Aircraft Handling Qualities Data, NASA CR-2144, 1972.
7. Larimer, S.J. An Interactive Computer-Aided Design Program for Digital and Continuous System Analysis and Synthesis (TOTAL), AFIT Thesis GE/GGC/EE/78-2. Wright-Patterson Air Force Base, Ohio: Air Force Institute of Technology, 1978.
8. Etkin, Bernard, Dynamics of Atmospheric Flight, New York: John Wiley and Sons, Inc., 1972.
9. Rudolph, R.J. Stability Analysis of an F-4C Aircraft in Steady Level Turning Flight, AFIT Thesis GAE/MC/74-9. Wright-Patterson Air Force Base, Ohio: Air Force Institute of Technology, 1978.
10. Military Specification - Flying Qualities of Piloted Airplanes, MIL-F-8785C, 8 November 1980.
11. Moorhouse, D.J., et. al., Background Information and User Guide for MIL-F-8785C, Technical Report AFWAL-TR-81-3109, July 1982.
12. Monagan, Stephen J., et. al., Head-Up-Display Flight Tests, Symposium Proceedings of the Twenty-Fourth SETP Aerospace Symposium, 27 September 1980.

13. Flight Demonstrations with the USAF/CALSPAN NT-33A Variable Stability Aircraft for the USAF Test Pilot School, CALSPAN Corporation, March 1983.
14. AFFDL-TR-70-71, System Description and Performance Data for the USAF/CAL Variable Stability T-33 Airplane, Aug 1970.
15. USAF Series T-33A Aircraft, T.O. 1T-33A-1, 31 January 1973, Change 7, 30 August 1976.
16. Engel, Richard L., Major, et al., Advanced Flight Control Instruction at the Air Force Test Pilot School, 1982 Report of the 26th SETP Symposium Proceedings, 25 September 1982.
17. USAF TPS Report 82A-4, Letter Report NT-33A, Limited Evaluation of Longitudinal Flying Qualities of a Centerstick Controlled Aircraft with Various Stick Force and Deflection Gradients and Longitudinal Dynamics, 30 November 1982.
18. Engel, Richard L. Unpublished class notes from Test Pilot School Simulation Course, December 1982.

APPENDIX A
ANALYSIS OF THE EFFECTS OF LOAD FACTOR
ON FREQUENCY RESPONSE OF THE NT-33A

INTRODUCTION

When doing aircraft design studies, the decoupling of the longitudinal and lateral axes makes the problem tractable. However, many practical flight conditions require banked, turning flight which causes coupling between the axes of motion. By investigating the frequency response of a NT-33A in several steady, level turns, this appendix determines the validity of using decoupled equations to study flight conditions where the axes are coupled.

Eight interdependent equations of motion are required to model three dimensional flight. This model is based on three force equations, three moment equations, and two kinematic relationships which were all linearized about an equilibrium condition.

The data for this analysis were extracted from NASA CR-2144 (Ref. 6). The NASA data are listed in two formats, graphs and tabular charts. The graphical data were non-dimensional and in stability axes. The tabular data were dimensional and in body axes. To accomplish the analysis, all data were transformed into dimensional form and set in the stability axis system appropriate for straight and level (1g) flight. The change in angle of attack required to maintain each load factor was then determined. Finally, the data were transformed to the sets of stability axes corresponding to each load factor and the frequency response for the appropriate control input was determined using TOTAL, a computer program for analyzing linear dynamical systems (Ref. 7).

VARIABLES OF INTEREST

The important variables in a handling qualities study are those that are easily perceived and controlled by the pilot. Rate variables such as q , the pitching rate, and p , the rolling rate, are not affected by the orientation of the coordinate system. Thus, q and p were chosen as the variables of interest. Theta was chosen so it could be compared to q .

The frequency range of 10^{-3} to 10^2 radians per second was chosen as this encompassed the response characteristics of a typical pilot.

EQUATIONS OF MOTION

Assuming a flat, nonrotating earth, a rigid, symmetric vehicle, and a stationary atmosphere makes the following equations applicable to the problem.

Force Equations: $X - mg \sin \theta = m (\dot{u} + qw - rv)$

$$Y + mg \cos \theta \sin \phi = m (\dot{v} + ru - pw)$$

$$Z + mg \cos \theta \cos \phi = m (\dot{w} + pv - qu)$$

Moment Equations: $L = I_x \dot{p} - I_{zx} (\dot{r} + pq) - (I_y - I_z) qr$

$$M = I_y \dot{q} - I_{zx} (r^2 - p^2) - (I_z - I_x) rp$$

$$N = I_z \dot{r} - I_{zx} (\dot{p} - qr) - (I_x - I_y) pq$$

Kinematic Relations: $\dot{\phi} = p + q \sin \phi \tan \theta + r \cos \phi \tan \theta$

$$\dot{\theta} = q \cos \phi - r \sin \phi$$

$$\dot{\psi} = (q \cos \phi + r \sin \phi) \sec \theta$$

Note: The $\dot{\psi}$ equation is independent of the other equations so it is not required for this study.

These equations were linearized about a trim condition representing a steady, level turn. The following substitutions were made:

1. $\Theta_e = 0$ by definition of a steady, level turn.
2. $\cos \beta_e \cong 1$ and $\sin \beta_e \cong 0$ as the largest β_e for the load factors investigated was $\beta_e = 0.00253$ radians.
3. $p_e = 0$ when $\Theta_e = 0$.

The change in angle of attack for each flight condition was determined by (Ref. 8:426):

$$\begin{bmatrix} C_{m_{\alpha}} & C_{m_{\dot{\alpha}}} \\ C_{L_{\alpha}} & C_{L_{\dot{\alpha}}} \end{bmatrix} \begin{bmatrix} \Delta \alpha_e \\ \Delta \dot{\alpha}_e \end{bmatrix} = - \begin{bmatrix} C_{m_q} \\ C_{L_q} \end{bmatrix} \omega c \sin \phi / (2 V) + \begin{bmatrix} 0 \\ (n - 1) C_W \end{bmatrix}$$

The change in angle of sideslip was checked using:

$$\begin{bmatrix} C_{Y_{\beta}} & C_{Y_{\dot{\beta}}} & C_{Y_{\delta_a}} \\ C_{L_{\beta}} & C_{L_{\dot{\beta}}} & C_{L_{\delta_a}} \\ C_{N_{\beta}} & C_{N_{\dot{\beta}}} & C_{N_{\delta_a}} \end{bmatrix} \begin{bmatrix} \beta \\ \dot{\beta} \\ \delta_a \end{bmatrix} = \begin{bmatrix} C_{Y_p} & C_{Y_r} \\ C_{L_p} & C_{L_r} \\ C_{N_p} & C_{N_r} \end{bmatrix} \begin{bmatrix} - \cos \phi_e \end{bmatrix} \omega b / (2 V_e)$$

The equilibrium values of p , q , and r are (Ref 3:424):

$$\begin{bmatrix} p \\ q \\ r \end{bmatrix} = \begin{bmatrix} 0 \\ \sin \phi_e \\ \cos \phi_e \end{bmatrix} \omega$$

The computer programs which solve these sets of equations are listed in Appendix B.

The resulting equations are:

$$[m] \frac{\dot{\Delta V}}{\Delta V} = [T_v \cos \alpha_{te} - D_v] \Delta V + [m R_e V_e] \Delta \beta \\ + [-T_e \sin \alpha_{te} + L_e - D_\alpha - m q_e V_e] \Delta \alpha \\ + [-mg] \Delta \theta + [D_{\delta e}] \Delta \delta_e$$

$$[m V_e] \frac{\dot{\Delta \beta}}{\Delta \beta} = [m r_e] \Delta V + [Y_\beta] \Delta \beta + [Y_p] \Delta P \\ + [-m V_e + Y_r] \Delta r + [mg \cos \phi_e] \Delta \phi + [Y_\delta] \Delta \delta$$

$$[m V_e + L_\alpha] \frac{\dot{\Delta \alpha}}{\Delta \alpha} = [-m q_e - T_v \sin \alpha_{te} - L_v] \Delta V \\ + [-T_e \cos \alpha_{te} - D_e - L_\alpha] \Delta \alpha + [m V_e - L_q] \Delta q \\ + [-mg \sin \phi_e] \Delta \phi + [L_{\delta e}] \Delta \delta_e$$

$$[I_x] \frac{\dot{\Delta \dot{P}}}{\Delta \dot{P}} + [-I_{zx}] \frac{\dot{\Delta \dot{r}}}{\Delta \dot{r}} = [L_\beta] \Delta \beta + [L_p + I_{zx} q_e] \Delta P \\ + [(I_y - I_z) r_e] \Delta q \\ + [L_r + (I_{yy} - I_{zz}) q_e] \Delta r + [L_\alpha] \Delta \delta$$

$$[I_y] \frac{\dot{\Delta \dot{q}}}{\Delta \dot{q}} + [-M_\alpha] \frac{\dot{\Delta \dot{\alpha}}}{\Delta \dot{\alpha}} = [M_v] \Delta V + [M_\alpha] \Delta \alpha \\ + [(I_z - I_x) r_e] \Delta P + [M_q] \Delta q \\ + [2 I_{zx} r_e] \Delta r + [M_{\delta e}] \Delta \delta_e$$

$$[I_z] \frac{\dot{\Delta \dot{r}}}{\Delta \dot{r}} + [-I_{zx}] \frac{\dot{\Delta \dot{P}}}{\Delta \dot{P}} = [N_\beta] \Delta \beta + [N_p + (I_x - I_y) q_e] \Delta P \\ + [-I_{zx} r_e] \Delta q + [N_r - I_{zx} q_e] \Delta r \\ + [N_\delta] \Delta \delta$$

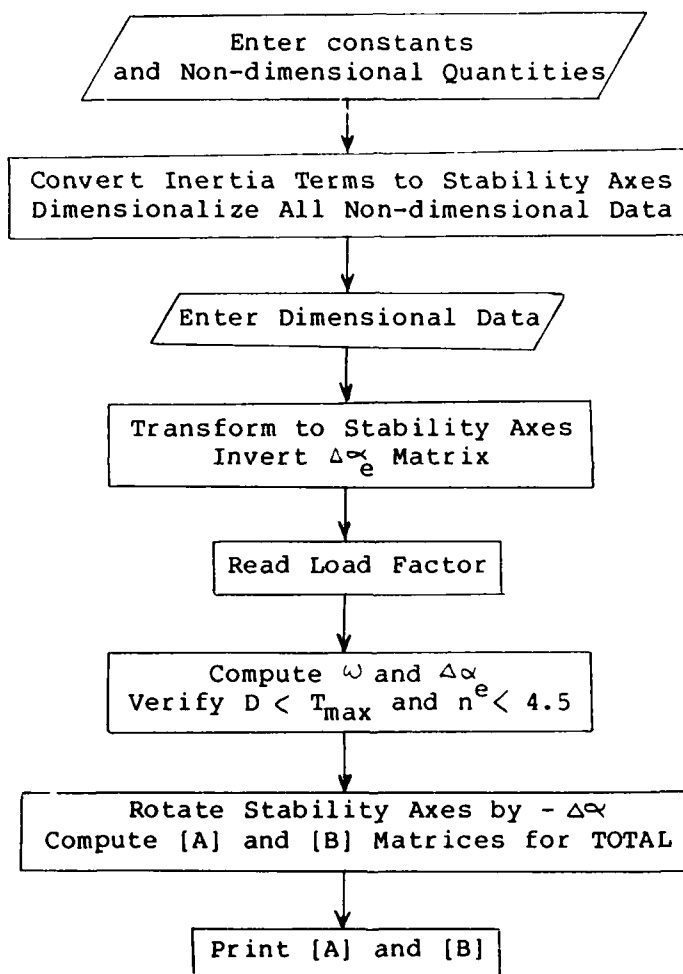
$$\frac{\dot{\Delta \phi}}{\Delta \phi} = \Delta P + [q_e \sin \phi_e + r_e \cos \phi_e] \Delta \theta$$

$$\frac{\dot{\Delta \theta}}{\Delta \theta} = [\cos \phi_e] \Delta q + [-\sin \phi_e] \Delta r + [-q_e \sin \phi_e - r_e \cos \phi_e] \Delta \phi$$

DATA MANIPULATION

The following algorithm was computerized for the transfer of data from its raw form to that required by TOTAL:

FLOW CHART FOR DATA PROCESSING



The computer code is listed in Appendix B.

FREQUENCY RESPONSE

The program TOTAL takes equations of the form

$$\dot{\underline{x}} = [A] \underline{x} + [B] \underline{u}$$

$$\dot{\underline{y}} = [C] \underline{x}$$

and generates the transfer functions between user designated inputs and outputs. From these transfer functions, the program is able to generate Bode plots.

RESULTS

The Bode plots in Appendix B show the frequency response of the NT-33A.

In each case, the Θ/ξ_e response is of the same general form with a spike at the damped frequency of the phugoid. This occurs at higher frequency as the load factor is increased (Figure B1-B5). The corner frequency of the Bode plot is the short period frequency of 3.0 radians per second. The response is reduced due to the effects of the bank angle. That is, as the aircraft increases its equilibrium bank angle, the aircraft's pitch rate response produces less pitch attitude change. This can be seen by examining the $\dot{\Delta\Theta}$ equation for increasing ϕ_e . As the aircraft approaches 90° of bank, pitching motion produces no change in pitch attitude.

The η/ξ_e is generally unchanged for differing values of load factor (Figure B6-B10). It contains a spike at the same frequency as the spike in the Θ/ξ_e transfer function. The short period frequency is also 3.0 radians per second.

The ζ/ξ_e response is not altered significantly by load factor. The response using the uncoupled lateral equations and the coupled equations with zero bank angle is the same (Figure B11-B12). At load factors greater than one, a spike at the phugoid frequency occurs and the very low frequency response does not go to zero as rapidly (Figure B12-B14). These two results occur because of coupling between axes.

CONCLUSIONS

During steady, level turns, the frequency response between NT-33A aircraft dynamics and control inputs is not significantly altered when the load factor is varied. In the range of normal input frequencies, these variables are especially consistent.

Thus, designs optimized for a flight condition such as straight and level will retain the same response characteristics in a steady, level turn, which is a coupled flight condition.

APPENDIX B
COMPUTER LISTINGS AND
BODE PLOTS

```

10 REM  THESIS AID:  FINDS THE 'A' AND 'B' MATRICES FOR THE
20 REM  BASIC COUPLED AIRCRAFT EQUATIONS.
30 REM
40 REM  BY JIM PAYNE
50 REM  MARCH/APRIL 1982
60 REM
70 DIM A(8,8),E(2,2),F(2),H(2),Q(2),U(8),Z(2,2)
80 DEF FN H(I) = INT (I * 1000000 + .5) / 1000000
90 REM
100 REM  ENTER CONSTANTS
110 REM
120 REM  NT-33A  MACH = .4  H = SEA LEVEL
130 REM
140 DR = 57.29578
150 G = 32.1725
160 B = 37.54
170 C = 6.72
180 S = 234.8
190 WT = 13700
200 M = WT / G
210 IX = 23800
220 IY = 21100
230 IZ = 43800
240 ZX = 480
250 REM
260 REM  ENTER VARIABLE QUANTITIES
270 READ RO,V,DO,IM,AO,CL,CD
280 DATA .002378,447,.0185,5200,.9,.24,.02
290 AO = AO / DR
300 REM
310 REM  ENTER NON-DIMENSIONAL DATA
320 REM
330 READ DA,YP,YR,LA,LQ,LE,LV,DV
340 DATA .133,0,0,5.9,0,.345,.000183,0
350 CW = CL
360 KK = (CD - DO) / (CL * CL)
370 D3 = DA
380 READ LB,LP,LR,NB,NF,NR
390 DATA -.09,-.58,.095,.057,-.008,-.148
400 READ MD,MQ,ME,MA,MV
410 DATA -4.3,-10.33,-.90,-.51,0
420 Q(1) = MQ;Q(2) = LQ
430 Z(1,1) = MA;Z(1,2) = ME
440 Z(2,1) = LA;Z(2,2) = LE
450 REM
460 REM  CONVERT INERTIA TO STABILITY AXIS
470 REM
480 CA = COS ( - AO)
490 SA = SIN ( - AO)
500 I1 = IX * CA * CA + 2 * ZX * CA * SA + IZ * SA * SA
)

```

```

510 I3 = IZ * CA * CA - 2 * ZX * CA * SA + IX * SA * SA
520 ZX = (IZ - IX) * CA * SA + ZX * (CA * CA - SA * SA)
530 IX = I1; IZ = I3
540 REM
550 REM   CONVERT TO DIMENSIONAL DATA
560 TV = 0
570 QQ = RU * V * V * S / 2
580 DV = QQ * DV
590 DA = QQ * DA
600 LV = QQ * LV
610 LB = QQ * B * LB
620 LA = QQ * LA
630 LP = QQ * B * LP
640 LQ = QQ * LQ
650 LR = QQ * B * LR
660 LE = QQ * LE
670 MV = QQ * C * MV
680 MA = QQ * C * MA
690 MD = QQ * C * MD
700 MQ = QQ * C * MQ
710 ME = QQ * C * ME
720 NB = QQ * B * NB
730 NP = QQ * B * NP
740 NR = QQ * B * NR
750 YP = QQ * YP
760 YR = QQ * YR
770 REM
780 REM   ENTER DIMENSIONAL DATA
790 REM
800 READ XU,YB,ZU,XE,XW,ZW,ZE
810 DATA -.0104,-.181 ,-.128,.620,.0562,-1.73,-44.4
820 REM
830 REM   TRANSFORM BODY TO STABILITY AXIS
840 REM
850 DV = - (XU * CA * CA - (XW + ZU) * CA * SA + ZW * SA * SA)
860 D3 = - (XW * CA * CA + (XU - ZW) * CA * SA - ZU * SA * SA)
870 LV = - (ZU * CA * CA - (ZW - XU) * CA * SA - XW * SA * SA)
880 L3 = - (ZW * CA * CA + (ZU + XW) * CA * SA + XU * SA * SA)
890 DE = - (XE * CA - ZE * SA)
900 L9 = - (ZE * CA + XE * SA)
910 REM
920 REM   REDEFINE NASA DATA FOR EQUATIONS OF MOTION
930 REM
940 YB = M * V * YB
950 DV = DV * M
960 D3 = D3 * M * V
970 LV = LV * M
980 L3 = L3 * M * V
990 DE = DE * M
1000 L9 = L9 * M

```

)

```

1010 MD = MD * C / (2 * V)
1020 Mq = Mq * C / (2 * V)
1030 LD = LD * C / (2 * V)
1040 LP = LP * B / (2 * V)
1050 LR = LR * B / (2 * V)
1060 NP = NP * B / (2 * V)
1070 NR = NR * B / (2 * V)
1080 REM
1090 REM   LOAD MATRIX FOR DELTA ALPHA SOVLER
1100 REM
1110 FOR I = 1 TO 2
1120 FOR J = 1 TO 2
1130 E(I,J) = Z(I,J)
1140 NEXT
1150 NEXT
1160 REM
1170 REM   FIGURE TRIANGULAR FACTORS OF MATRIX SOLVER
1180 REM
1190 NN = 2
1200 F(NN) = 1
1210 FOR K = 1 TO NN - 1
1220 MM = K
1230 FOR I = K + 1 TO NN
1240 IF ABS (E(I,K)) < = ABS (E(MM,K)) THEN 1260
1250 MM = I
1260 NEXT I
1270 F(K) = MM
1280 IF MM = K THEN 1300
1290 F(NN) = - F(NN)
1300 P = E(MM,K)
1310 E(MM,K) = E(K,K)
1320 E(K,K) = P
1330 FOR I = K + 1 TO NN
1340 E(I,K) = - E(I,K) / P
1350 NEXT I
1360 FOR J = K + 1 TO NN
1370 T = E(MM,J)
1380 E(MM,J) = E(K,J)
1390 E(K,J) = T
1400 IF T = 0 GOTO 1440
1410 FOR I = K + 1 TO NN
1420 E(I,J) = E(I,J) + E(I,K) * T
1430 NEXT I
1440 NEXT J
1450 NEXT K
1460 REM
1470 REM   THE MAIN LOOP
1480 REM
1490 READ N
1500 DATA 4

```

)

```

1510 FE = ATN ( SQR (N * N - 1)) + (SGN (N) - 1) * 1.5707963
1520 W = G * TAN (FE) / V
1530 FF = W * C * SIN (FE) / (2 * V)
1540 H(1) = - Q(1) * FF
1550 H(2) = - Q(2) * FF + (N - 1) * CW
1560 WE = W * SIN (FE)
1570 RE = W * COS (FE)
1580 REM
1590 REM BACK SUBSTITUTE TO FIND DELTA ALPHA
1600 REM
1610 FOR K = 1 TO NN - 1
1620 MM = F(K)
1630 SS = H(MM)
1640 H(MM) = H(K)
1650 H(K) = SS
1660 FOR I = K + 1 TO NN
1670 H(I) = H(I) + E(I,K) * SS
1680 NEXT
1690 NEXT
1700 FOR J = 1 TO NN - 1
1710 K = NN - J + 1
1720 H(K) = H(K) / E(K,K)
1730 SS = - H(K)
1740 FOR I = 1 TO NN - J
1750 H(I) = H(I) + E(I,K) * SS
1760 NEXT
1770 NEXT
1780 H(1) = H(1) / E(1,1)
1790 AD = H(1)
1800 REM CHECK THAT DRAG < THRUST
1810 L = N * WT
1820 CL = 2 * L / (RO * V * V * S)
1830 D = RO * V * V * S * (DO + KK * CL * CL) / 2
1840 IF D > TM THEN PRINT : PRI "N = ";N;" , DRAG > THRUST": END
1850 REM
1860 REM MOVE STABILITY AXIS BY DELTA ALPHA
1870 REM
1880 CA = COS ( - AD)
1890 SA = SIN ( - AD)
1900 D1 = DV * CA * CA - (LV + DA / V) * SA * CA + (LA / V) * SA * SA
1910 D3 = (DA / V) * CA * CA + (DV - LA / V) * SA * CA - LV * SA * SA
1920 D3 = D3 * V
1930 Y4 = YF * CA - YR * SA
1940 Y6 = YR * CA + YF * SA
1950 L1 = LV * CA * CA - ((LA / V) - DV) * SA * CA - (DA / V) * SA * SA
1960 LX = (LD / V) * CA * CA + (DD / V) * SA * CA
1970 LX = LX * V
1980 L5 = L4 * CA + D4 * SA
1990 L3 = (LA / V) * CA * CA + (LV + DA / V) * SA * CA + DV * SA * SA
2000 L3 = L3 * V
)

```

```

2010 I4 = (IZ - IX) * CA * SA + ZX * (CA * CA - SA * SA)
2020 I1 = IX * CA * CA + 2 * ZX * SA * CA + IZ * SA * SA
2030 L2 = (LB / V) * CA - (NB / V) * SA
2040 L2 = L2 * V
2050 I4 = LP * CA * CA - (LR + NP) * SA * CA + NR * SA * SA
2060 I3 = IZ * CA * CA - 2 * ZX * SA * CA + IX * SA * SA
2070 L6 = LR * CA * CA - (NR - LP) * SA * CA - NP * SA * SA
2080 N2 = (NB / V) * CA + (LB / V) * SA
2090 N2 = N2 * V
2100 M4 = NP * CA * CA - (NR - LP) * SA * CA - LR * SA * SA
2110 N6 = NR * CA * CA + (LR + NP) * SA * CA + LP * SA * SA
2120 M1 = MV * CA - (MA / V) * SA
2130 M4 = (MD / V) * CA
2140 M4 = M4 * V
2150 M3 = (MA / V) * CA + MV * SA
2160 M3 = M3 * V
2170 D9 = DE * CA - LE * SA
2180 L9 = LE * CA + DE * SA
2190 REM
2200 REM   FIGURE ELEMENTS OF 'A' MATRIX
2210 REM
2220 A(1,1) = (TV * COS (AO + AD) - D1) / M
2230 A(1,2) = RE * V
2240 A(1,3) = (- D * SIN (AO + AD) + L - M * QE * V - D3) / M
2250 A(1,8) = - G
2260 A(2,1) = RE / V
2270 A(2,2) = YB / (M * V)
2280 A(2,4) = Y4 / (M * V)
2290 A(2,6) = - 1 + Y6 / (M * V)
2300 A(2,7) = G * COS (FE) / V
2310 A(3,1) = (- TV * SIN (AO + AD) - L1 - QE * M) / (M * V + LX)
2320 A(3,3) = (- L3 - D * COS (AO + AD) - D) / (M * V + LX)
2330 A(3,5) = (V * M - L5) / (M * V + LX)
2340 A(3,7) = (- WT * SIN (FE)) / (M * V + LX)
2350 A(4,2) = L2 / I1
2360 A(4,4) = (I4 + I4 * QE) / I1
2370 A(4,5) = ((IY - I3) * RE) / I1
2380 A(4,6) = (L6 + (IY - I3) * QE) / I1
2390 I = I4 * (I4 / I1)
2400 A(6,2) = (N2 + I4 * A(4,2)) / (I3 - I)
2410 A(6,4) = (N4 + (I1 - IY) * QE + I4 * A(4,4)) / (I3 - I)
2420 A(6,5) = (- I4 * RE + I4 * A(4,5)) / (I3 - I)
2430 A(6,6) = (N6 - I4 * QE + I4 * A(4,6)) / (I3 - I)
2440 I = 1 / I1
2450 A(4,2) = I * A(6,2) + A(4,2)
2460 A(4,4) = I * A(6,4) + A(4,4)
2470 A(4,5) = I * A(6,5) + A(4,5)
2480 A(4,6) = I * A(6,6) + A(4,6)
2490 A(5,1) = (M1 + M4 * A(3,1)) / IY
2500 A(5,3) = (M3 + M4 * A(3,3)) / IY

```

```

2510 A(5,4) = ((I3 - I1) * RE) / IY
2520 A(5,5) = (M4 + M4 * A(3,5)) / IY
2530 A(5,6) = 2 * I4 * RE / IY
2540 A(5,7) = M4 * A(3,7) / IY
2550 A(7,4) = 1
2560 A(7,8) = QE * SIN (FE) + RE * COS (FE)
2570 A(8,5) = COS (FE)
2580 A(8,6) = - SIN (FE)
2590 A(8,7) = - QE * SIN (FE) - RE * COS (FE)
2600 REM
2610 REM  FIGURE ELEMENTS OF 'B' MATRIX
2620 REM
2630 U(1) = - D9 / M
2640 U(3) = - L9 / (M * V + LX)
2650 U(5) = (ME + M4 * U(3)) / IY
2660 REM
2670 REM  PRINT RESULTS
2680 REM
2690 PRINT "THE 'A' MATRIX FOR LOAD FACTOR, N = ";N
2700 PRINT : PRINT "BANK ANGLE, FE = ";FE * DR;" DEGREES"
2710 PRINT "DELTA ALPHA, AD = ";AD * DR;" DEGREES"
2720 PRINT
2730 FOR I = 1 TO 8
2740 FOR J = 1 TO 8
2750 PRINT FN R(A(I,J));" ";
2760 NEXT
2770 PRINT
2780 NEXT
2790 PRINT
2800 PRINT "THE 'B' MATRIX TRANSPOSED IS"
2810 PRINT
2820 FOR I = 1 TO 8
2830 PRINT FN R(U(I));" ";
2840 NEXT
2850 PRINT : PRINT
)

```


RUN
THE 'A' MATRIX FOR LOAD FACTOR, N = 4

BANK ANGLE, FE = 75.5224885 DEGREES
DELTA ALPHA, AD = 7.31234296 DEGREES

```
-0.064255 31.150889 -105.687431 0 0 0 0 -32.1725  
1.56E-04 -.181 0 0 0 -1 .017994 0  
-1.428E-03 0 -1.702174 0 1 0 -.069689 0  
0 -7.134195 0 -2.07948 -.064927 .289606 0 0  
-1.766E-03 0 -8.017326 .064257 -1.94903 -.015636 .039692 0  
0 3.678639 0 .22388 7.36E-03 -.338186 0 0  
0 0 0 1 0 0 0 .278755  
0 0 0 0 .25 -.968246 -.278755 0
```

THE 'B' MATRIX TRANSPOSED IS

```
-5.829034 0 -.10026 0 -15.932007 0 0 0
```

)

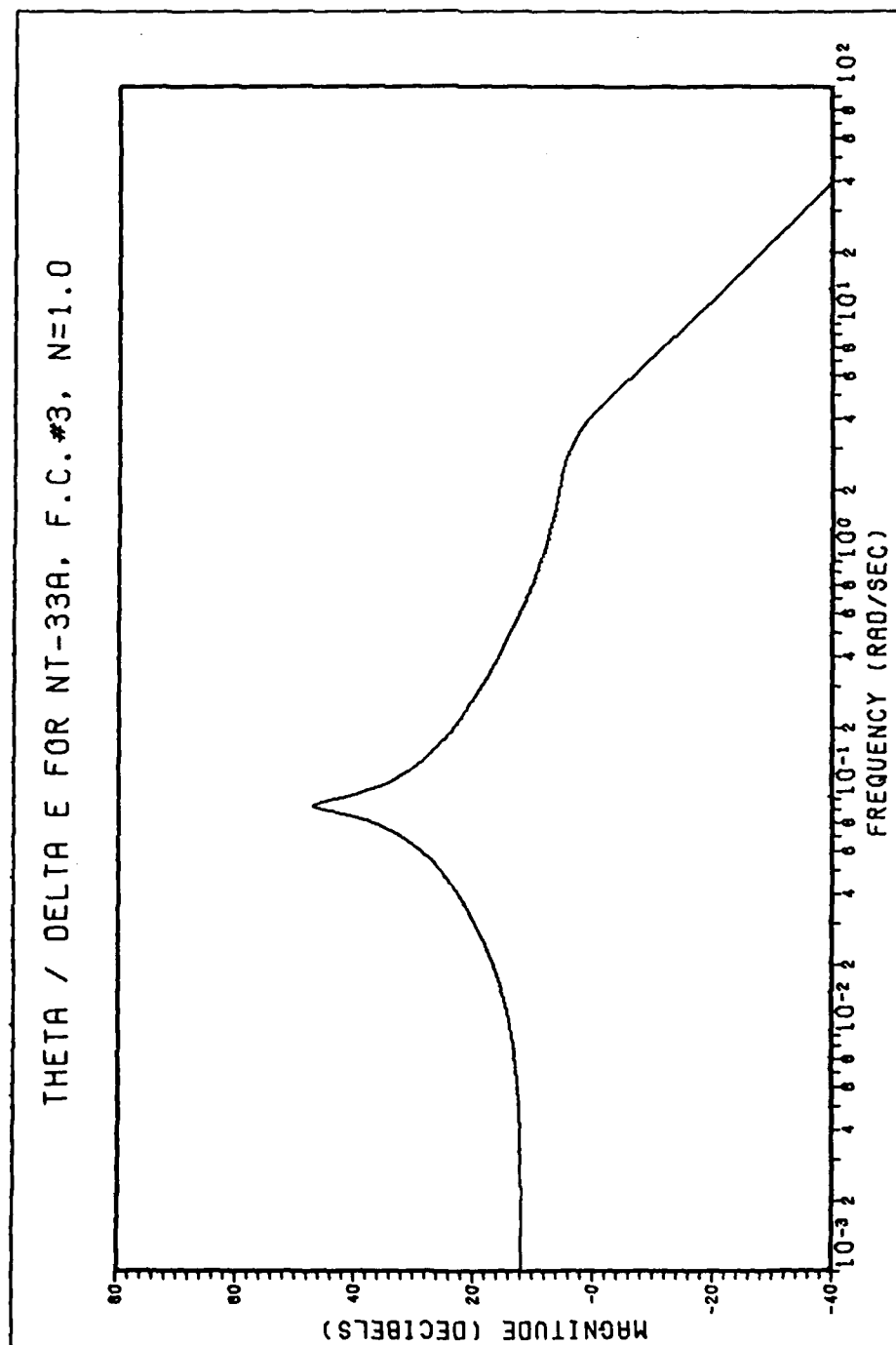


Figure B1.

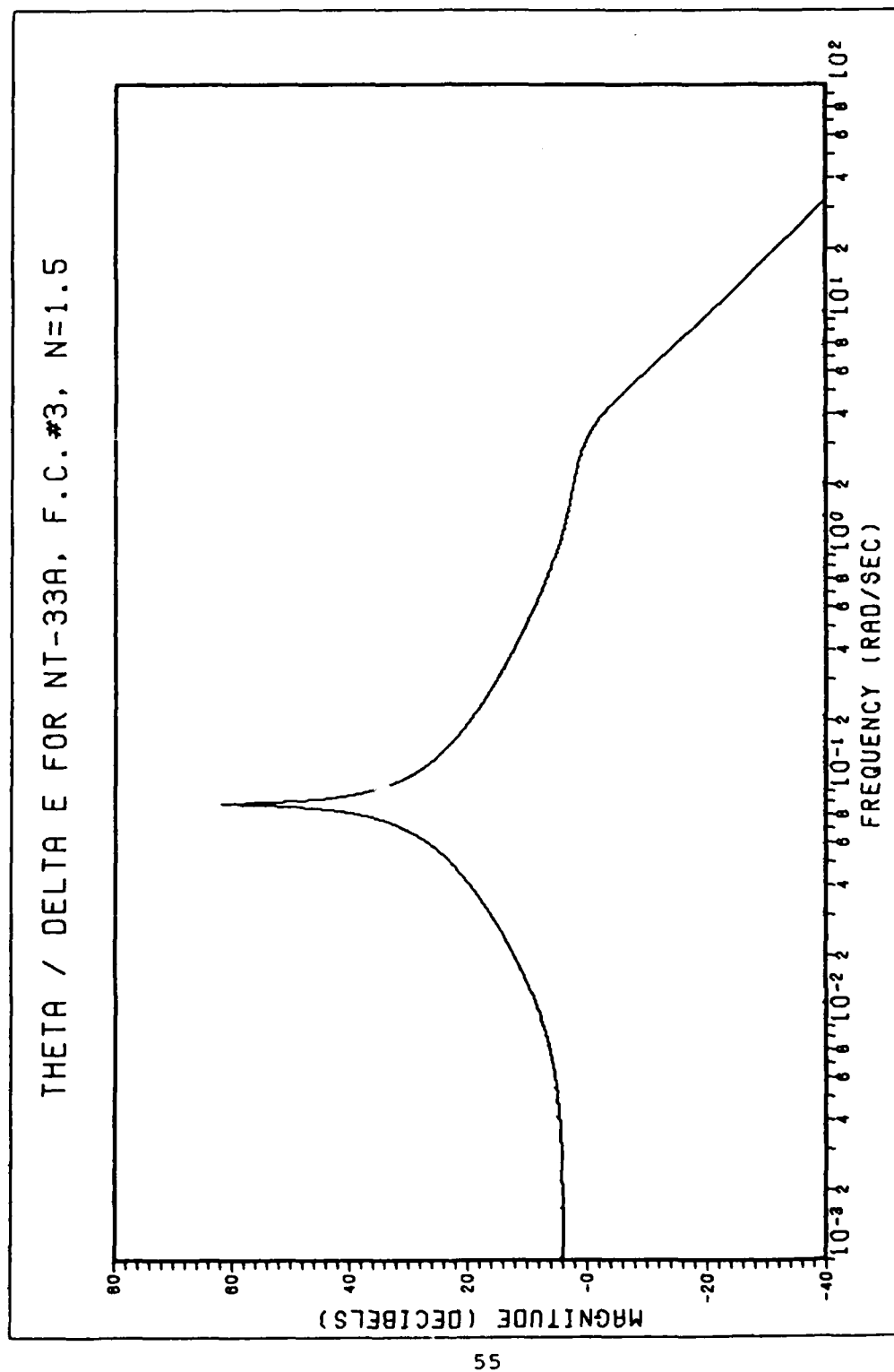


Figure B2.

THETA / DELTA E FOR NT-33A, F.C.#3, N=2.0

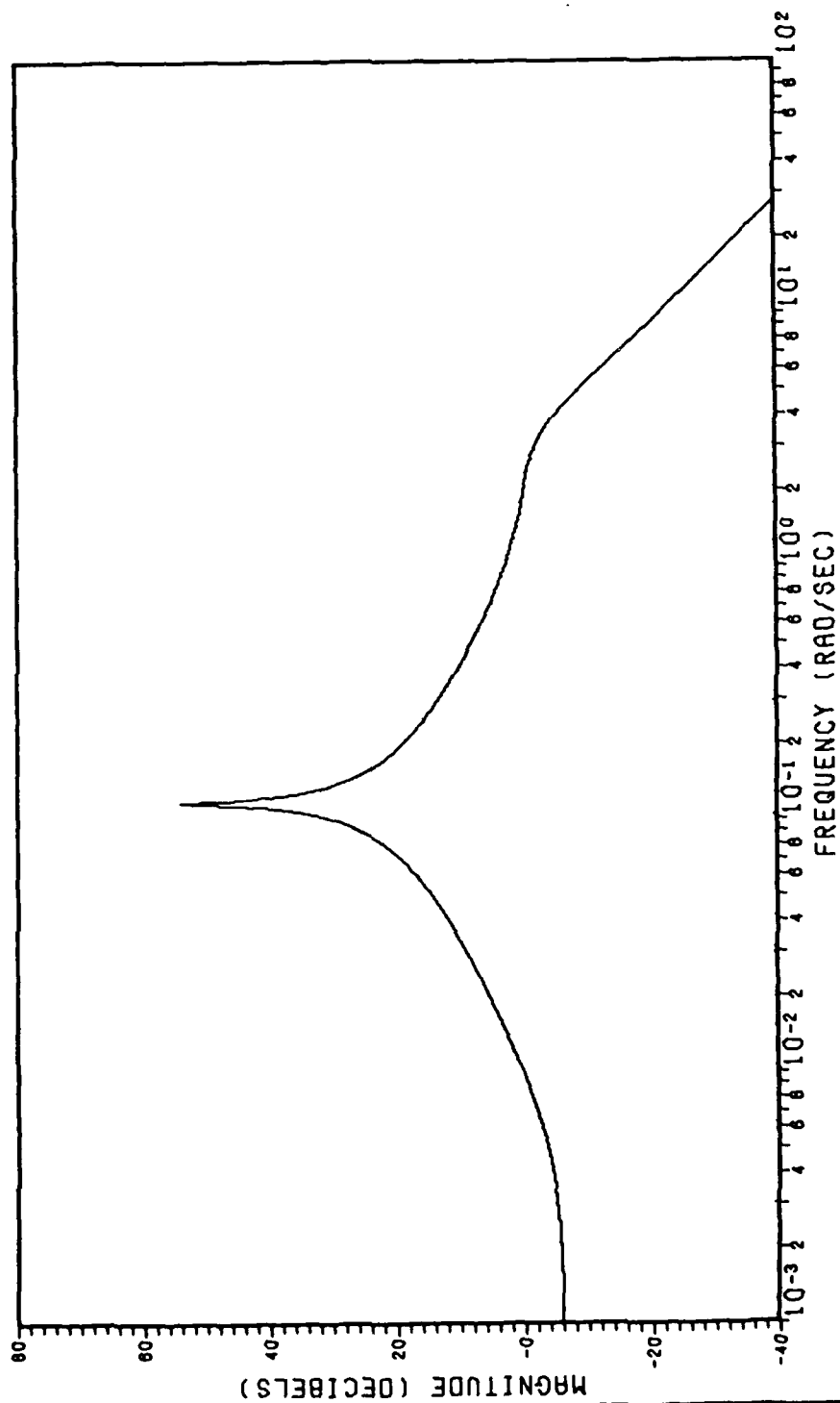


Figure B3.

THETA / DELTA E FOR NT-33A, F.C.#3, N=3.0

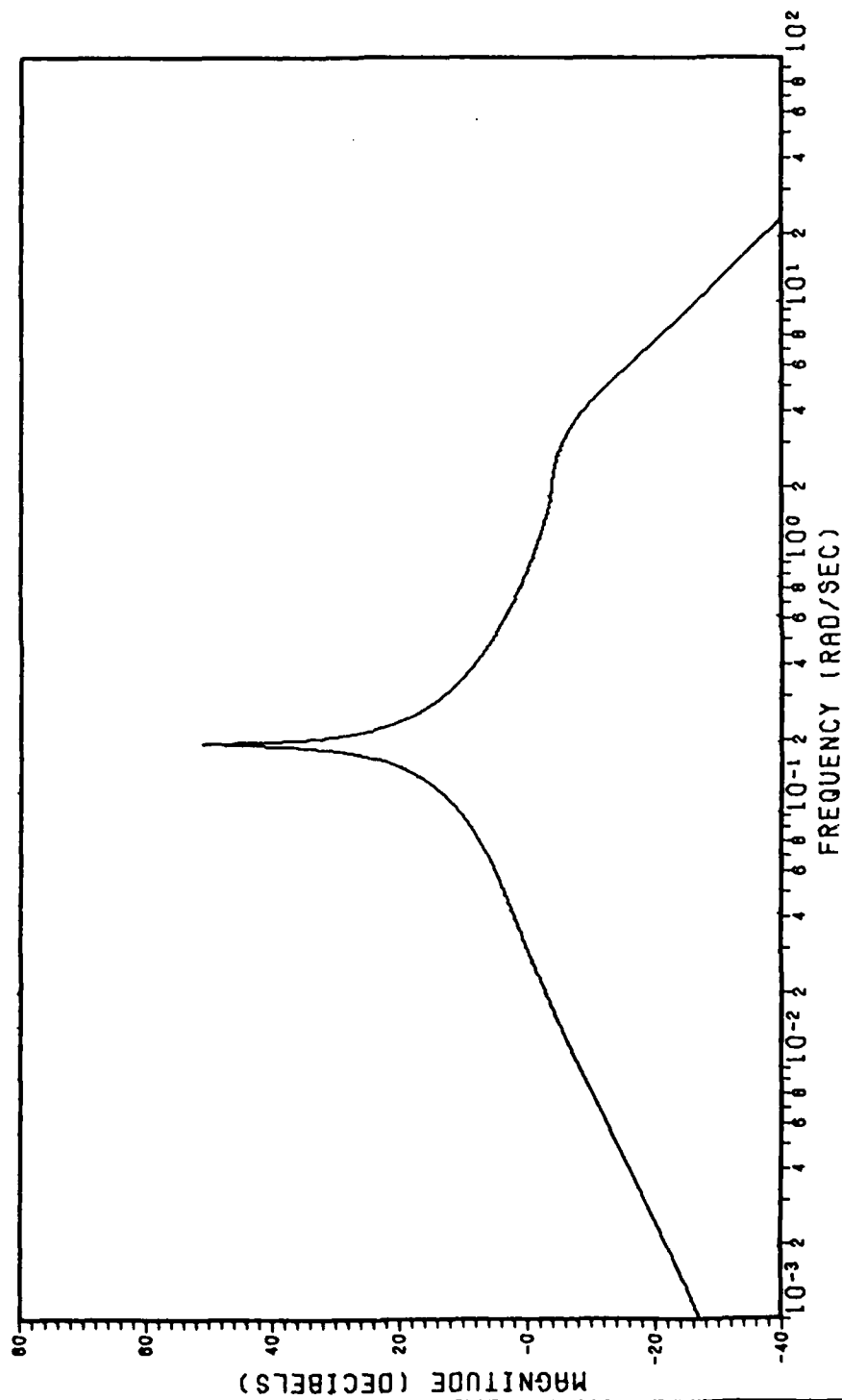


Figure B4.

THETA / DELTA E FOR NT-33A, F.C.#3, N=4.0

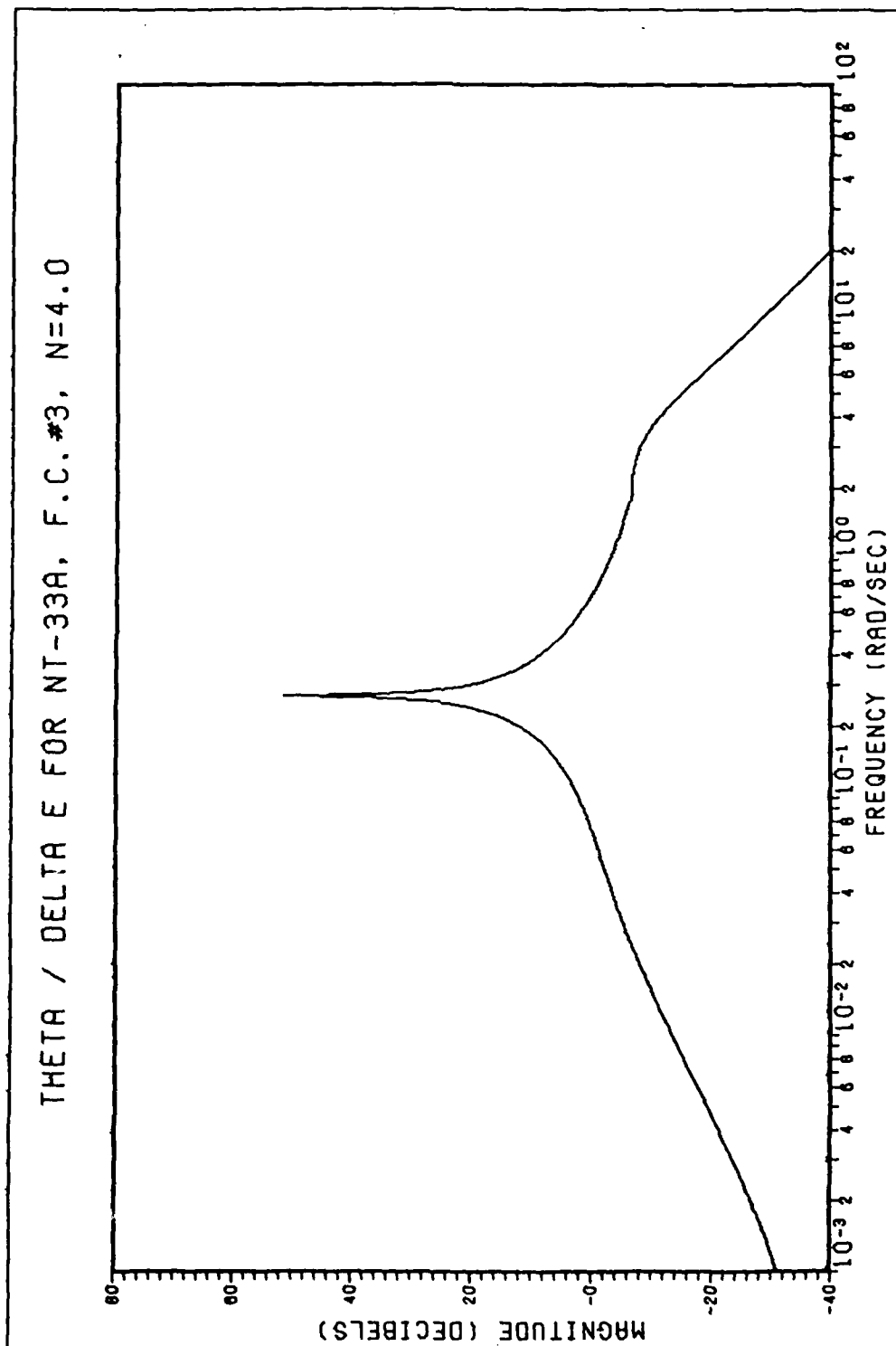


Figure B5.

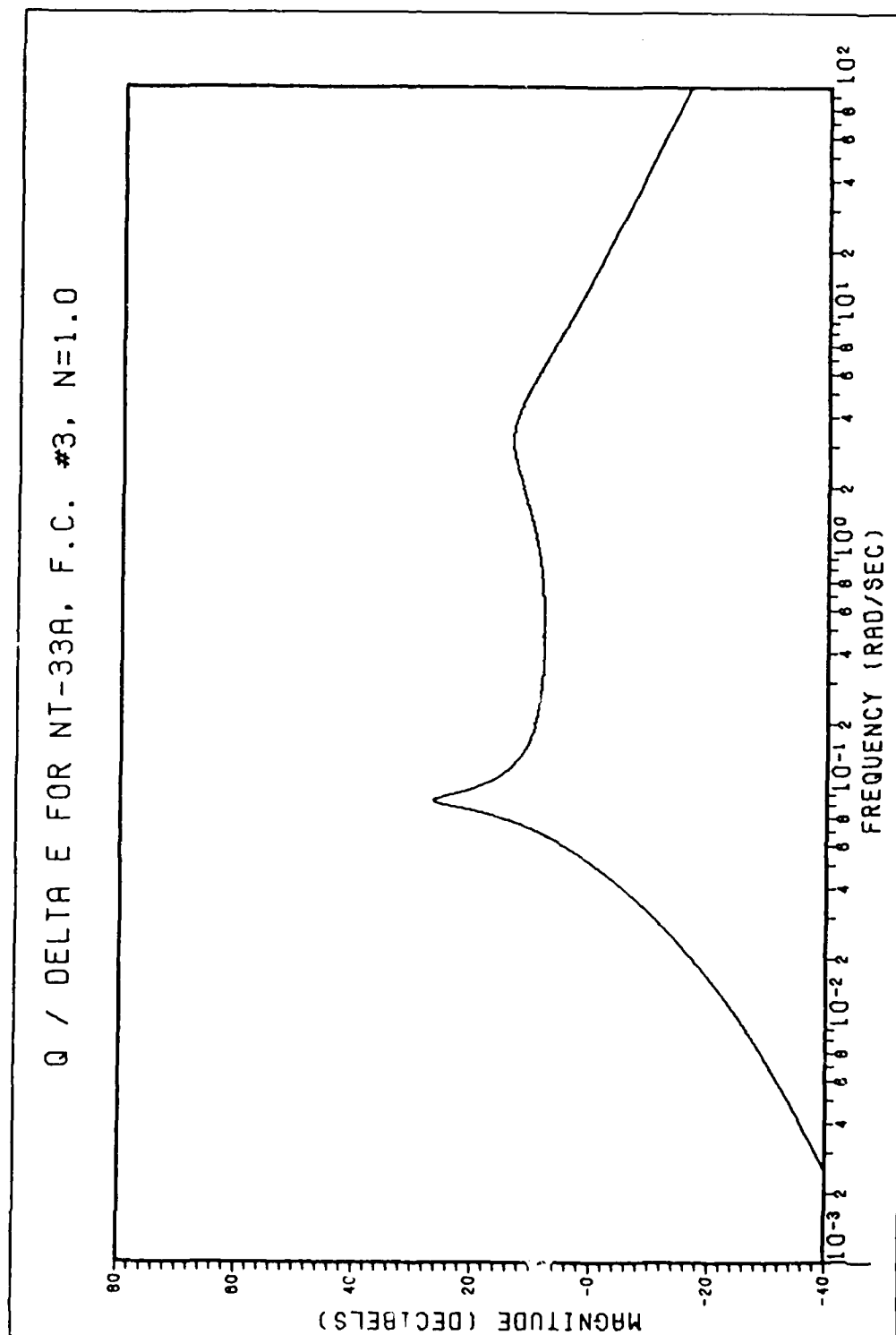


Figure B6.

Q / DELTA E FOR NT-33A, F.C.#3, N=1.5

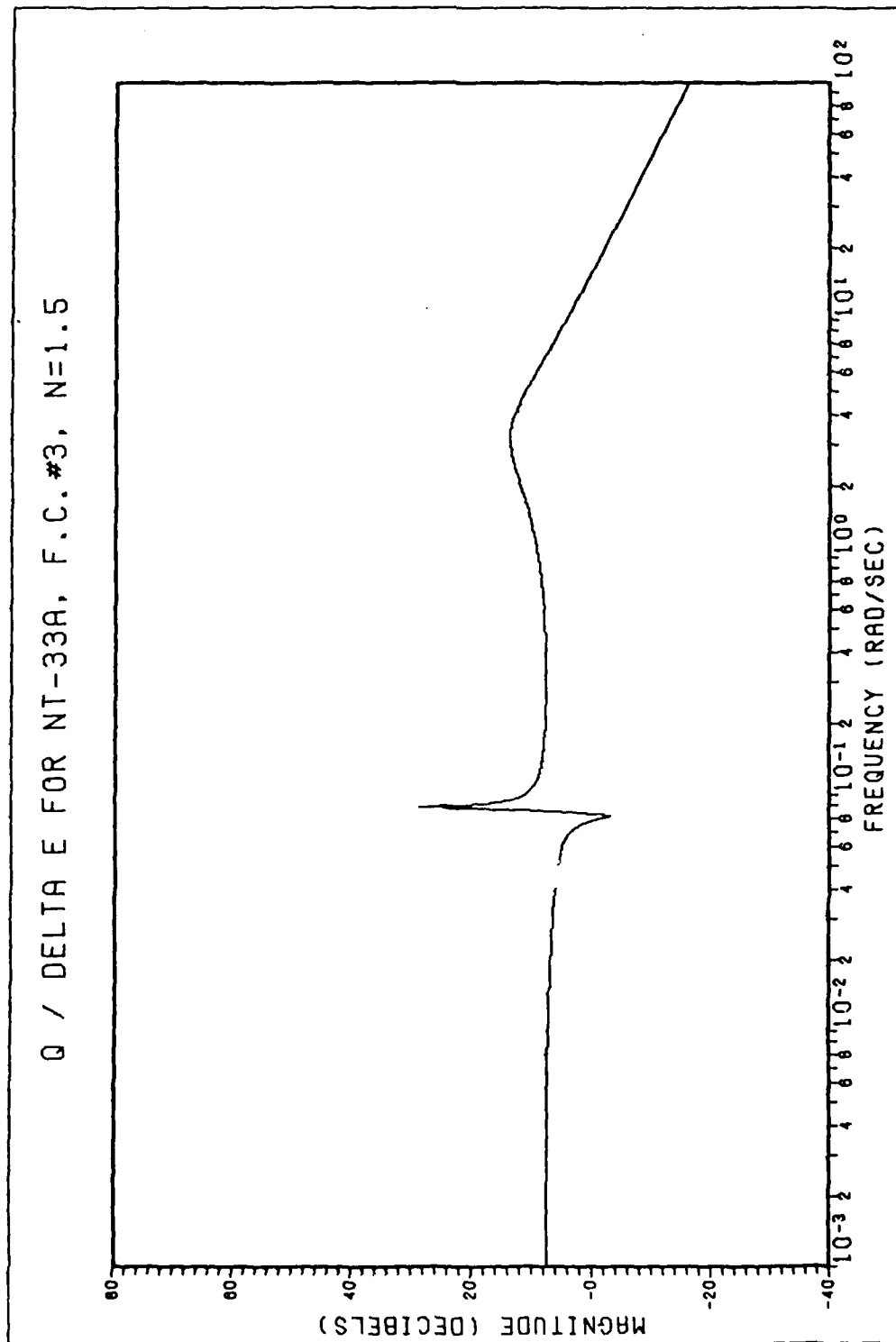


Figure B7.

Q / DELTA E FOR NT-33A, F.C. #3, N=2.0

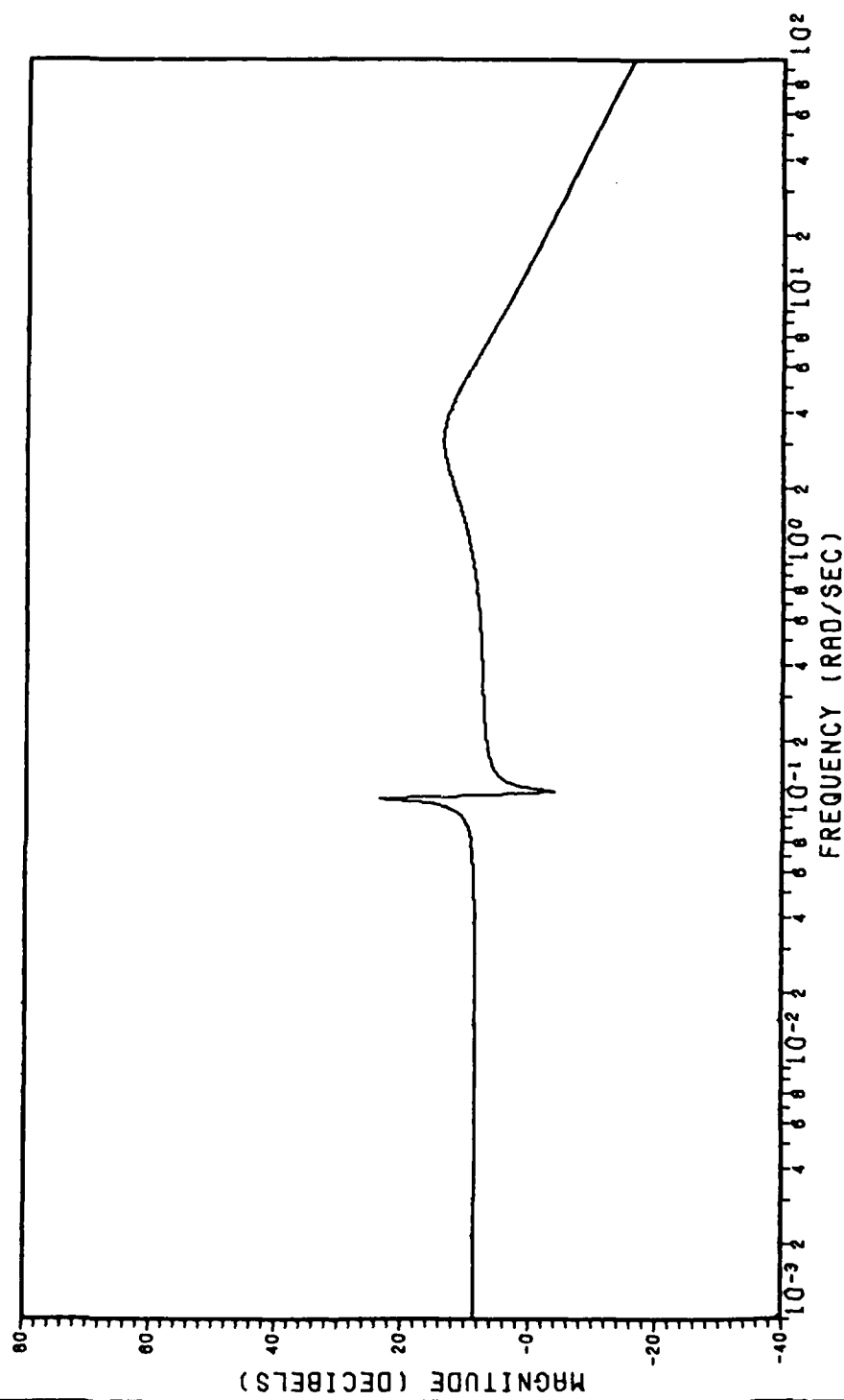


Figure B8.

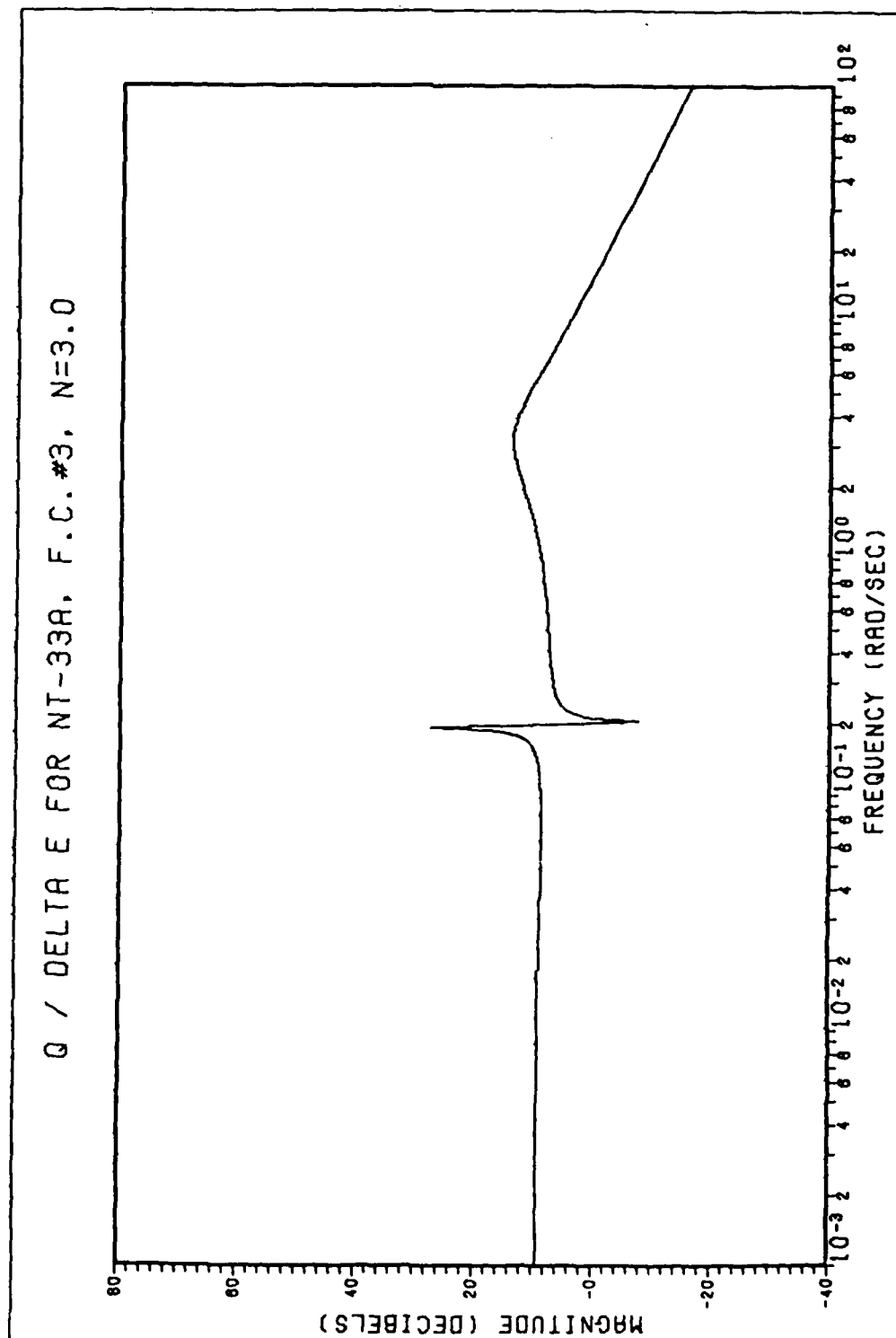


Figure B9.

Q / DELTA E FOR NT-33A, F.C.#3, N=4.0

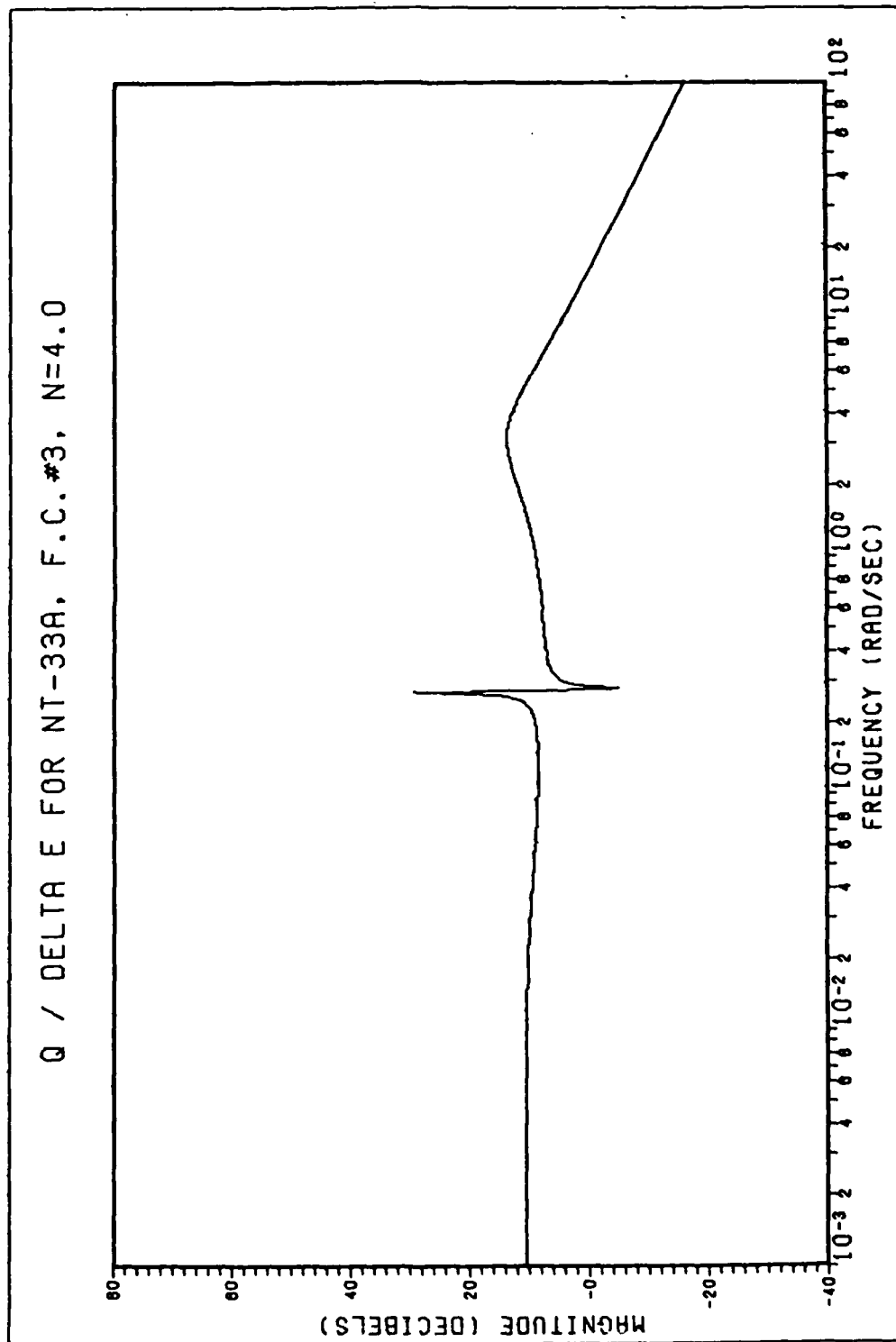


Figure B10.

P / DELTA A FOR NT-33A, F.C. #3, N=1

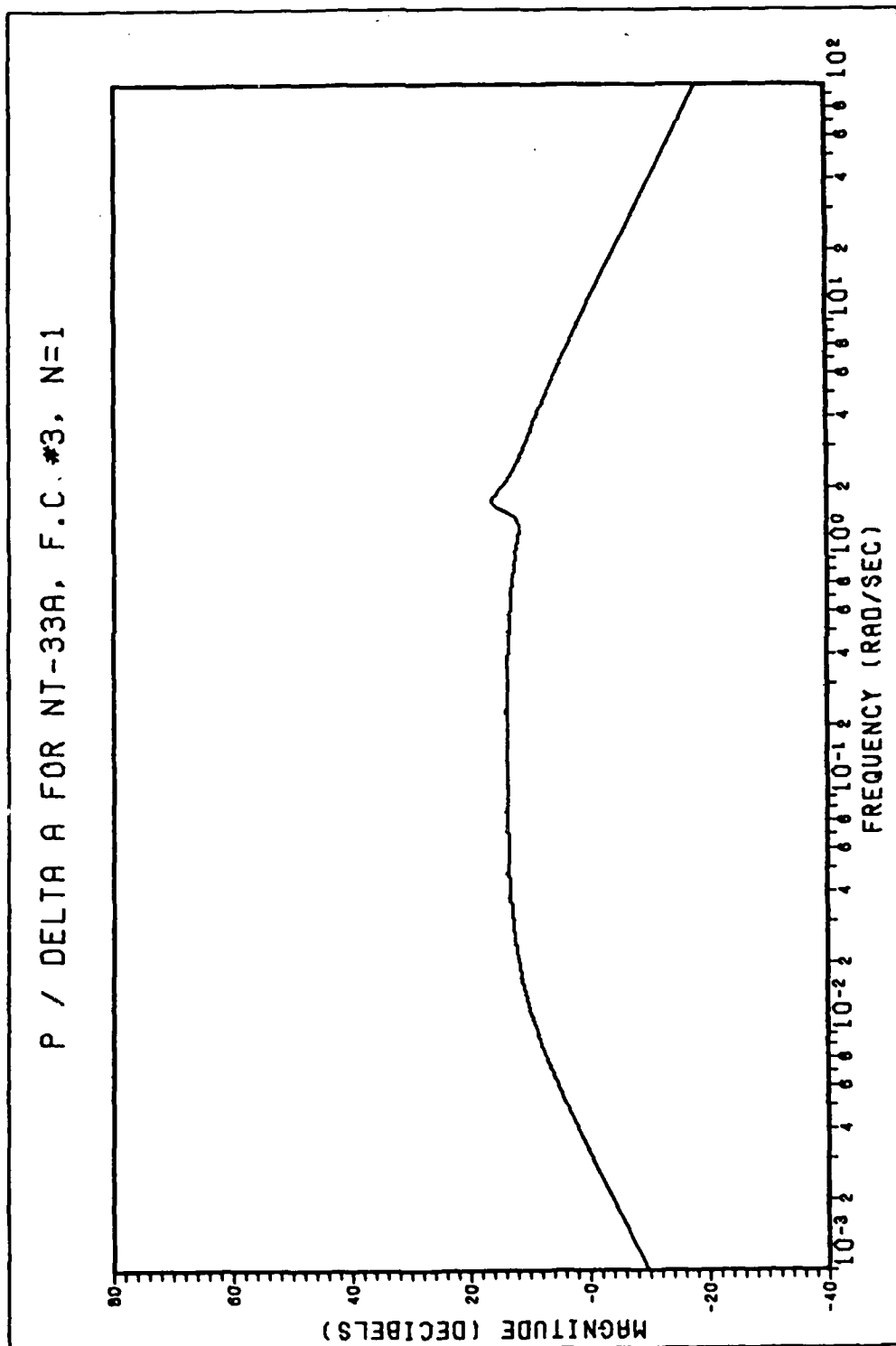


Figure B11.

P / DELTA A FOR NT-33A. F.C. #3, N=1

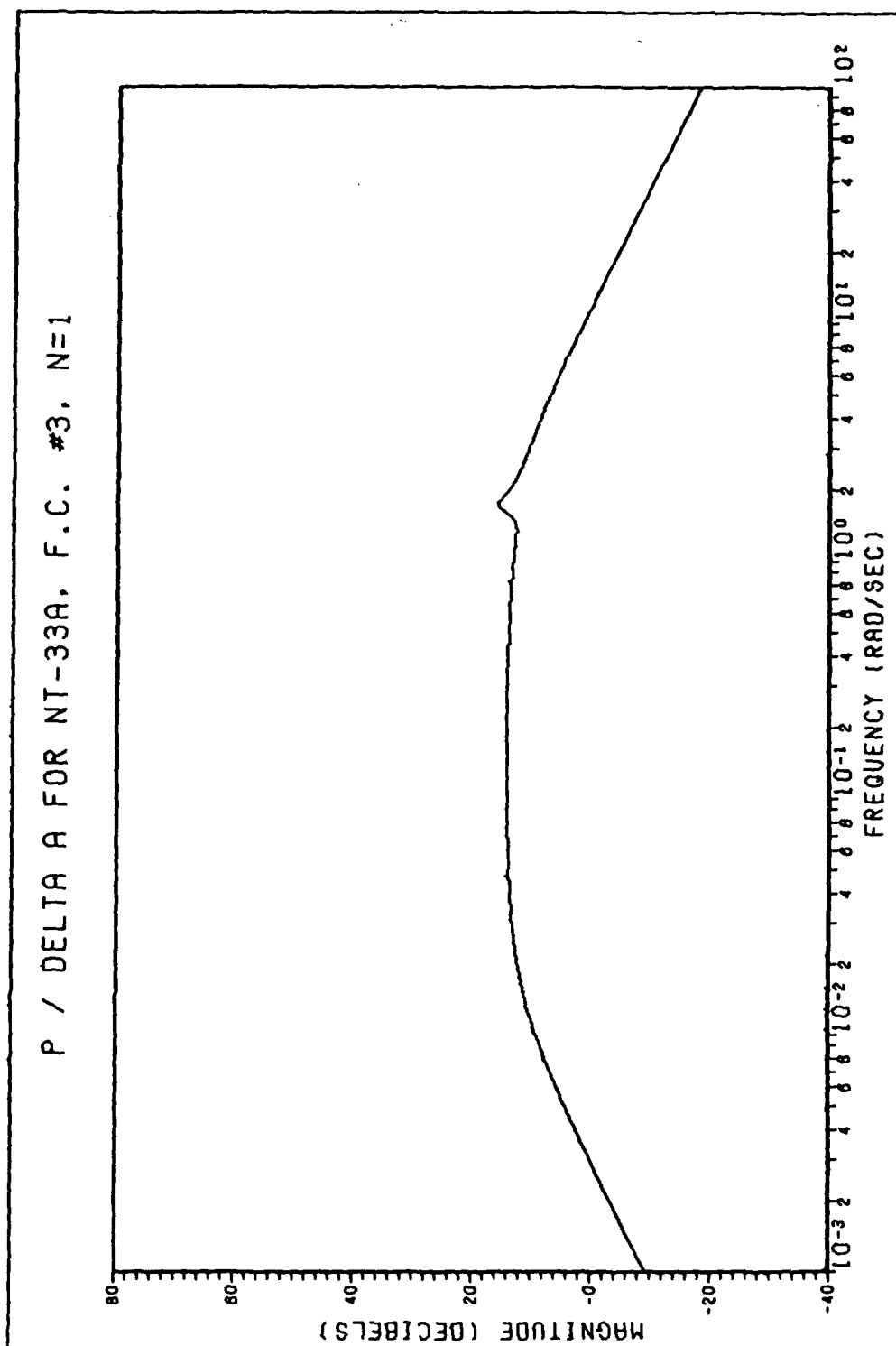


Figure B12.

P / DELTA A FOR NT-33A. F.C. #3, N=2

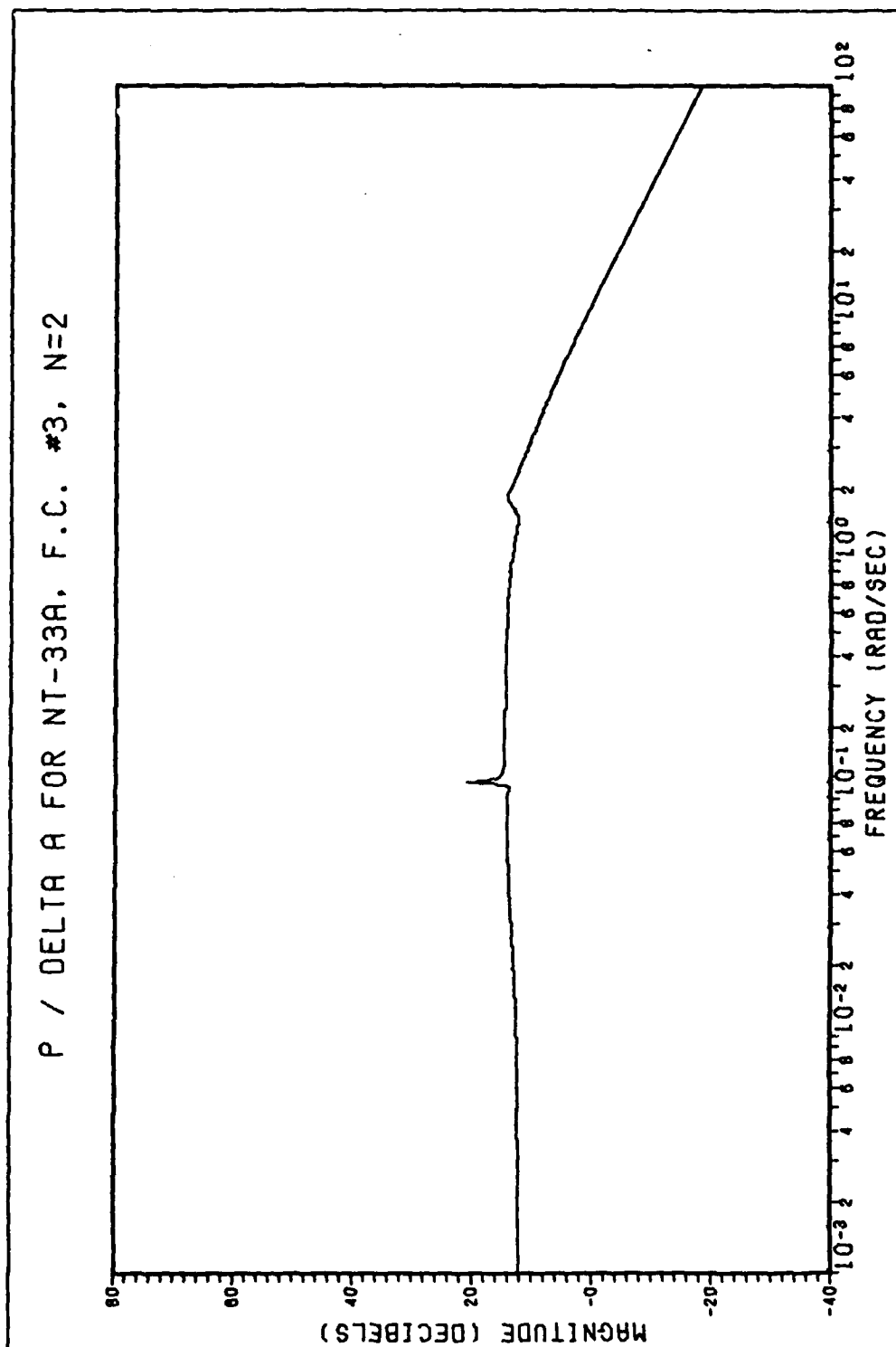


Figure B13.

P / DELTA A FOR NT-33A, F.C. #3, N=4

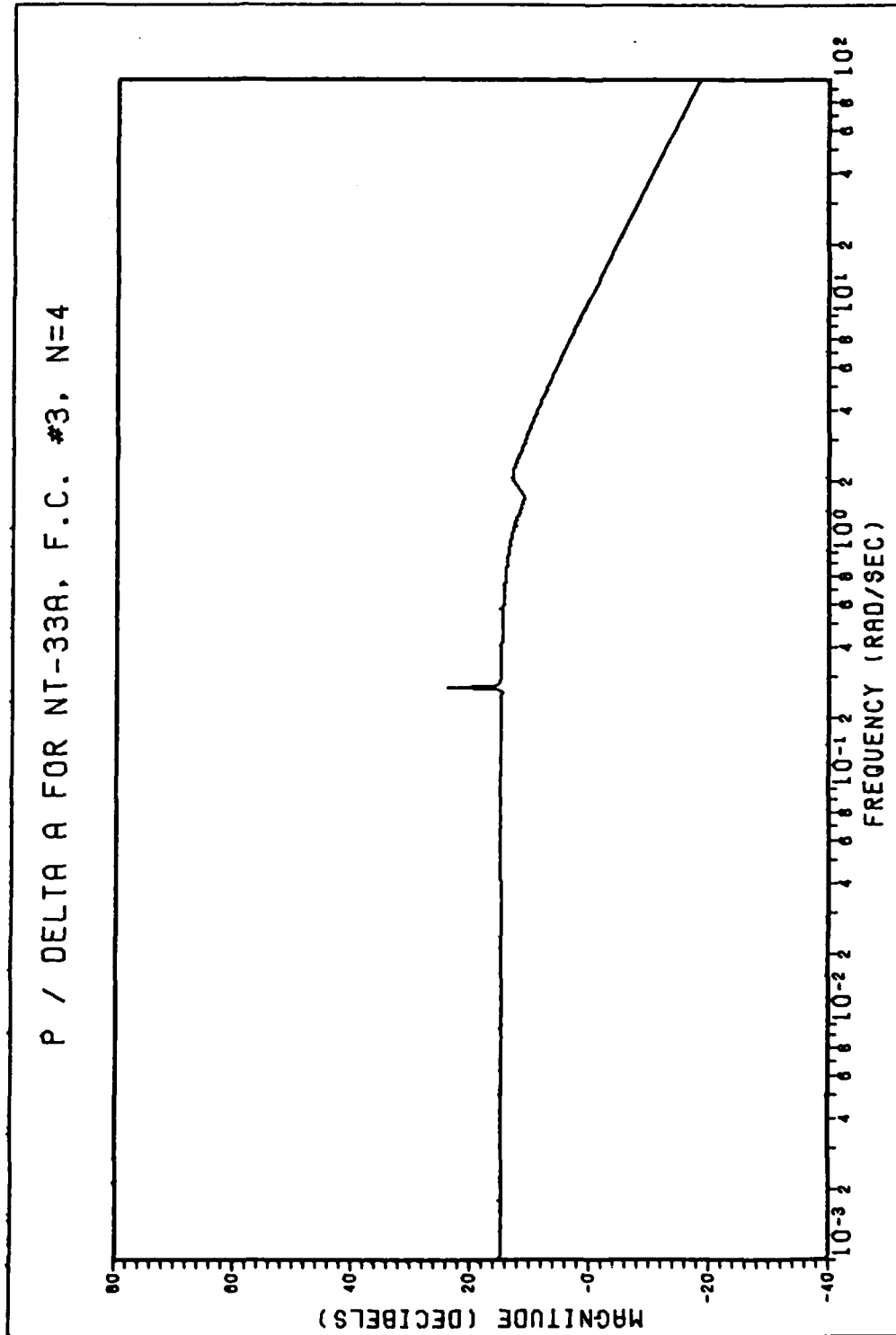
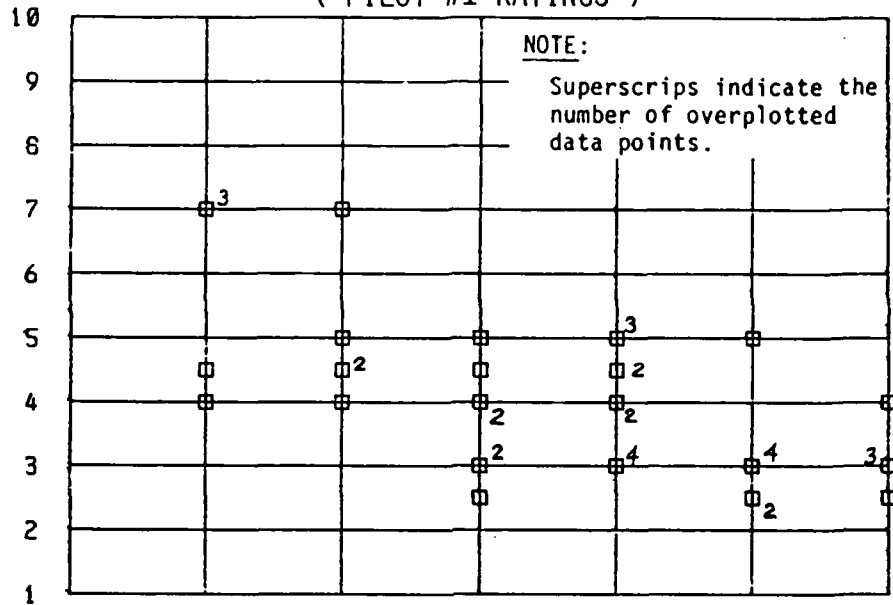


Figure B14.

APPENDIX C
DATA PLOTS

COOPER-HARPER VS OMEGA AT 1G
 SAFTD TV TRACKING TASK
 $N / \text{ALPHA} = 29 \text{ G} / \text{RAD}$
 0.7 DAMPING RATIO , 1G/2ND ORDER
 (PILOT #1 RATINGS)

C-H RATINGS



C-H RATINGS

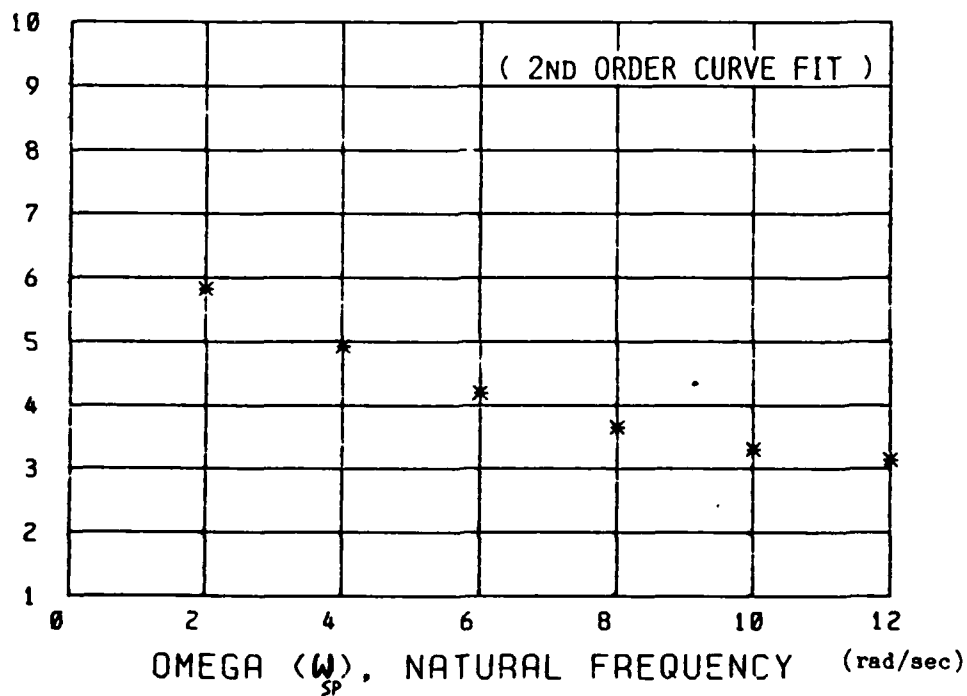


Figure c1. COOPER-HARPER VS OMEGA

COOPER-HARPER VS OMEGA AT 1G
 SAFTD TV TRACKING TASK
 $N / \text{ALPHA} = 29 \text{ G} / \text{RAD}$
 0.7 DAMPING RATIO , 1G/2ND ORDER
 (PILOT #2 RATINGS)

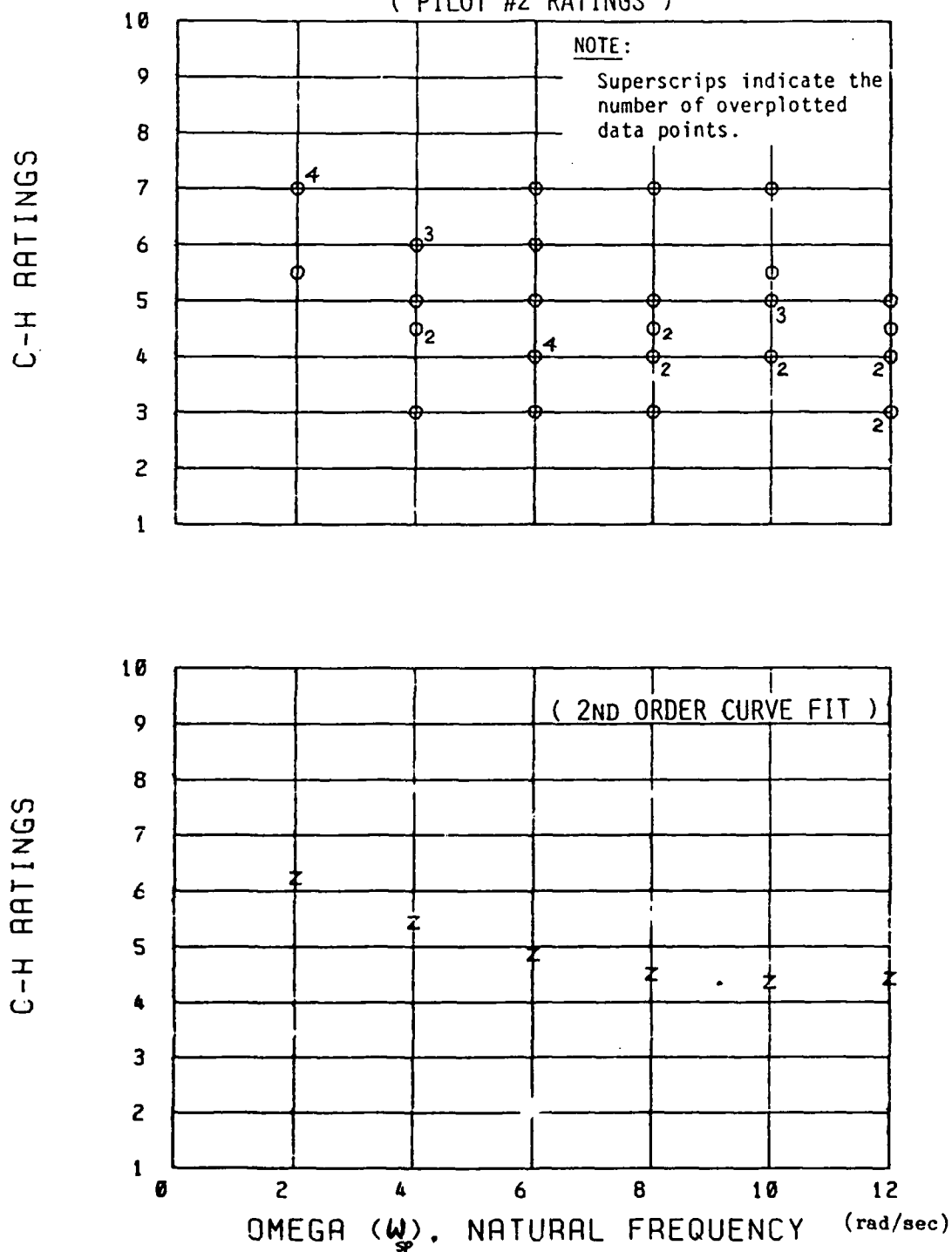
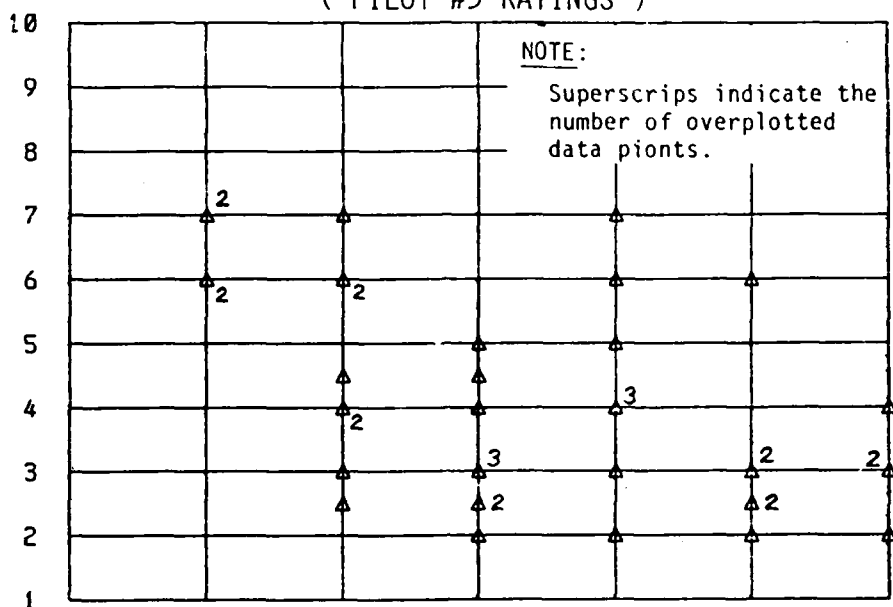


Figure C2. COOPER-HARPER VS OMEGA

COOPER-HARPER VS OMEGA AT 1G
 SAFTD TV TRACKING TASK
 $N / \text{ALPHA} = 29 \text{ G} / \text{RAD}$
 0.7 DAMPING RATIO . 1G/2ND ORDER
 (PILOT #3 RATINGS)

C-H RATINGS



C-H RATINGS

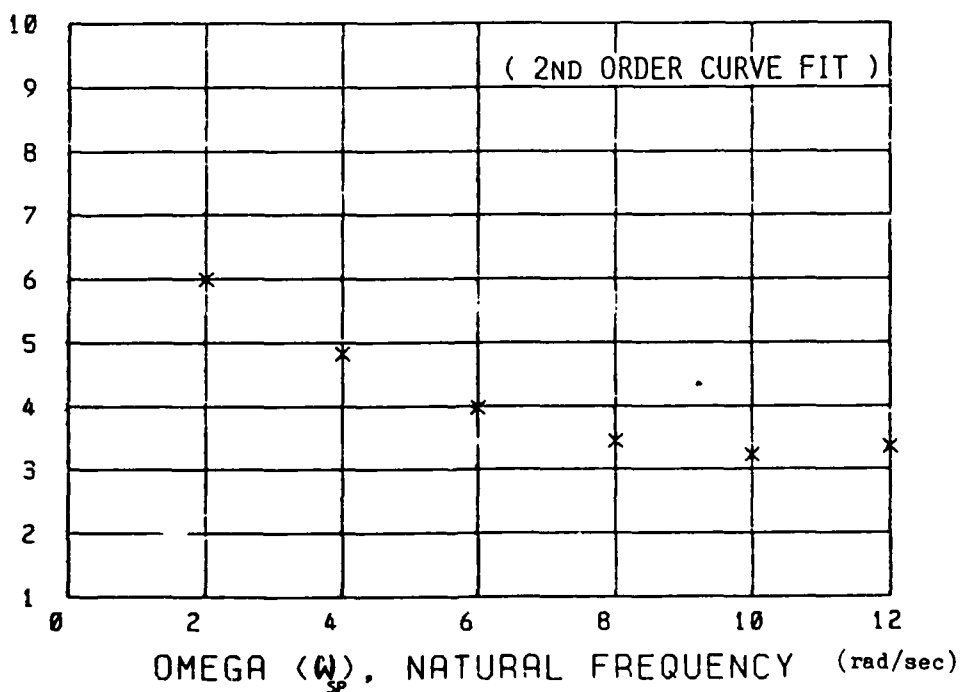


Figure C3. COOPER-HARPER VS OMEGA

COOPER-HARPER VS OMEGA AT 1G
SAFTD TV TRACKING TASK
N / ALPHA = 29 G / RAD
0.7 DAMPING RATIO , 1G/2ND ORDER

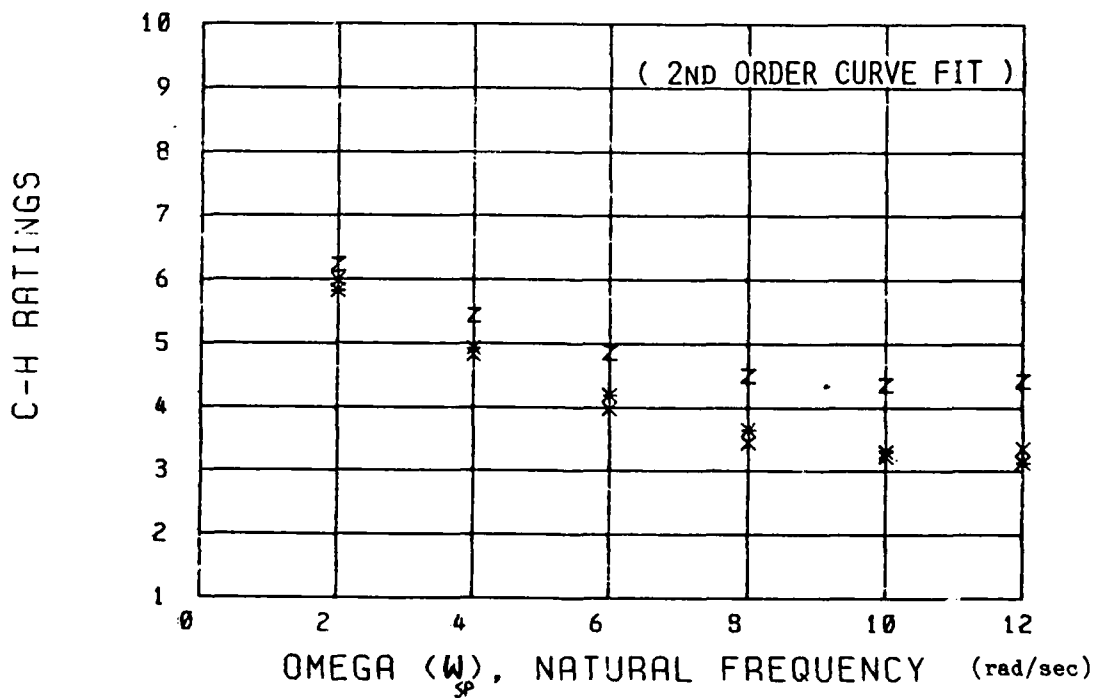
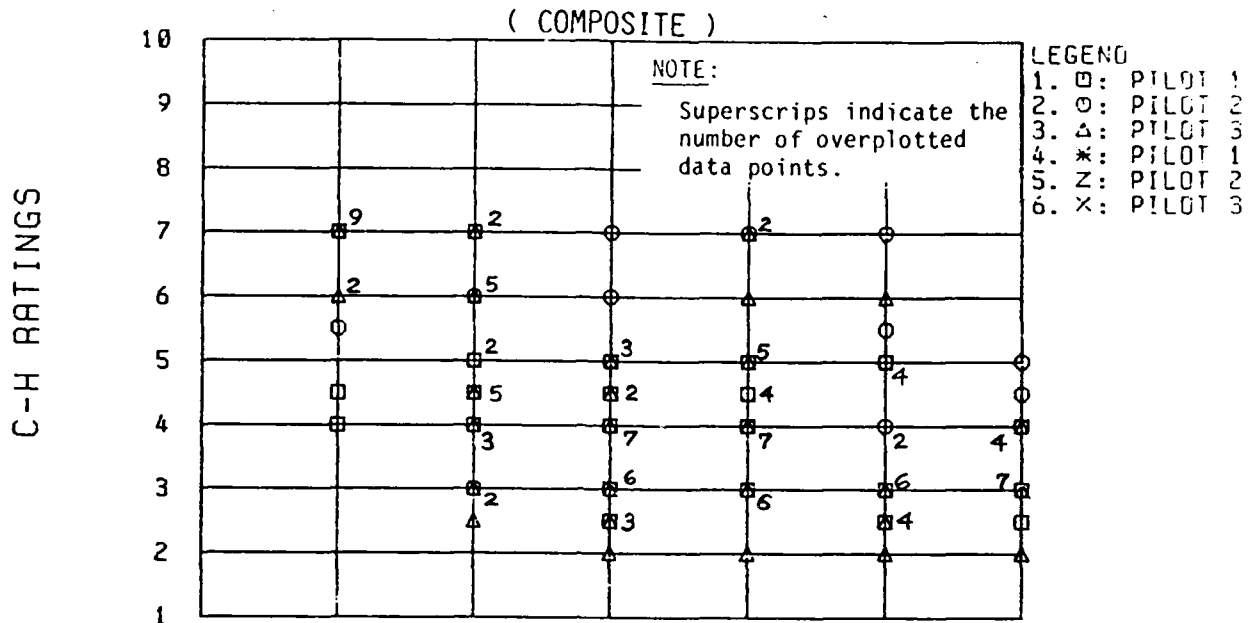


Figure C4. COOPER-HARPER VS OMEGA

COOPER-HARPER VS OMEGA AT 2G
 SAFTD TV TRACKING TASK
 $N / \text{ALPHA} = 29 \text{ G} / \text{RAD}$
 0.7 DAMPING RATIO, 2G/2ND ORDER

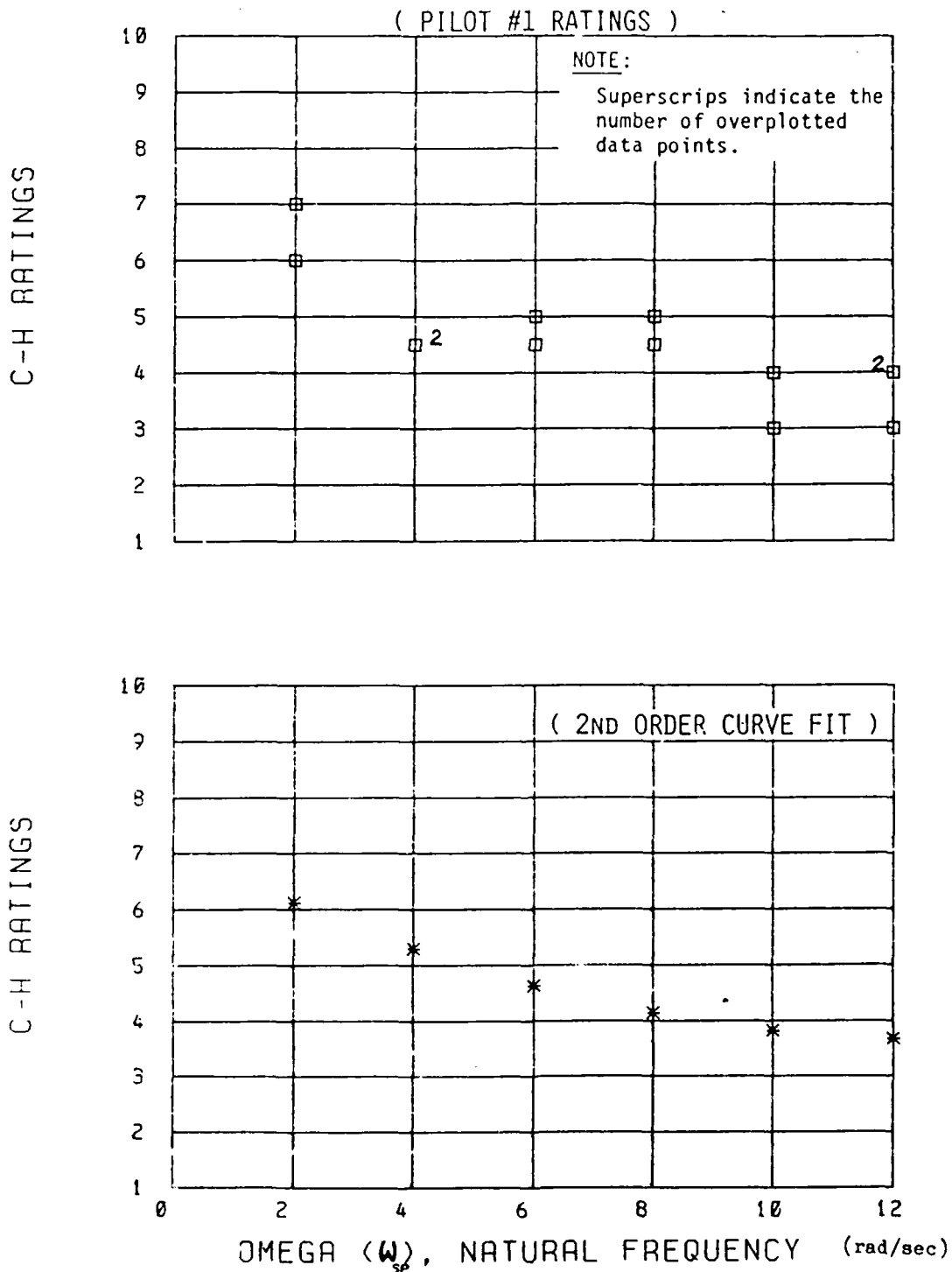
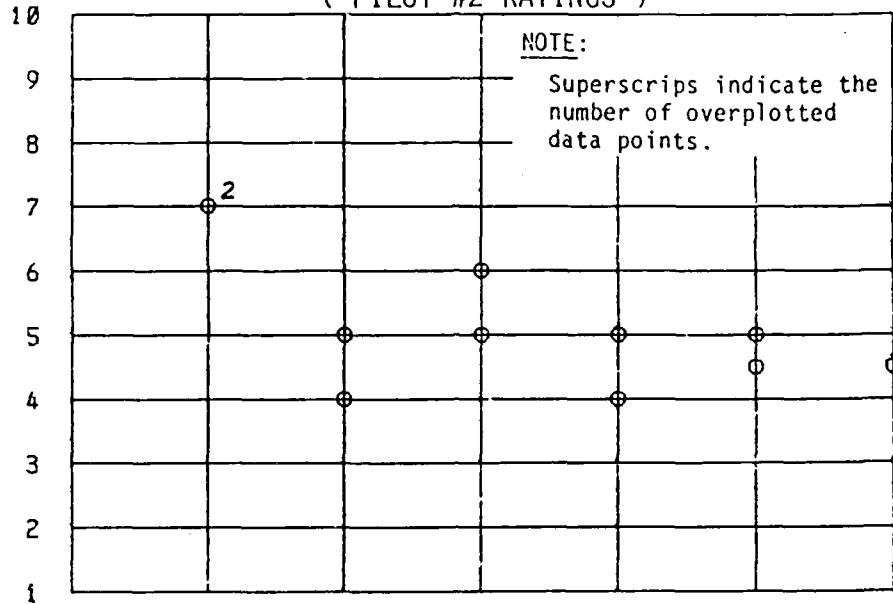


Figure C5. COOPER-HARPER VS OMEGA

COOPER-HARPER VS OMEGA AT 2G
 SAFTD TV TRACKING TASK
 $N / \text{ALPHA} = 29 \text{ G} / \text{RAD}$
 0.7 DAMPING RATIO, 2G/2ND ORDER

(PILOT #2 RATINGS)

C-H RATINGS



C-H RATINGS

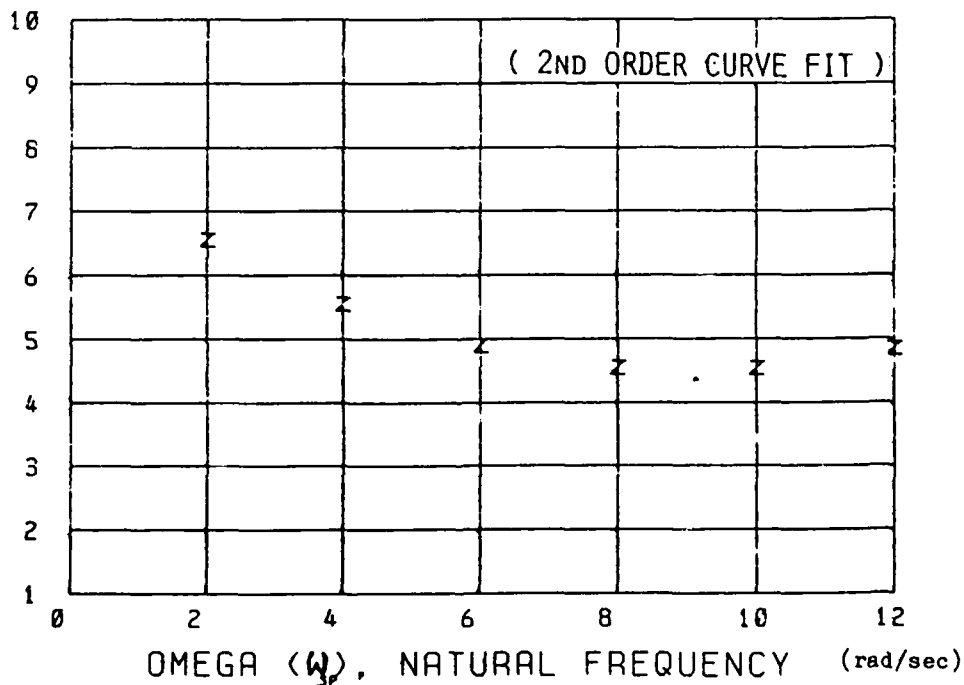
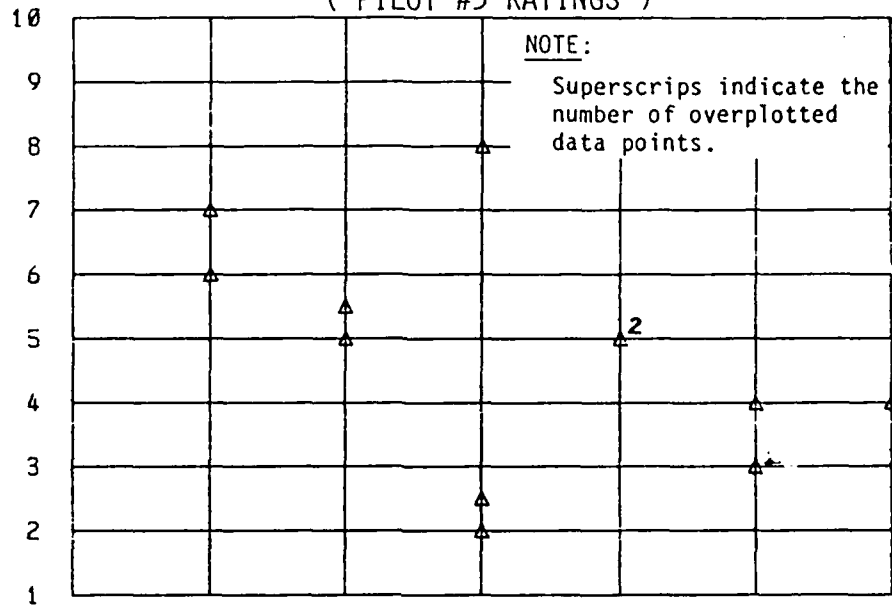


Figure C6. COOPER-HARPER VS OMEGA

COOPER-HARPER VS OMEGA AT 2G
 SAFTD TV TRACKING TASK
 $N / \text{ALPHA} = 29 \text{ G} / \text{RAD}$
 0.7 DAMPING RATIO, 2G/2ND ORDER

(PILOT #3 RATINGS)

C-H RATINGS



C-H RATINGS

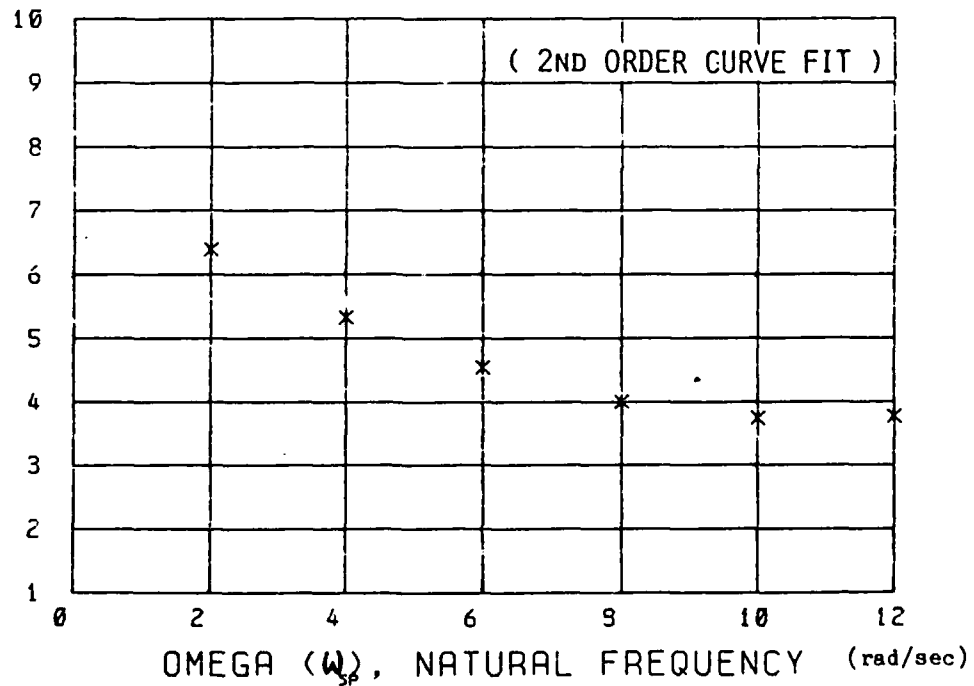


Figure C7. COOPER-HARPER VS OMEGA

COOPER-HARPER VS OMEGA AT 2G
SAFTD TV TRACKING TASK
N / ALPHA = 29 G / RAD
0.7 DAMPING RATIO, 2G/2ND ORDER
(COMPOSITE)

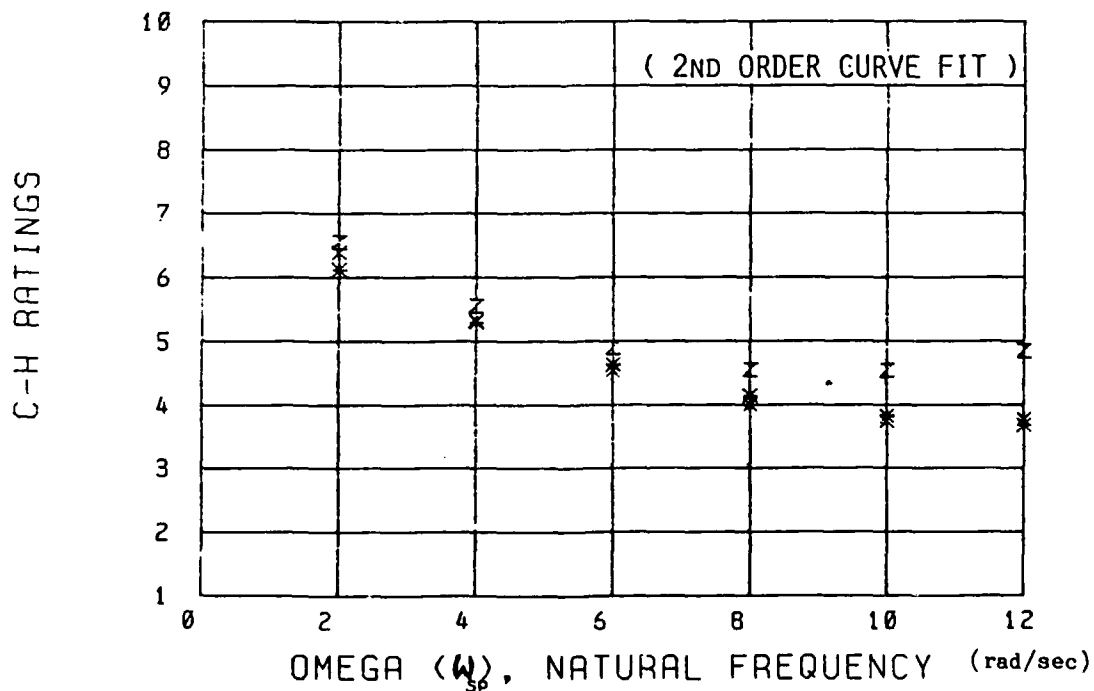
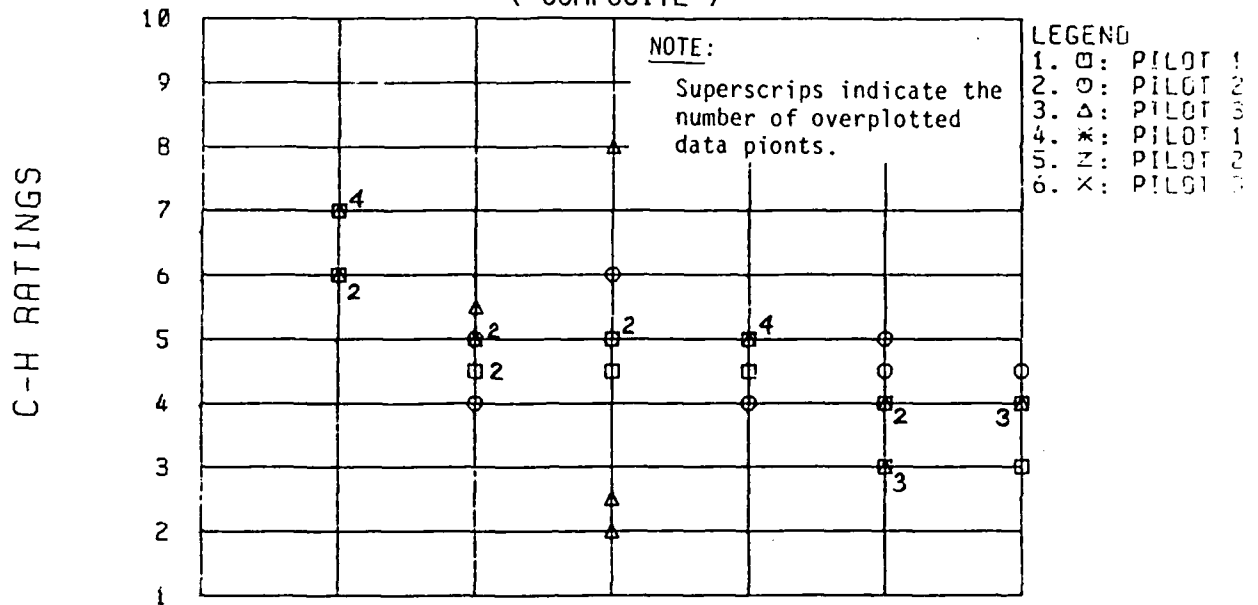
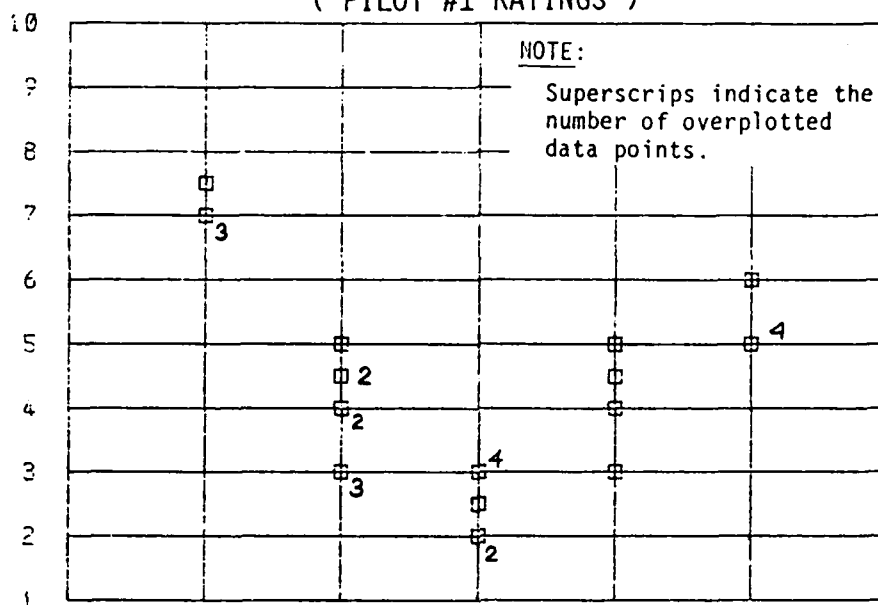


Figure C8. COOPER-HARPER VS OMEGA

COOPER-HARPER VS OMEGA AT 1G
 NT-33A PROJECT HUD TRACKING
 $N / \text{ALPHA} = 29 \text{ G} / \text{RAD}$
 0.7 DAMPING RATIO, 10/4TH ORDER

(PILOT #1 RATINGS)

C-H RATINGS



C-H RATINGS

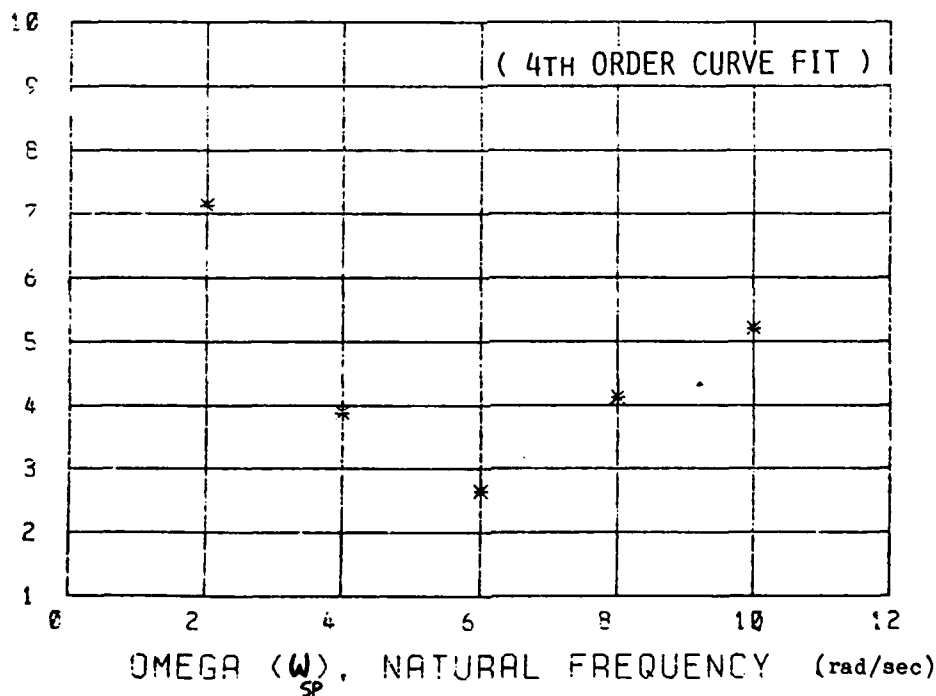
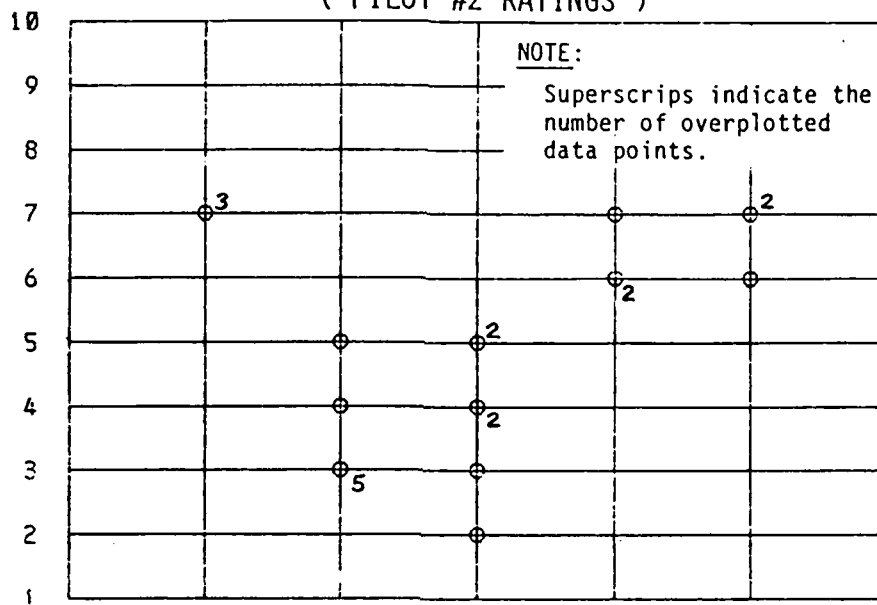


Figure C9. COOPER-HARPER VS OMEGA

COOPER-HARPER VS OMEGA AT 1G
 NT-33A PROJECT HUD TRACKING
 $N / \text{ALPHA} = 29 \text{ G} / \text{RAD}$
 0.7 DAMPING RATIO , 1G/4TH ORDER
 (PILOT #2 RATINGS)

C-H RATINGS



C-H RATINGS

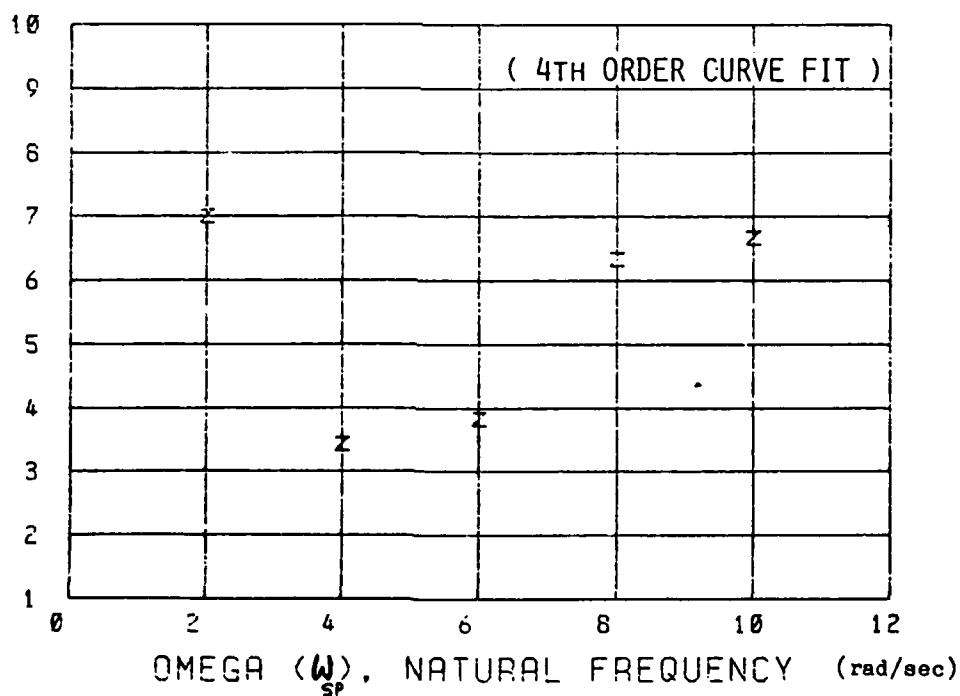
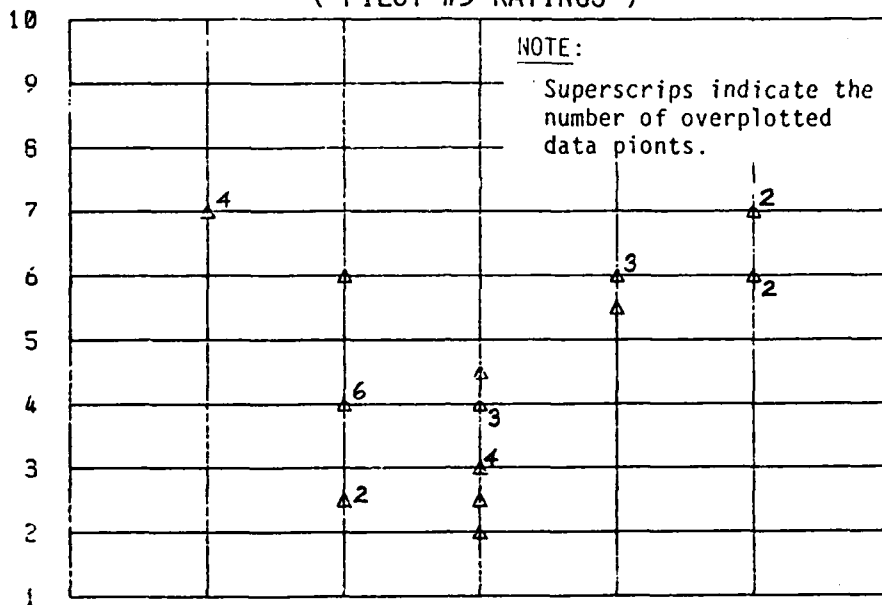


Figure c10. COOPER-HARPER VS OMEGA

COOPER-HARPER VS OMEGA AT 1G
 NT-33A PROJECT HUD TRACKING
 $N / \text{ALPHA} = 29 \text{ G} / \text{RAD}$
 0.7 DAMPING RATIO . 1G/4TH ORDER
 (PILOT #3 RATINGS)

C-H RATINGS



C-H RATINGS

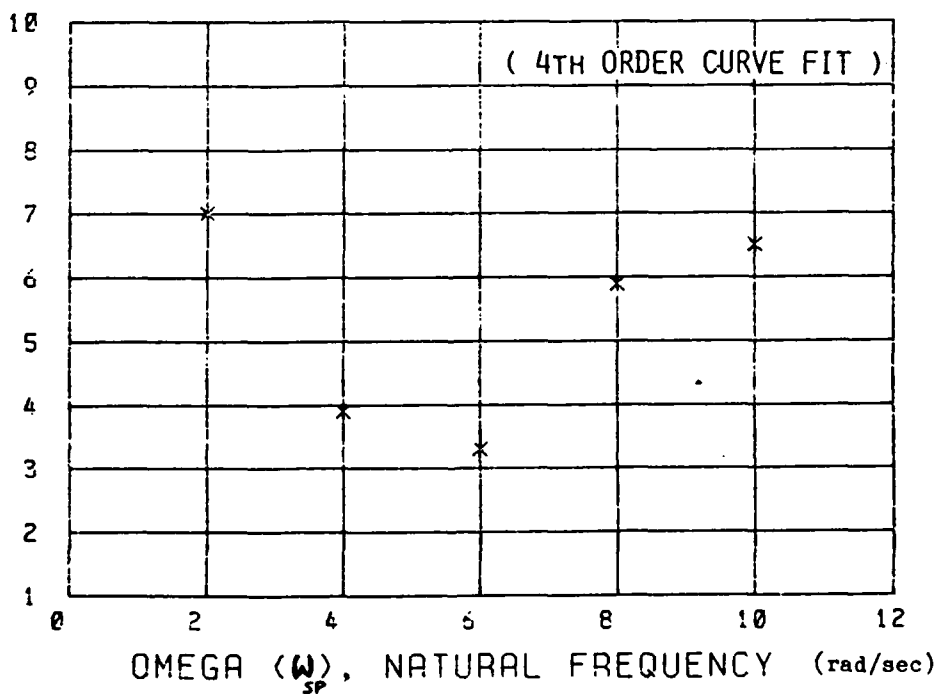
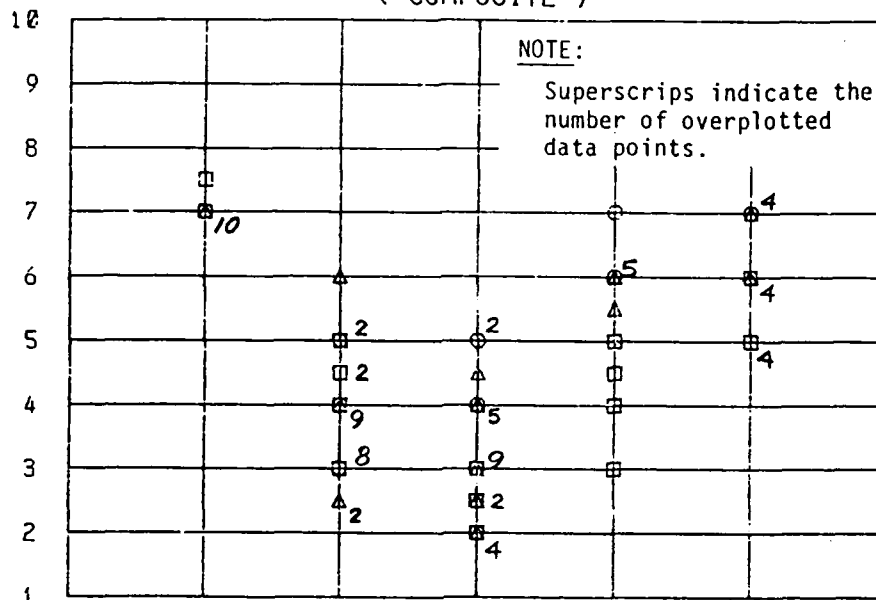


Figure c11. COOPER-HARPER VS OMEGA

COOPER-HARPER VS OMEGA AT 1G
 NT-33A PROJECT HUD TRACKING
 $N / \text{ALPHA} = 29 \text{ G} / \text{RAD}$
 0.7 DAMPING RATIO , 1G/4TH ORDER
 (COMPOSITE)

C-H RATINGS



LEGEND
 1. □: PILOT 1
 2. ○: PILOT 2
 3. △: PILOT 3
 4. *: PILOT 1
 5. Z: PILOT 2
 6. X: PILOT 3

C-H RATINGS

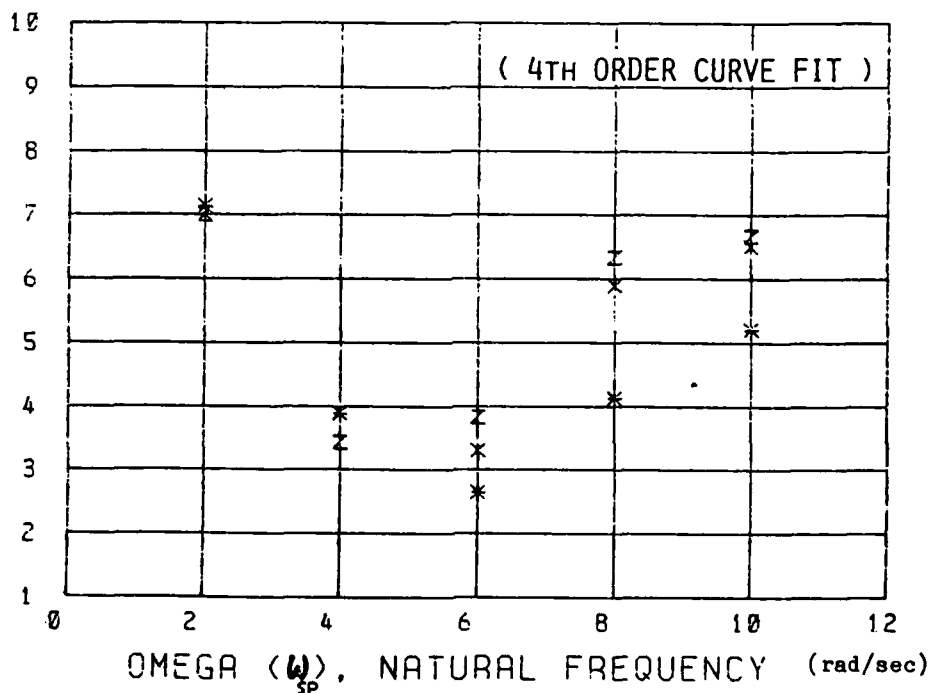
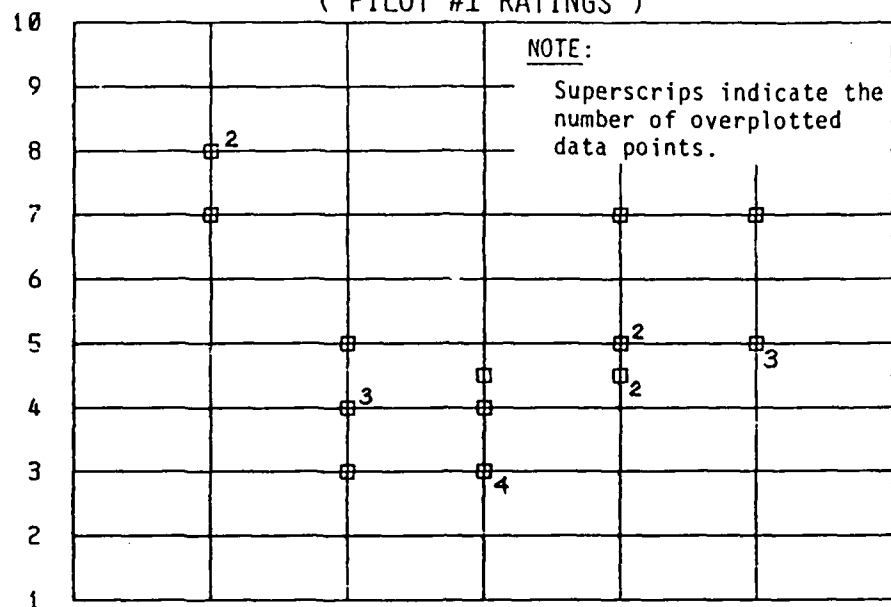


Figure C12. COOPER-HARPER VS OMEGA

COOPER-HARPER VS OMEGA AT 2G
 NT-33A PROJECT HUD TRACKING
 $N / \text{ALPHA} = 29 \text{ G} / \text{RAD}$
 0.7 DAMPING RATIO , 2G/4TH ORDER
 (PILOT #1 RATINGS)

C-H RATINGS



C-H RATINGS

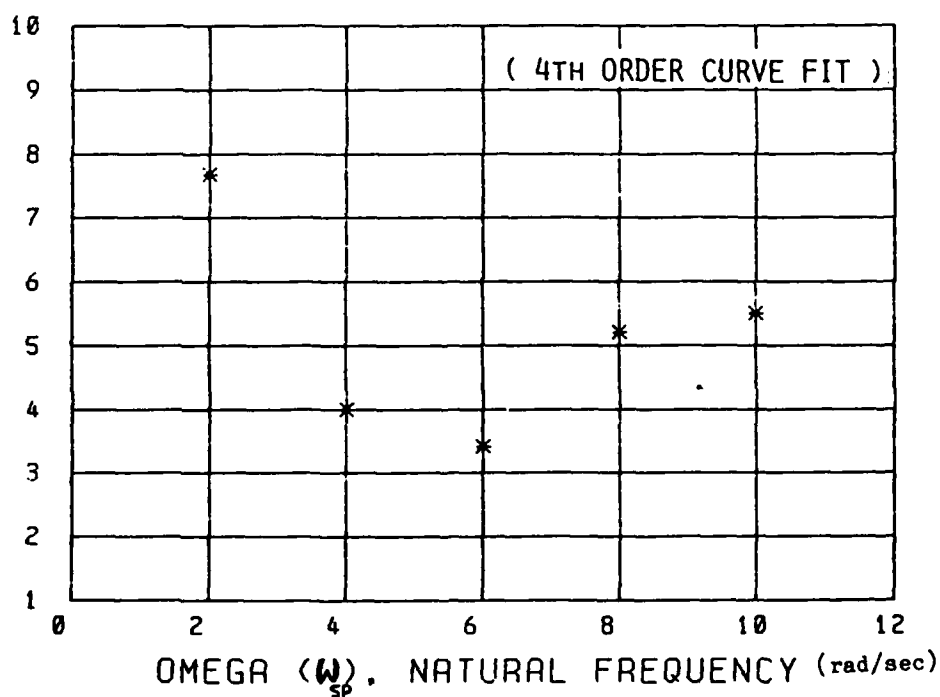


Figure c13. COOPER-HARPER VS OMEGA

COOPER-HARPER VS OMEGA AT 2G
 NT-33A PROJECT HUD TRACKING
 $N / \text{ALPHA} = 29 \text{ G} / \text{RAD}$
 0.7 DAMPING RATIO , 2G/4TH ORDER

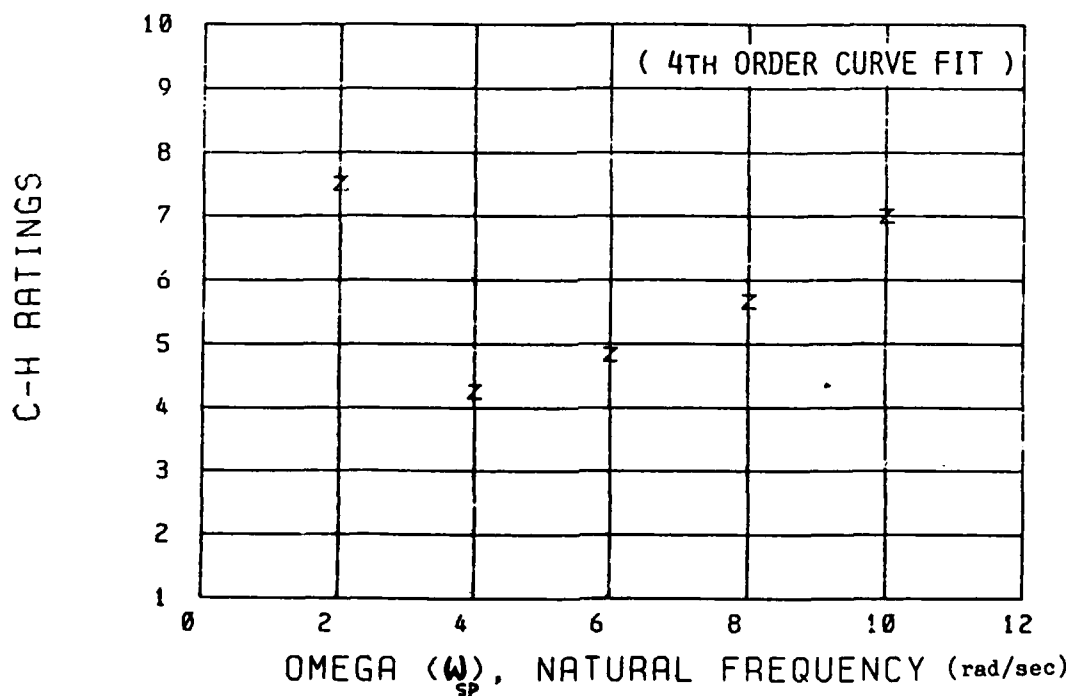
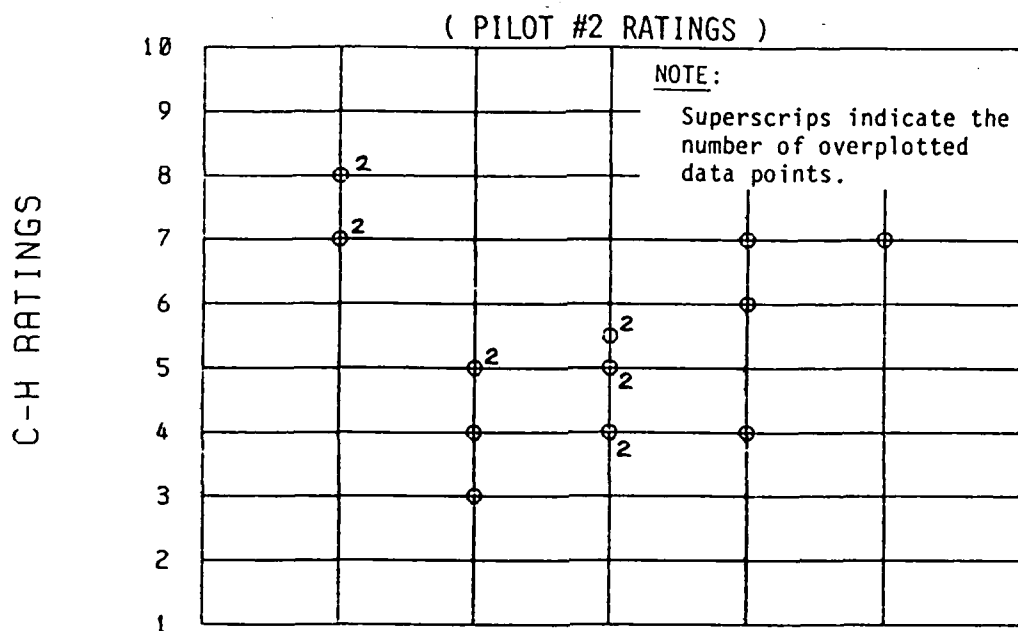


Figure c14. COOPER-HARPER VS OMEGA

COOPER-HARPER VS OMEGA AT 2G
 NT-33A PROJECT HUD TRACKING
 $N / \text{ALPHA} = 29 \text{ G} / \text{RAD}$
 0.7 DAMPING RATIO , 2G/4TH ORDER

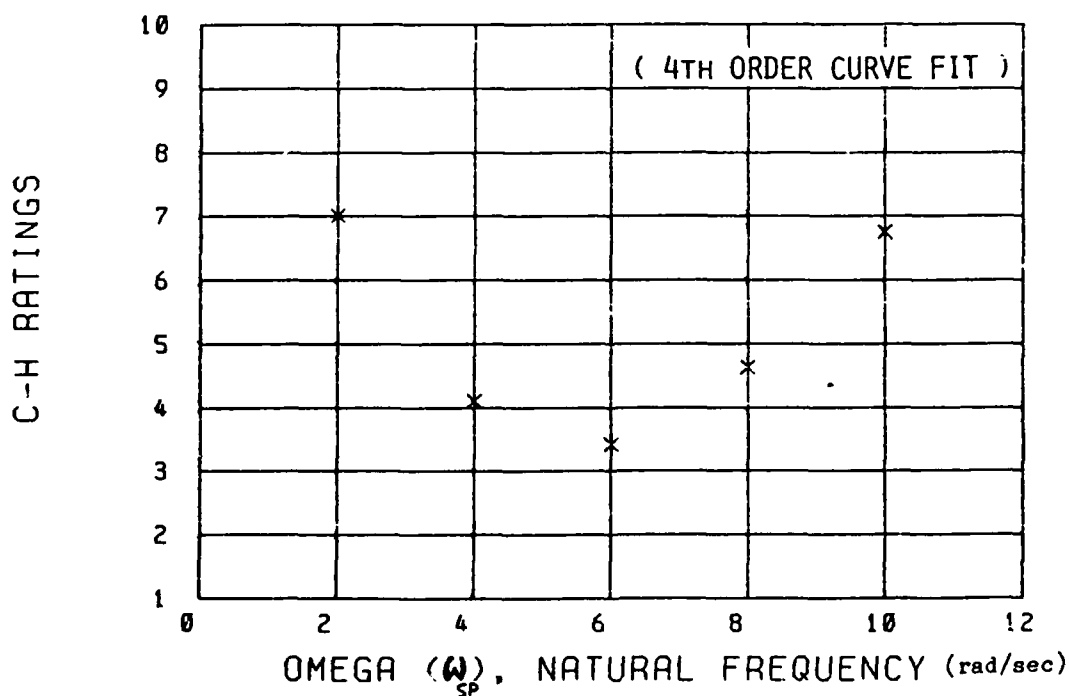
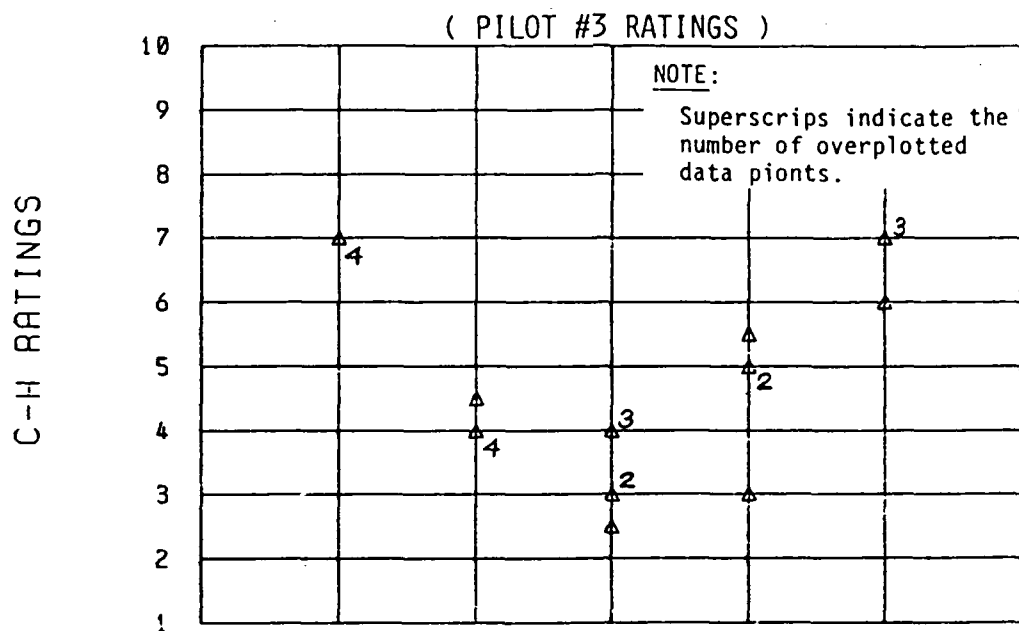
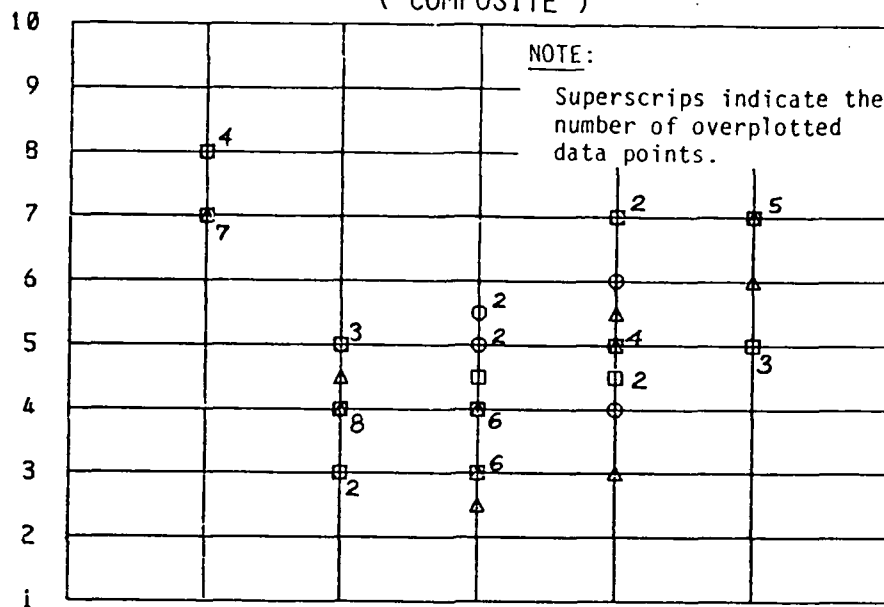


Figure C15. COOPER-HARPER VS OMEGA

COOPER-HARPER VS OMEGA AT 2G
 NT-33A PROJECT HUD TRACKING
 $N / \text{ALPHA} = 29 \text{ G} / \text{RAD}$
 0.7 DAMPING RATIO , 2G/4TH ORDER
 (COMPOSITE)

C-H RATINGS



C-H RATINGS

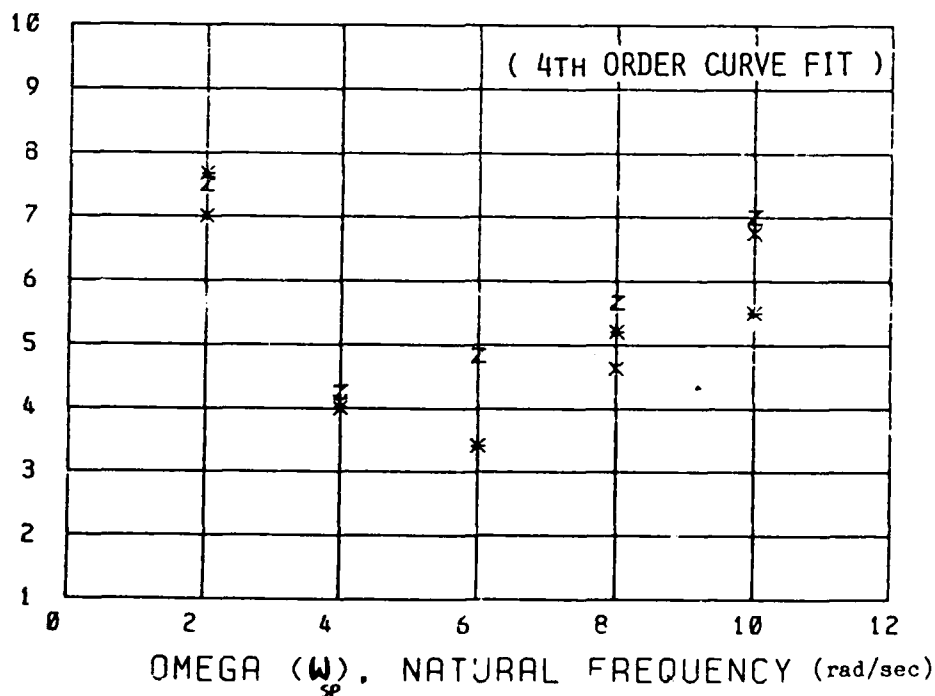


Figure C16. COOPER-HARPER VS OMEGA

PILOT #1 / SAFID 1G DATA
 NT-33A PROJECT HUD TRACKING TASK
 N/ALPHA = 29 G/RAD
 0.7 DAMPING RATIO

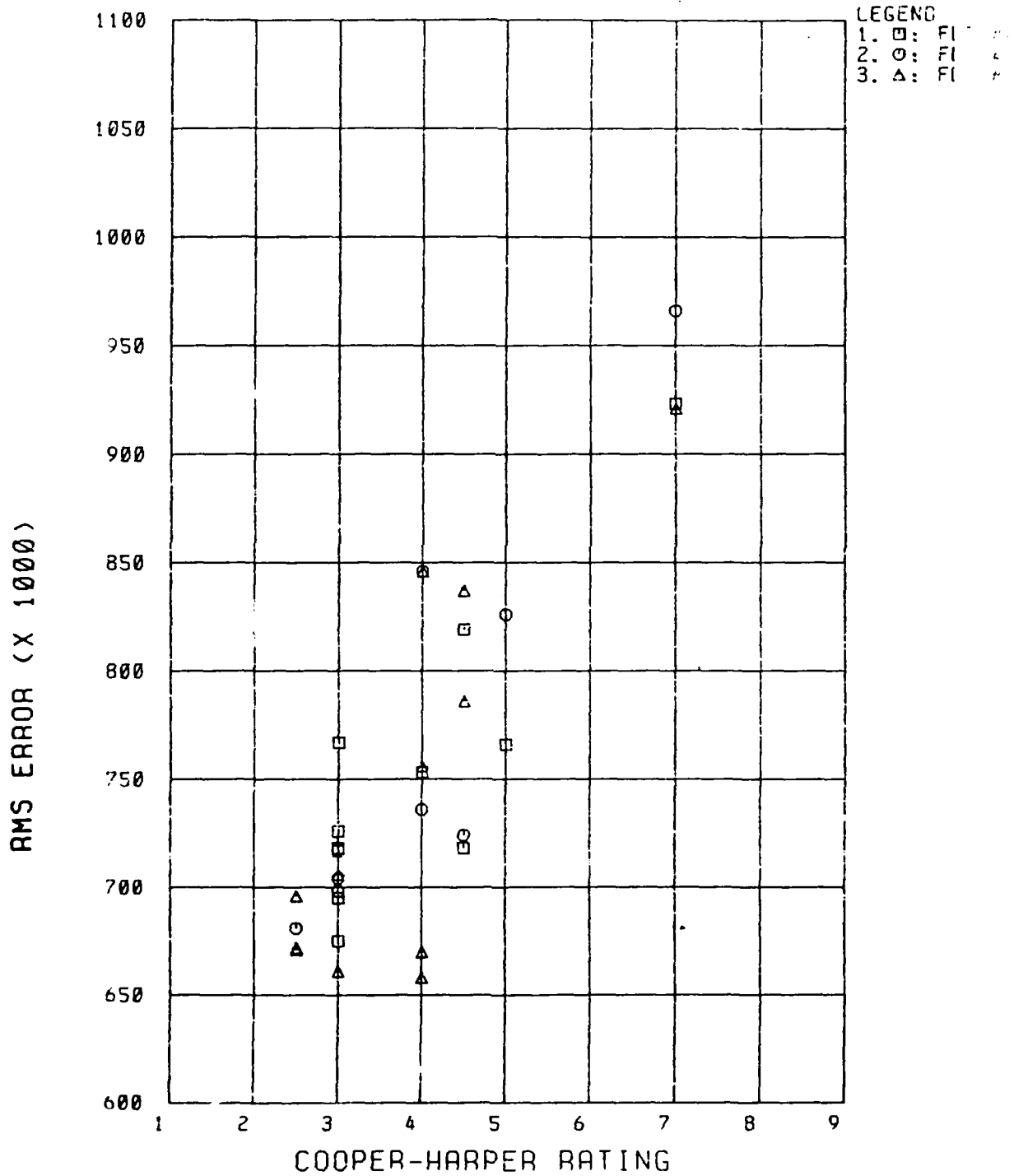


Figure 17. RMS VERSUS COOPER-HARPER RATING

PILOT #2 / SAFTD 1G DATA
 NT-33A PROJECT HUD TRACKING TASK
 N/ALPHA = 29 G/RAD
 0.7 DAMPING RATIO

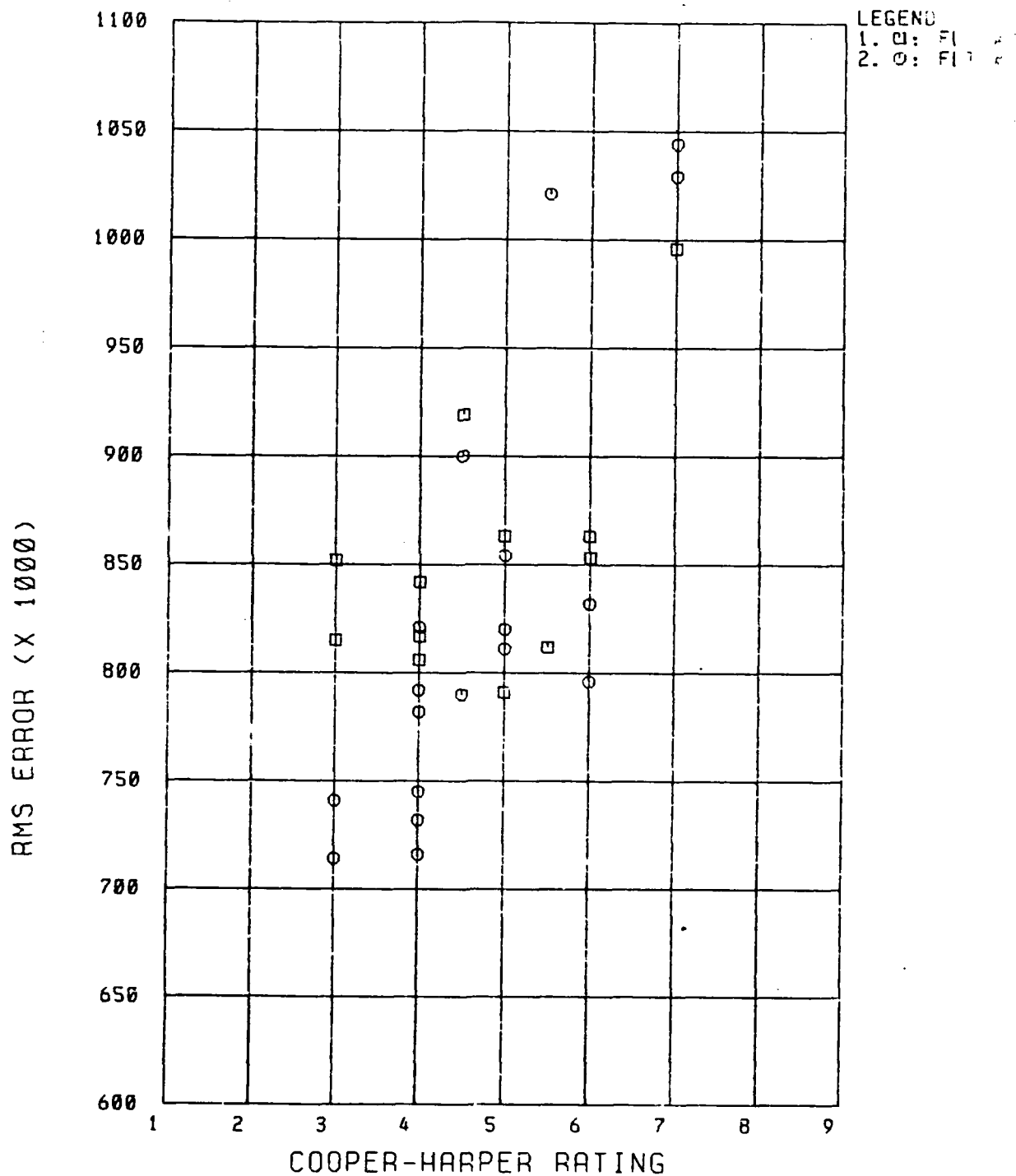


Figure C18. RMS VERSUS COOPER-HARPER RATING

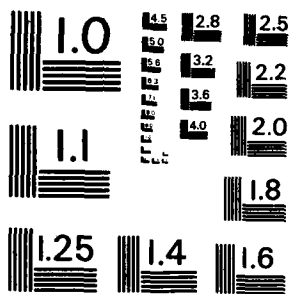
AD-A135 853

COMPARISON OF THE LONGITUDINAL FLYING QUALITIES OF AN
OPTIMAL PILOT MODEL (W) AIR FORCE INST OF TECH
WRIGHT-PATTERSON AFB OH SCHOOL OF ENGL. J M PAYNE
SEP 83 AFIT/GAE/DA/833-5 F/C 1A/2 NL

2/2

UNCLASSIFIED





MICROCOPY RESOLUTION TEST CHART
NATIONAL BUREAU OF STANDARDS-1963-A

PILOT #3 / SAFTD 1G DATA
 NT-530 PROJECT HUD TRACKING TASK
 N/ALPHA = 29 G/RAD
 0.7 DAMPING RATIO

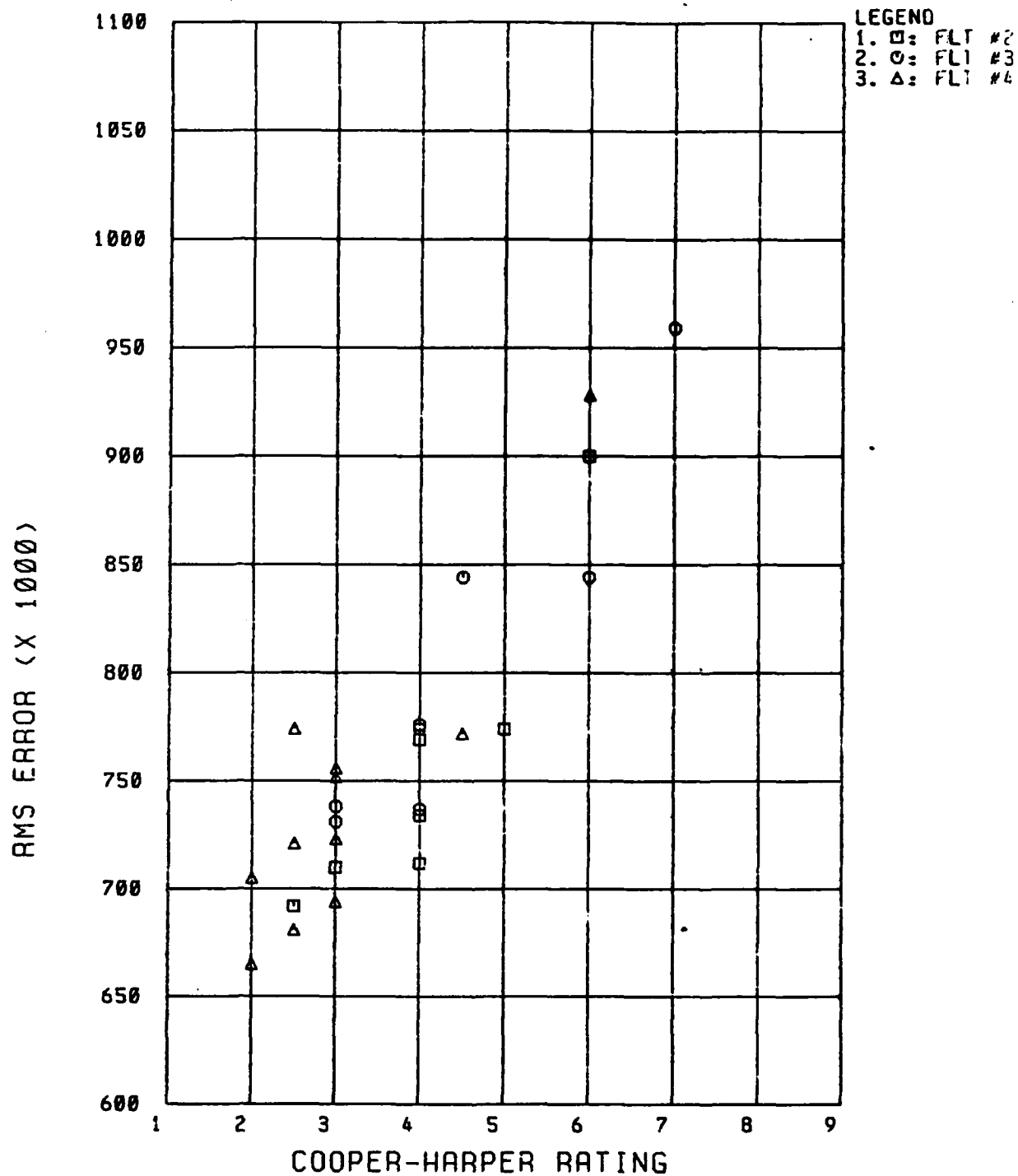


Figure C19. RMS VERSUS COOPER-HARPER RATING

PILOT #1 / SAFTD 1G DATA
 NT-33A PROJECT HUD TRACKING TASK
 N/ALPHA = 29 G/RAD
 0.7 DAMPING RATIO

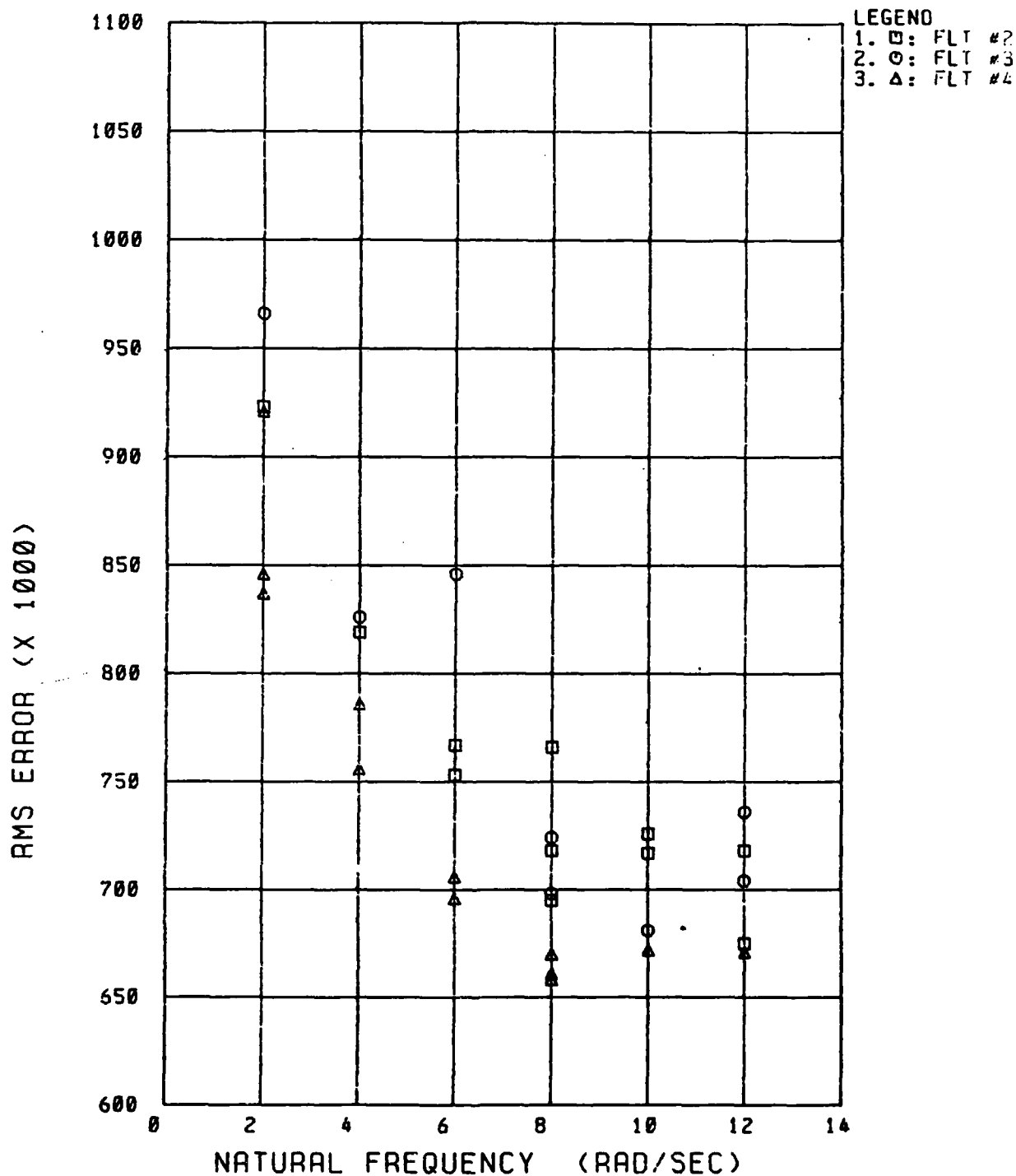


Figure C20. RMS VERSUS SHORT PERIOD NATURAL FREQUENCY

PILOT #2 / SAFTD 1G DATA
 NT-33A PROJECT HUD TRACKING TASK
 $N/\alpha = 29 \text{ G/RAD}$
 $0.7 \text{ DAMPING RATIO}$

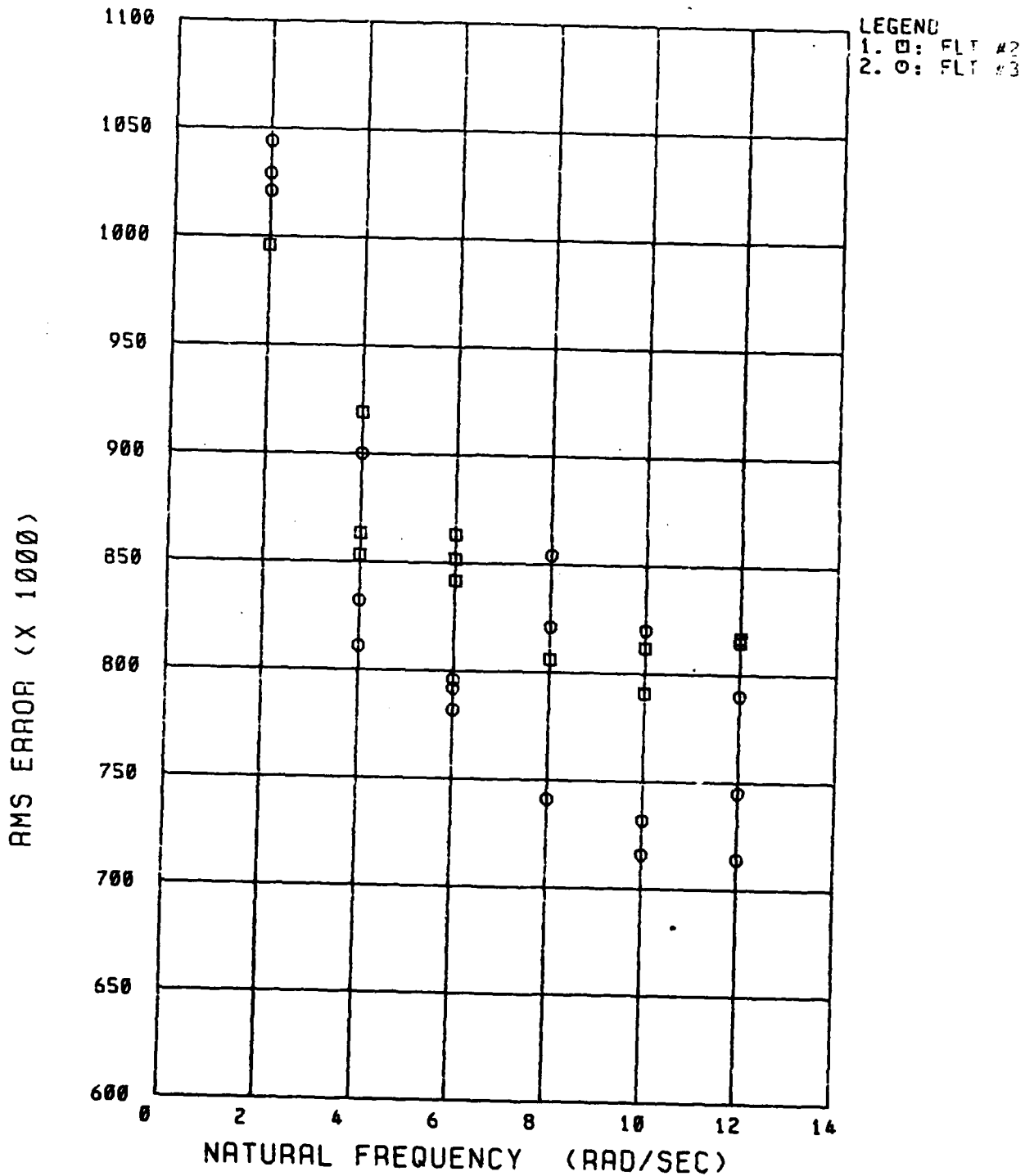


Figure C21. RMS VERSUS SHORT PERIOD NATURAL FREQUENCY

PILOT #3 / SAFTD 1G DATA
 NT-33A PROJECT HUD TRACKING TASK
 $N/\text{ALPHA} = 29 \text{ G/RAD}$
 0.7 DAMPING RATIO

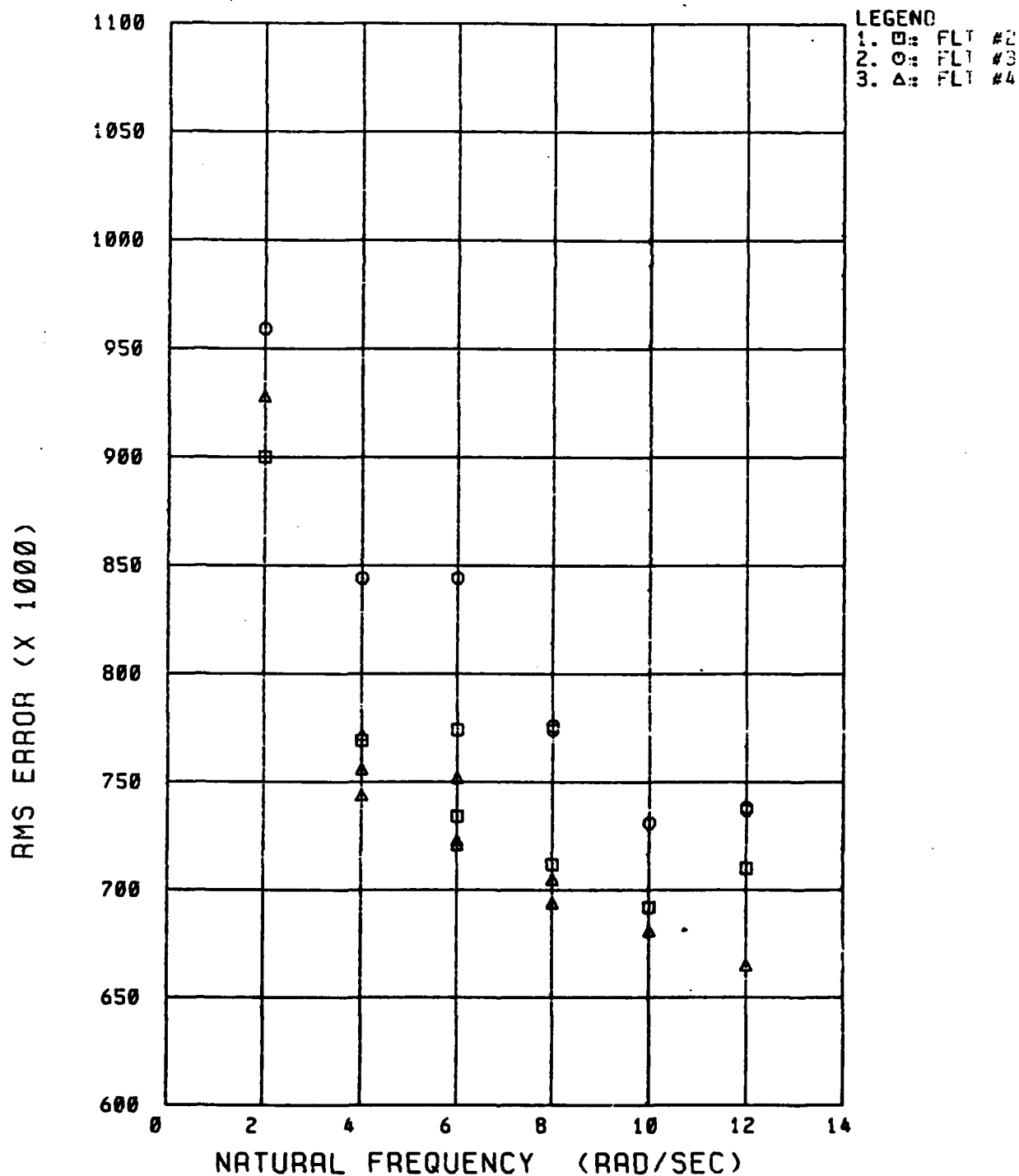


Figure C22. RMS VERSUS SHORT PERIOD NATURAL FREQUENCY

PILOT #1 SAFIO 2G DATA
 NT-33A PROJECT HUD TRACKING TASK
 $N/\alpha = 29 \text{ G/RAD}$ $FS/G = 6.5 \text{ LB/G}$
 $0.7 \text{ DAMPING RATIO}$

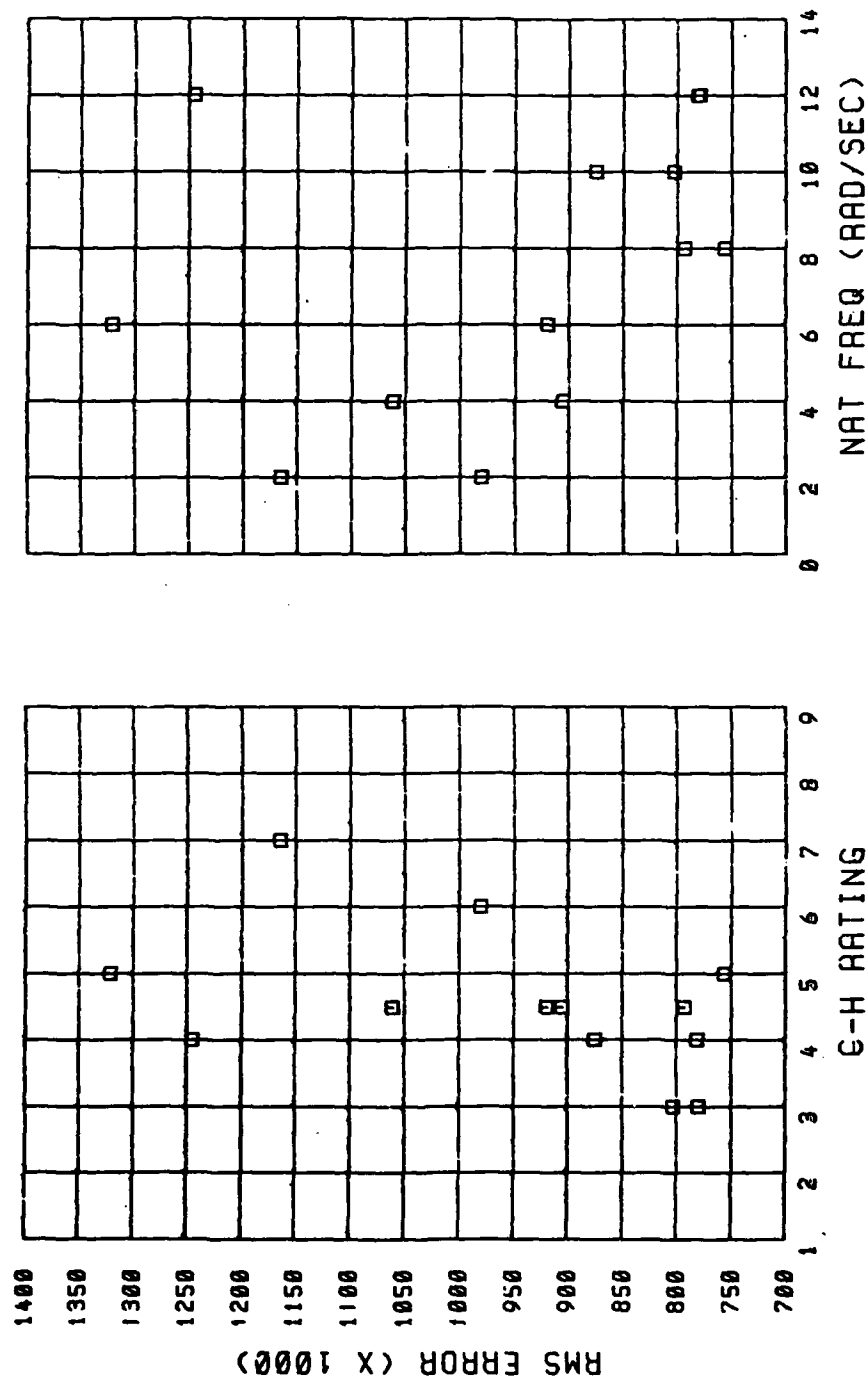


Figure C23. RMS ERROR (X 1000) vs. DAMPING RATIO/NATURAL FREQUENCY

PILOT #2 SAFTD 2G DATA
 NT-33A PROJECT HUD TRACKING TASK
 N/ALPHA = 29 G/RAD FS/G = 6.5 LB/G
 0.7 DAMPING RATIO

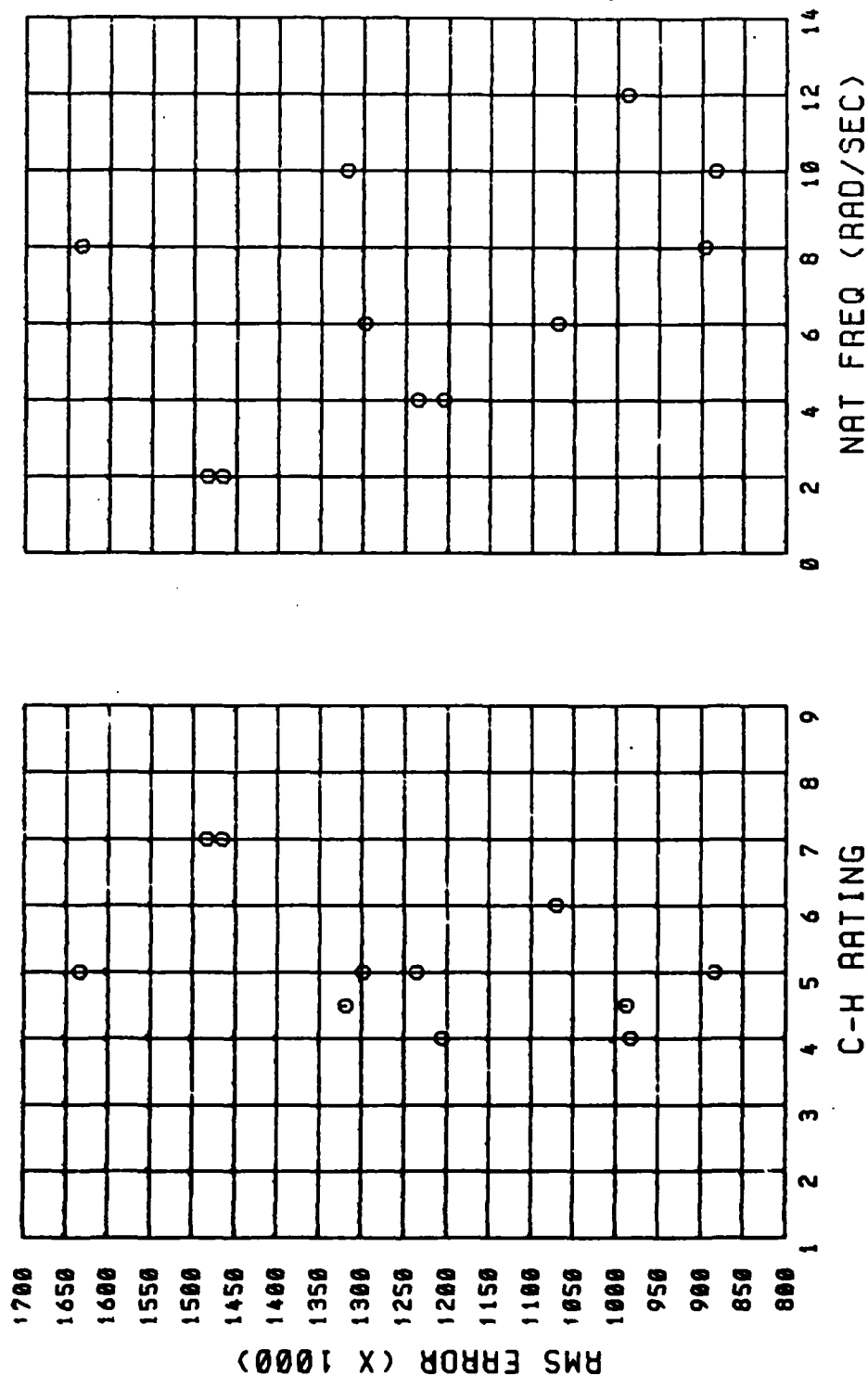


Figure c24. RMS VERSUS COOPER HARPER RATING/NATURAL FREQUENCY

PILOT #3 SAFID 2G DATA
 NT-33A PROJECT HUD TRACKING TASK
 N/ALPHA = 29 G/RAD FS/G = 6.5 LB/G
 0.7 DAMPING RATIO

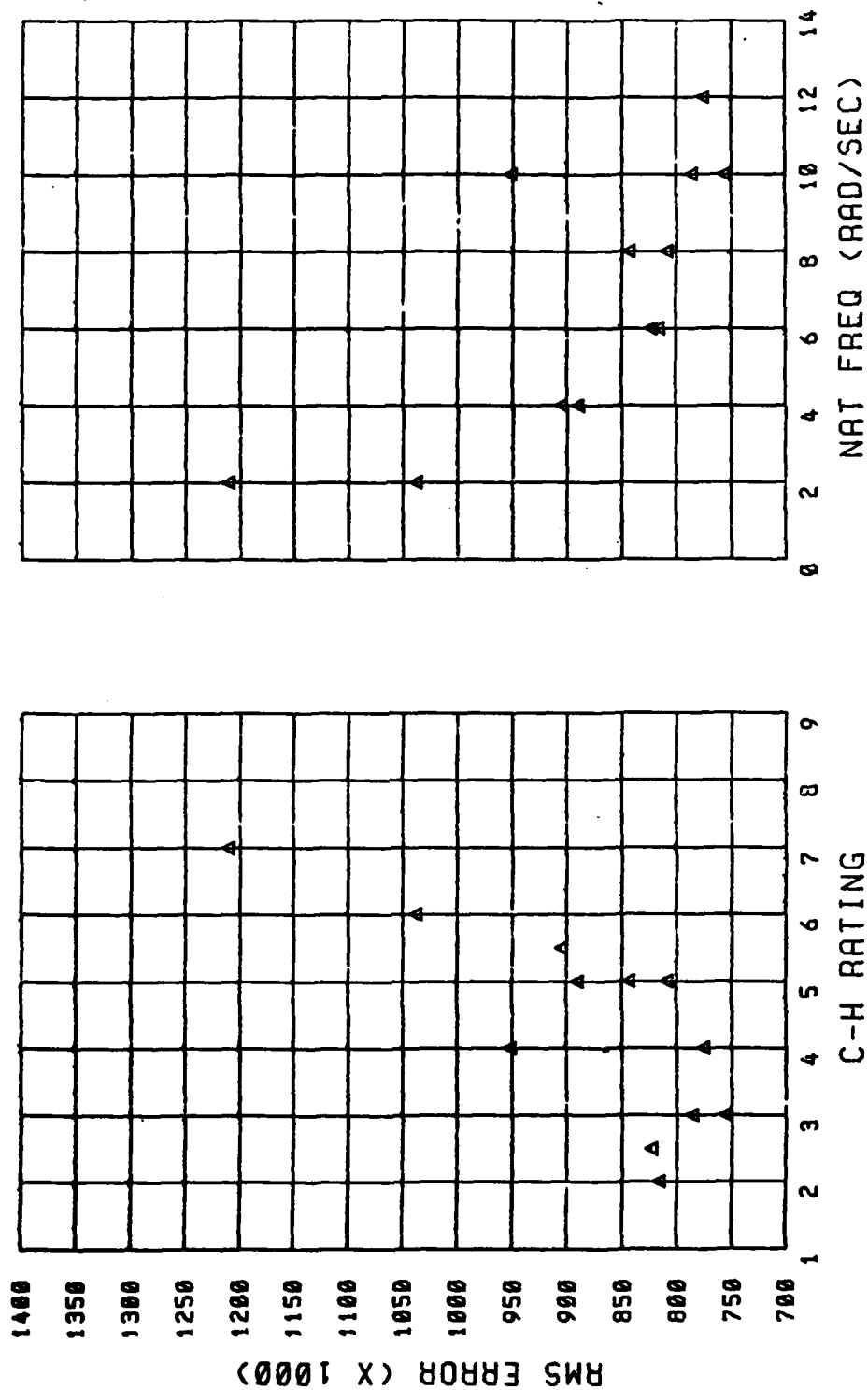


Figure C25. RMS VERSUS COOPER HARPER RATING/NATURAL FREQUENCY

SAFTD 2G DATA
 NT-33A PROJECT HUD TRACKING TASKS
 N/ALPHA = 29 G/RAD FS/G = 6.5 LB /G
 0.7 DAMPING RATIO

LEGEND
 1. ○: PILOT #1
 2. □: PILOT #2
 3. △: PILOT #3

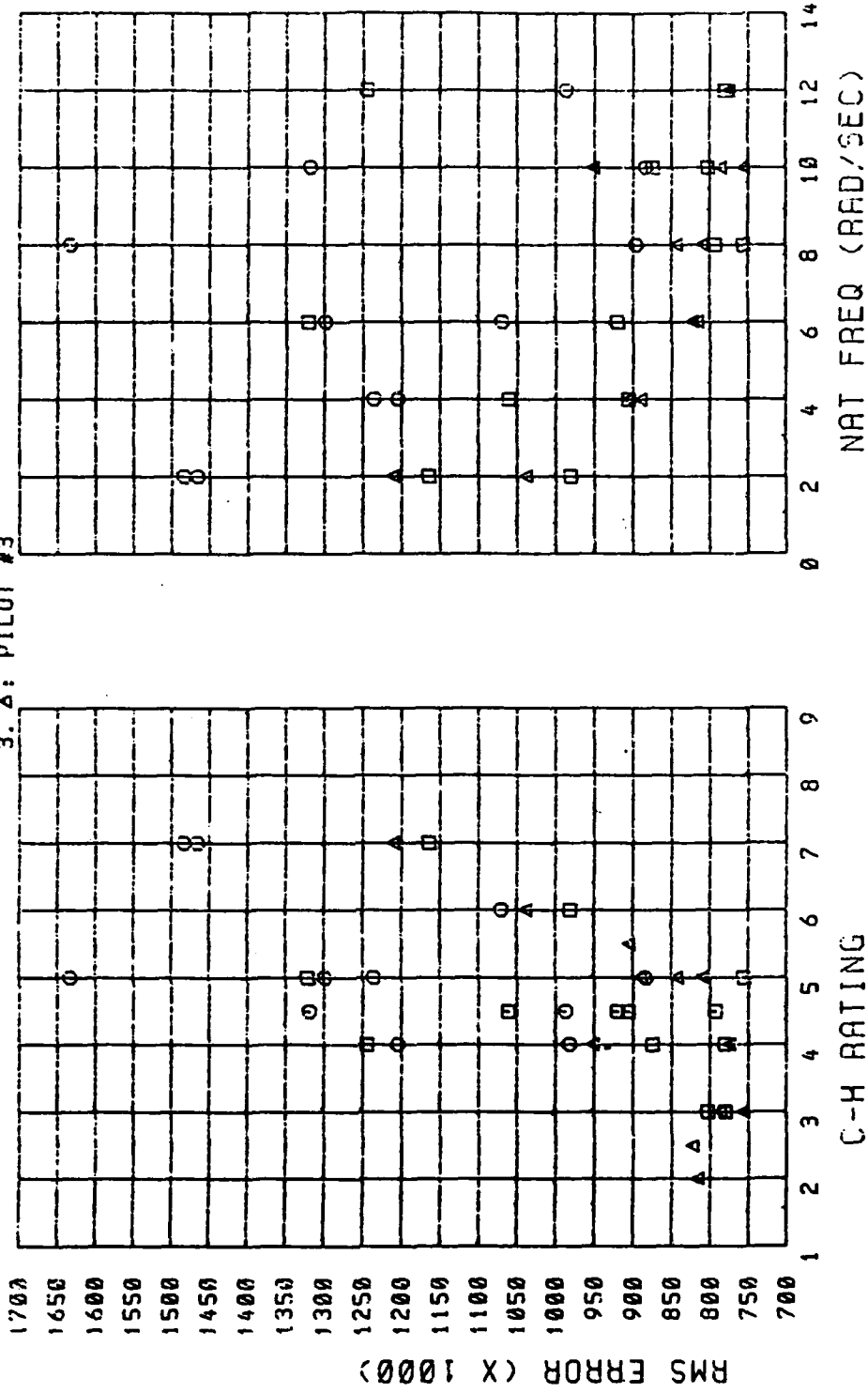


Figure C26. RMS ERROR vs C-H RATING/NATURAL FREQUENCY

PILOT #2 / NT-33A 1G DATA
 NT-33A PROJECT HUD TRACKING TASK
 N/ALPHA = 29 G/RAD
 0.7 DAMPING RATIO

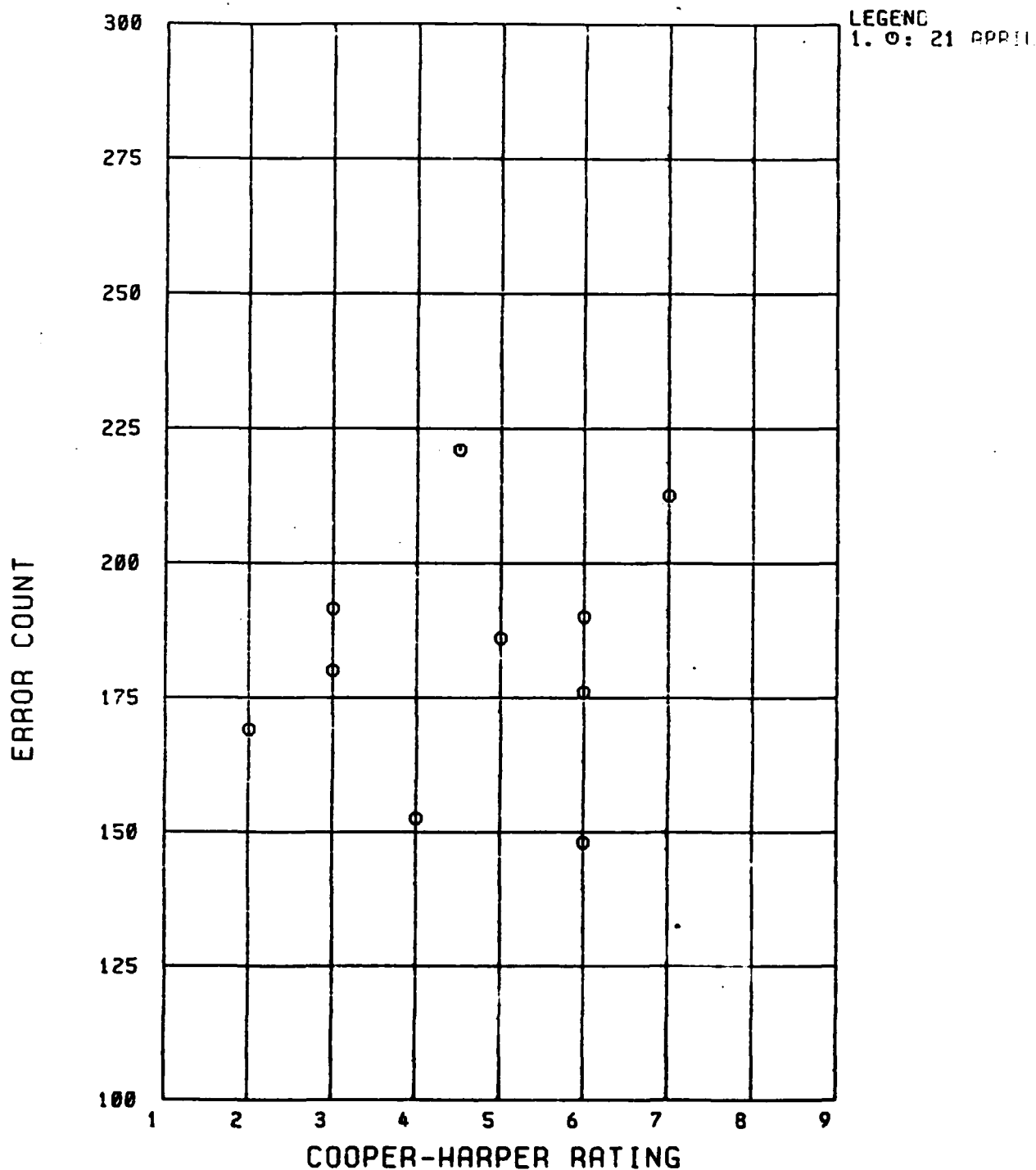


Figure C27. ERROR COUNT VERSUS COOPER-HARPER RATING

PILOT #3 / NT-33A 1G DATA
NT-33A PROJECT HUD TRACKING TASK
N/ALPHA = 29 G/RAD
0.7 DAMPING RATIO

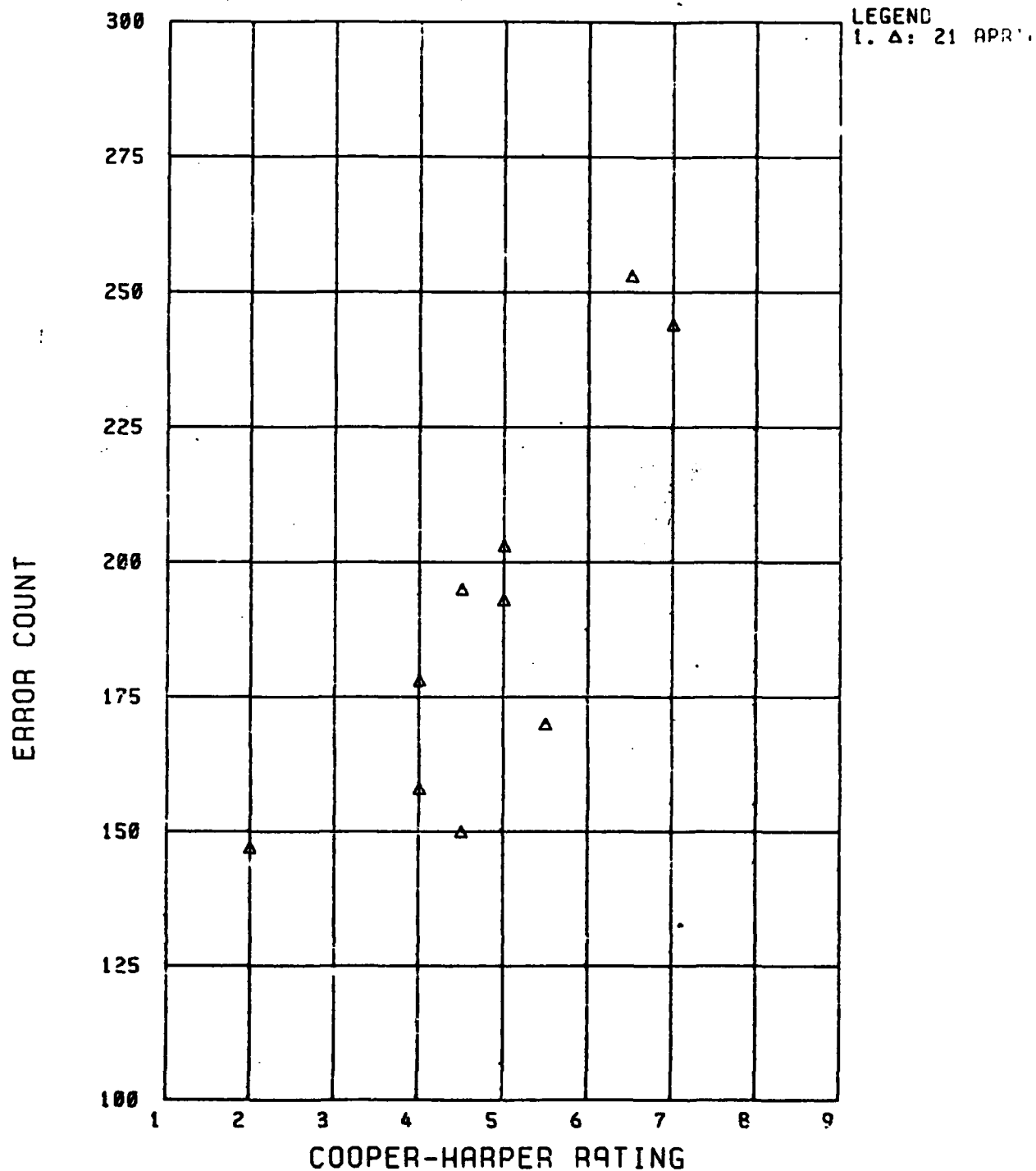


Figure C28. ERROR COUNT VERSUS COOPER-HARPER RATING

PILOT #2 / NT-33A 1G DATA
 NT-33A PROJECT HUD TRACKING TASK
 $N/\alpha = 29 \text{ G/RAD}$
 0.7 DAMPING RATIO

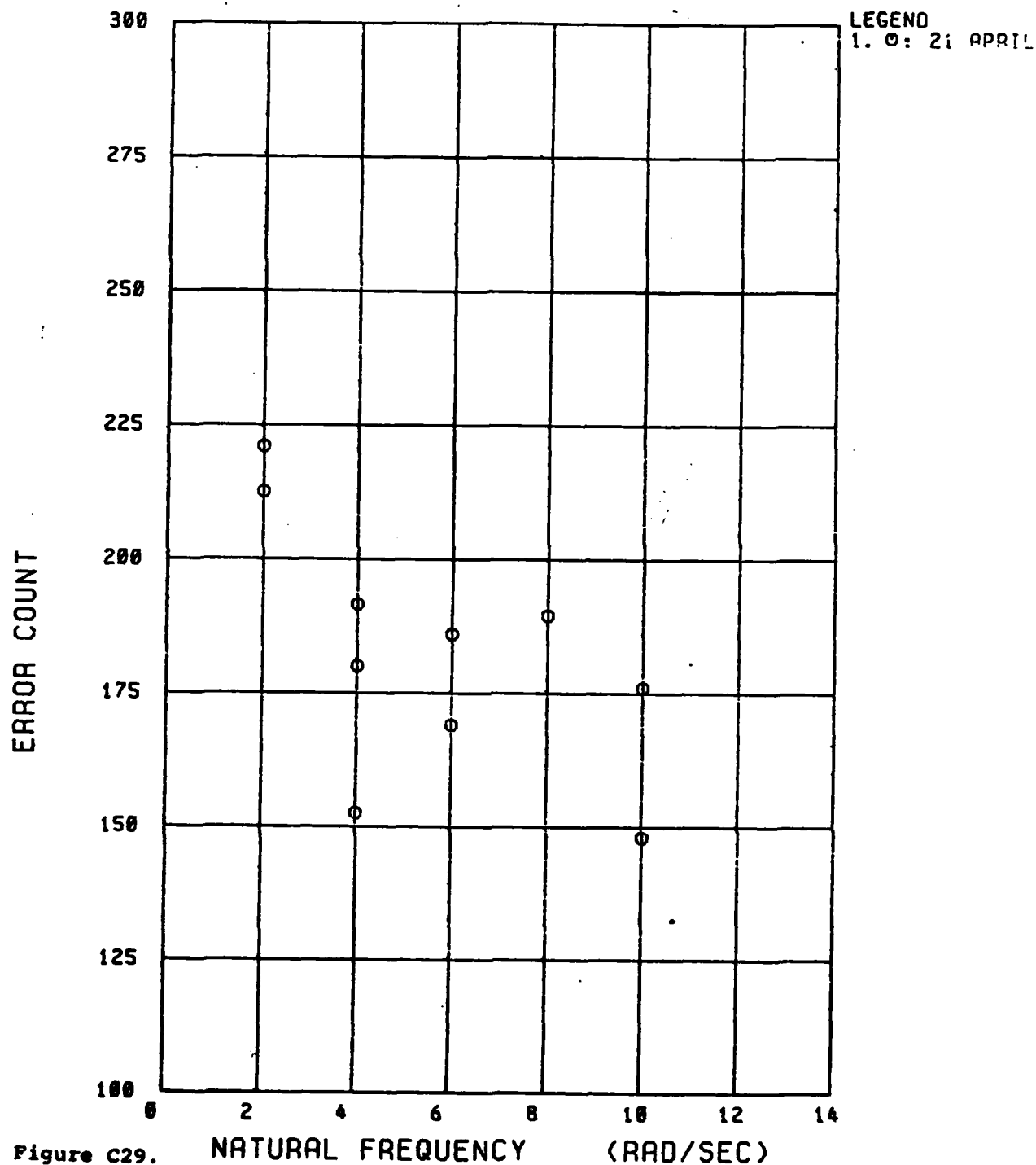


Figure C29. NATURAL FREQUENCY (RAD/SEC)
 ERROR COUNT VERSUS SHORT PERIOD NATURAL FREQUENCY

PILOT #3 / NT-33A 1G DATA
 NT-33A PROJECT HUD TRACKING TASK
 N/ALPHA = 29 G/RAD
 0.7 DAMPING RATIO

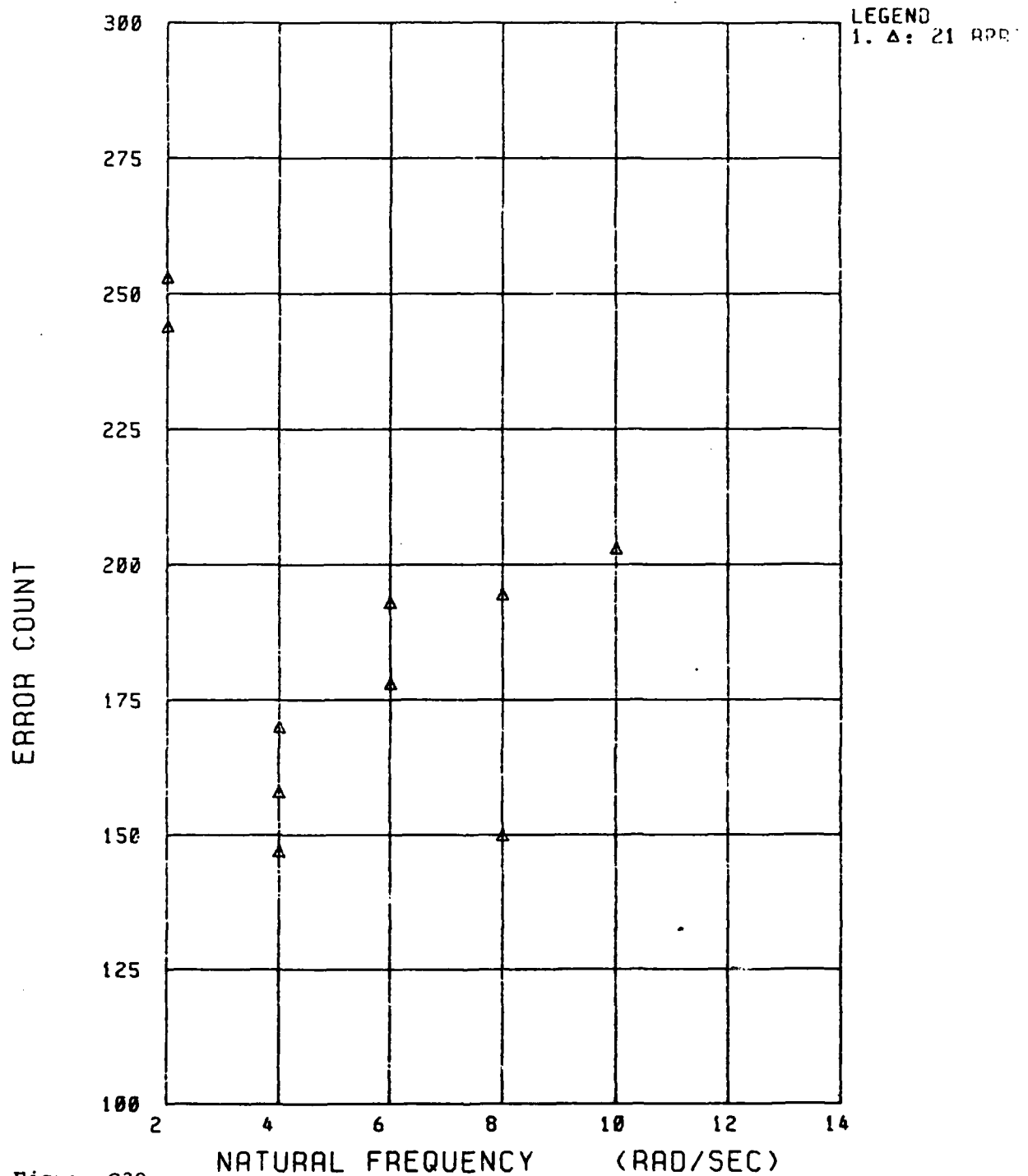


Figure C30.

ERROR COUNT VERSUS SHORT PERIOD NATURAL FREQUENCY

APPENDIX D
DIGITAL TAPE PARAMETERS

Table D1
SAFTD STRIP CHART OUTPUTS

<u>Parameter</u>	<u>Description</u>	<u>Strip Chart Range</u>
Fs	Long. Stick Force	\pm 30 lbs
Fs/Nz	Stick Force per g	0 to 10 lbs per g
Nz	Normal Acceleration	0 to 4 g's
RMS	Root Mean Square	0 to 2
Test Pulse	SAFTD Tracking Task	event
$\Delta\theta$	Error Between Tracking Task and Pitch Angle	\pm 10 deg
θ	Pitch Angle	\pm 10 deg
α	Angle of Attack	\pm 10 deg

Note: Strip charts were played back at 0.5mm per second at a scale factor of 0.2 volts per division.

Table D2
NT-33A STRIP CHART OUTPUTS

<u>Digital Channel No.</u>	<u>Parameter</u>	<u>Description</u>	<u>VSS Output P.P.</u>	<u>Scale Factor (x per volt)</u>
3*	Vi	Indicated Velocity	106	27.5 Kt
18	Fes	Long. Stick Force	26	20.0 lb
2	Nz	Normal Acceleration	16	0.5 g
24	α_v	AOA (vane)	38	2.0 deg
4	q	Pitch Rate	4	5.0 deg/sec
5	$\sin\theta$	Pitch Angle	28	5.88 deg
11	ϵ_{ec}	Tracking Task Error	D/A#1	2.5 deg
1**	hp	Pressure Altitude	107	1,300 feet

- Notes: 1. * Zero knots equalled 10.00 volts.
2. ** 720 feet equalled 8.45 volts.
3. Digital channels one through 12 had adjustable gain x1, x2, x5 and x10. Gains were x1.
4. Aircraft data tapes were played back at 1.0mm per second.
Strip chart sensitivity was 0.1 volt per division.

APPENDIX E
PILOT BACKGROUND

Table E1
PILOT BACKGROUND

PAYNE, JAMES M., Captain, USAF

EDUCATION: BS - General Engineering, US Air Force Academy, CO

FLIGHT TIME:	F-4C/E	602
	F-5E	521
	Other	870
	Total	1993

OPERATIONAL EXPERIENCE: F-4E pilot for one year in the 334th Tactical Fighter Squadron at Seymour Johnson AFB, NC; F-4C/E pilot for fifteen months in the 57th Fighter Interceptor Squadron, Keflavik NS, Iceland; F-5E Aggressor Dissimilar Air Combat Tactics Instructor Pilot for two years in the 527th Tactical Fighter Training Aggressor Squadron, RAF Alconbury, United Kingdom.

STEWART, CHARLES R., Captain, USAF

EDUCATION: BS/MS - Aeronautical and Astronautical Engineering
Purdue University, West Lafayette, Indiana

FLIGHT TIME:	A-10	1325
	Other	331
	Total	1656

OPERATIONAL EXPERIENCE: A-10 pilot for two years in the 356th Tactical Fighter Squadron at Myrtle Beach AFB, SC and then served another two year tour as an A-10 Instructor Pilot with the 92nd Tactical Fighter Squadron at RAF Bentwaters, United Kingdom.

TOMENY, TERRY E., Captain, USAF

EDUCATION: BS/ME - Mechanical Engineering,
Rensselaer Polytechnic Institute, Troy, NY

FLIGHT TIME:	T-38A	1350
	RF-4C	1000
	Other	100
	Total	2450

OPERATIONAL EXPERIENCE: T-38A Instructor Pilot for four years at Moody, AFB, GA. and Vance AFB, Okla; RF-4C Instructor Pilot/Flight Examiner for four years at Zweibrucken AB, Germany.

VITA

James M. Payne was born on July 2nd, 1952, in Eugene, Oregon, and grew up in Hastings, Michigan. Graduation from Hastings High School was followed by undergraduate schooling at the United States Air Force Academy. He graduated from the Academy in 1974 with a Bachelor of Science degree in General Engineering and a commission as a Second Lieutenant in the United States Air Force. He completed Undergraduate Pilot Training at Laughlin Air Force Base, Texas, in 1975, and F-4C combat training at Luke Air Force Base, Arizona, in 1976. After one year of flying F-4E's at Seymour Johnson Air Force Base, North Carolina, he was sent to Keflavik Naval Station, Iceland, for a fifteen month remote tour in F-4C/E's. He then attended Enemy Weapons School at Nellis Air Force Base, Nevada, and was subsequently assigned to the 527th Tactical Fighter Training Aggressor Squadron at Royal Air Force Alconbury, England. There he flew the F-5E in simulations of the enemy. In 1981, he was selected for a new combined Air Force Institute of Technology/Test Pilot School Education Program. He spent one year at AFIT followed by a year at TPS, where the requirements for a Master of Science in Aeronautical Engineering, specializing in Stability and Control, were completed.

Permanent address: 1970 North Broadway
Hastings, Michigan 49058

REPORT DOCUMENTATION PAGE		READ INSTRUCTIONS BEFORE COMPLETING FORM
1. REPORT NUMBER AFIT/GAE/AA/83S-5	2. GOVT ACCESSION NO.	3. RECIPIENT'S CATALOG NUMBER
4. TITLE (and Subtitle) Comparison of the Longitudinal Flying Qualities of an Optimal Pilot Model, a Ground-Based Simulator, and an Airborne Simulator	5. TYPE OF REPORT & PERIOD COVERED MS Thesis	
7. AUTHOR(s) James M. Payne Captain, USAF	6. PERFORMING ORG. REPORT NUMBER	
9. PERFORMING ORGANIZATION NAME AND ADDRESS Air Force Institute of Technology (AFIT-EN) Wright-Patterson AFB OH 45433	8. CONTRACT OR GRANT NUMBER(s)	
11. CONTROLLING OFFICE NAME AND ADDRESS	10. PROGRAM ELEMENT, PROJECT, TASK AREA & WORK UNIT NUMBERS	
14. MONITORING AGENCY NAME & ADDRESS (if different from Controlling Office)	12. REPORT DATE September 1983	
	13. NUMBER OF PAGES 114	
	15. SECURITY CLASS. (of this report) Unclassified	
15a. DECLASSIFICATION/DOWNGRADING SCHEDULE		
16. DISTRIBUTION STATEMENT (of this Report) Approved for public release; distribution unlimited.		
17. DISTRIBUTION STATEMENT (of the abstract entered in Block 20, if different from Report)		
18. SUPPLEMENTARY NOTES Approved for public release: IAW AFR 190-17. <i>W. L. WOLAYER</i> Dean for Research and Development Air Force Institute of Technology Wright-Patterson AFB, OH 45433 26 SEPT 83		
19. KEY WORDS (Continue on reverse side if necessary and identify by block number) flying qualities pilot model simulation HUD tracking NT-33A		
20. ABSTRACT (Continue on reverse side if necessary and identify by block number) A comparison of the longitudinal flying qualities as predicted by an analytical computer model, a ground based simulator, and an airborne simulator was accomplished. Short period natural frequency was varied with all other parameters held constant.		

20. (con't)

In the analytical model, pilot performance improved as frequency was increased. In the ground-based simulation, pilot ratings were a function of how well he could track. Performance improved with increased frequency.

In the airborne simulation, pilot preferred 4 to 6 radians per second. Lower frequencies were too slow and higher frequencies were too abrupt and uncomfortable despite better tracking performance.

UNCLASSIFIED

SECURITY CLASSIFICATION OF THIS PAGE (When Data Entered)

END

DATE
FILMED

1 84

DTIC